

THE PREDICTION OF POLYMER WEAR USING
POLYMER MECHANICAL PROPERTIES AND SURFACE
CHARACTERIZATION PARAMETERS

by

Jeffery Howard Warren

Dissertation submitted to the Graduate Faculty of the
Virginia Polytechnic Institute and State University
in partial fulfillment of the requirements for the degree of
DOCTOR OF PHILOSOPHY

in

Mechanical Engineering

APPROVED:

Dr. N. S. Eiss, Jr., Chairman

Dr. J. B. Jones, Dept. Head

Dr. H. H. Mabie

Dr. A. K. Furr

Dr. C. W. Smith

August, 1976

Blacksburg, Virginia

DEDICATED TO MY WIFE,

ACKNOWLEDGEMENTS

The author would like to thank Dr. N. S. Eiss, Jr., Chairman of his graduate committee, for the many hours of guidance and counseling he has given during this research. It is always a pleasure to work with such a fine man. The other members of the committee are also to be commended for the helpful discussions they gave during the development and completion of this research and dissertation.

Dr. T. F. Parkinson and the members of the Neutron Activation Analysis Laboratory deserve acknowledgement for their cooperation in the use of their facility for the wear measurements. Bradley Roscoe is especially thanked for his help in analyzing the data received from the radiation counting equipment in the NAA Laboratory.

of the Laboratory Support Service's Machine Shop is thanked for his help in preparing both steel and polymer specimens. is also thanked for her patience and excellent typing of this manuscript.

Thanks is also due to , operator of the scanning electron microscope, for his ability and desire to obtain outstanding photographs of the polymer wear tracks. Without his help, knowledge of the wear mechanism would have been greatly hindered. The author would also like to thank and his staff of Calspan Corporation for their help in characterizing the ground steel surfaces. The United States Army Research Office, Research Triangle Park, N.C., is gratefully thanked for its financial

support of this research.

The author also wants to thank his lovely wife, , for her patience and persistent help throughout the writing of this dissertation. His parents as well as his wife are also thanked for their encouragement throughout his educational program.

TABLE OF CONTENTS

	<u>Page</u>
ACKNOWLEDGEMENTS	iii
LIST OF FIGURES	vii
LIST OF TABLES	x
NOMENCLATURE	xii
1. <u>INTRODUCTION</u>	1
2. <u>LITERATURE SEARCH</u>	8
2.1. <u>Polymer Wear Theories</u>	8
2.2. <u>Surface Characterization Parameters</u>	24
3. <u>EXPERIMENTS</u>	27
3.1. <u>Wear Data</u>	27
3.1.1. Apparatus	27
3.1.2. Experimental Materials	29
3.1.3. Experimental Procedure	32
3.1.4. Wear Data Results	34
3.2. <u>Shear Angle Data</u>	38
3.2.1. Apparatus	38
3.2.2. Experimental Materials	40
3.2.3. Experimental Procedures	41
3.2.4. Shear Angle Results	43
3.3. <u>Surface Topography Data</u>	69
3.3.1. Apparatus, Materials, Procedure	69
3.3.2. Surface Characterization Results	70
4. <u>DISCUSSION OF RESULTS</u>	82

TABLE OF CONTENTS (cont'd)

	<u>Page</u>
4.1. <u>Single Point Orthogonal Cutting Theory</u>	82
4.2. <u>Types of Penetration</u>	90
4.2.1. Full Penetration	94
4.2.2. Partial Penetration	106
5. <u>CONCLUSIONS AND RECOMMENDATIONS</u>	113
6. <u>REFERENCES</u>	118
7. APPENDIX A: WEAR MEASUREMENT SENSITIVITY	123
8. APPENDIX B: SHEAR ANGLE MEASUREMENT	128
9. VITA	155

LIST OF FIGURES

<u>Figure Number</u>		<u>Page</u>
1	Abrasive Wear Model in which a cone removes material from a surface from Rabinowicz [15, p. 168]	10
2	Relationship of volume displaced per unit sliding distance to base angle of the conical indenter from Lancaster [4].	12
3	Schematic diagrams for derivation of Pv-factor from Halling [28].	15
4	Example of a typical Pv-diagram from Lewis [27]	17
5	Approximate σ - ϵ curves for PVC and PCTFE, . .	20
6	Dependence of wear resistance on other mechanical characteristics of plastics for wear on abrasive such as emery cloth from Ratner et al. [29].	21
7	Pin-on-disk machine.	28
8	a) A rectangular ground steel block with linear wear tracks.	39
	b) The configuration of the steel block in the SEM.	39
9	Conical Nylon 6-6 pin run on rectangular block 4, 14.7N load, 1 Pass, 5/21/76. . . .	44
10	Conical Nylon 6-6 pin run on rectangular block 4, 14.7N load, 1 Pass, 5/21/76. . . .	45
11	Conical Nylon 6-6 pin run on rectangular block 4, 14.7N load, 1 Pass, 5/21/76. . . .	46
12	Conical Nylon 6-6 pin run on rectangular block 4, 14.7N load, 1 Pass, 5/21/76. . . .	47
13	Conical PVC pin run on rectangular block 5, 9.8N load, 1 Pass, 6/3/76.	48

<u>Figure Number</u>		<u>Page</u>
14	Conical PVC pin run on rectangular block 5, 9.8N load, 1 Pass, 6/3/76	49
15	Conical PVC pin run on rectangular block 7, 2.45N load, 1 Pass, 6/8/76	50
16	Conical PCTFE pin run on rectangular block 3, 14.7N load, 1 Pass, 5/19/76	52
17	Conical PCTFE pin run on rectangular block 3, 14.7N load, 1 Pass, 5/19/76	53
18	PVC pin with 250,000 μm^2 area run on rectangular block 6, 9.8N load, 1 Pass, 6/10/76	54
19	Plot of Φ as a Function of Load for Nylon 6-6, PCTFE, and PVC.	58
20	A typical stylus profile of a ground steel surface.	83
21	Force Diagram Showing Geometric Relationships Between Forces at Tool Point When No Built-Up Edge Exists [44].	85
22	Shearing Process on the shear plane [46].	87
23	Conical PCTFE pin loaded normal to a ground steel surface.	91
24	Original Deformation of Conical Polymer Pin.	92
25	Examples of full and partial penetration	93
26	Forces acting on a single steel asperity	95
27	S_s/p_m versus α for different values of k	98
28	Plot of ϕ versus k for various values of α	100

<u>Figure Number</u>		<u>Page</u>
29	Volume of material removed by a given asperity for PVC and PCTFE.	102
30	Upper portion of bearing area curve for disks 18, 19, 20, 31 and 33.	108
31	Wear versus penetration depth for disks 18, 19, 20, 31 and 33.	109
32	Additional forces that might be acting on the steel asperity and polymer chip. . .	114
A1	Illustration of energy peak with background for gamma radiation.	125
B1	Illustration of polymer shear angle as measured.	130

LIST OF TABLES

<u>Table Number</u>	<u>Page</u>
1. Various Linear High Polymers With Name Abbreviations, Repeat Units, Glass Transition Temperature (T_g) and Crystalline Melting Point (T_m) [2].	3
2. Mechanical Property Data for Polymers.	30
3. Wear Data for PVC and PCTFE Conical Polymer Pins Run on Steel Disks 11 and 12.	35
4. Wear Data for PVC and PCTFE Polymer Pins Having a 250,000 μm^2 Circular Area.	36
5. Shear Angle Measurements.	55
6. Two Way Analysis of Variance Table.	56
7. Shear Angle Means and One Way Analysis of Variance Table for 2.45 N Load.	59
8. Shear Angle Means and One Way Analysis of Variance Table for 9.80 N Load.	60
9. Shear Angle Means and One Way Analysis of Variance Table for 14.70 N Load.	61
10. Duncan's Test for Loads of 2.45, 9.8 and 14.7 N.	63
11. Shear Angle Means and One Way Analysis of Variance Table for PCTFE.	64
12. Shear Angle Means and One Way Analysis of Variance Table for Nylon 6-6.	65
13. Shear Angle Means and One Way Analysis of Variance Table for PVC.	66
14. Duncan's Test for PVC.	68
15. Surface Topography Data for Disk 11.	71

<u>Table Number</u>		<u>Page</u>
16.	Surface Topography Data for Disk 22.	72
17.	Surface Topography Data for Steel Disk 18. .	74
18.	Surface Topography Data for Steel Disk 19. .	75
19.	Surface Topography Data for Steel Disk 20. .	76
20.	Surface Topography Data for Steel Disk 31. .	77
21.	Surface Topography Data for Steel Disk 33. .	78
22.	Percent Area Required to Support a Given Normal Load for Different Polymers According to the Disk Worn On. .	79
23.	Surface Topography Data for Rectangular Block 5. .	81
24.	Summary of Wear and Bottom Inside Profile Data for Disks 18, 19, 20, 31, and 33. . .	107
25.	Average Slope Data for Disks 19, 20, 31 and 33. .	112

NOMENCLATURE

A _a	actual area of contact
A _c	chip area
A _i	cross sectional area of asperity i
A _r	real area of contact
A _s	shear area
AA	arithmetic average roughness
C	constant used in Block-Halliday criterion, arccot(k)
d	sliding distance
d _l	incremental distance
dV	incremental volume
D _x	horizontal spacing between two points on steel disk profile
E	Young's modulus
ER	energy to rupture
F	frictional force
F _c	horizontal cutting force
F' _f	force which opposes the tendency for the polymer to slide from C to B in metal cutting theory
F _N	normal force
F _S	shear force
F _v	vertical cutting force
H	hardness
I	plasticity index
k	probability per unit encounter of a wear particle being produced, slope of shear strength versus compressive stress curve

NOMENCLATURE (cont'd)

K	wear coefficient
L	correlation length
n	number of observations
n_b, n_c	number of replications used to determine \bar{x}_b and \bar{x}_c , respectively
n_2	degrees of freedom of root mean square error
N	normal force
p	number of means
p_m	flow pressure
P	pressure
r	radius
R	resultant force
R_a	arithmetic average roughness
RMS	root mean square roughness
R_p	shortest significant range
S	standard deviation
S_N	normal stress
S_o	shear strength of a material under zero compressive stress
S_s	shear stress
S_S	shear strength of a material
T_g	glass transition temperature
T_m	crystalline melting point
v	velocity
V	total wear

NOMENCLATURE (cont'd)

V	volume wear rate
W	load supported by a given asperity
W'	normal load acting on AB
W _t	total normal load
x	depth of penetration
\bar{X}_b, \bar{X}_c	ranked means
Y	yield strength
Y(I)	profile height at point I
Z _{p,n₂}	tabulated value of studentized range used in Duncan's Test
α	notched impact strength, rake angle, significance level
β	average radius of curvature
ΔA	area of a given asperity
ε	normal strain
γ _s	shear strain
μ	10 ⁻⁶ , also coefficient of friction
φ	shear angle
φ _{min}	minimum shear angle
φ _{max}	maximum shear angle
Φ	average shear angle
σ	standard deviation of asperity heights, stress
τ	coefficient of friction between cutting tool and chip

NOMENCLATURE (cont'd)

θ	asperity base angle, angle between normal load and resultant force acting on a steel asperity
θ_m	measured shear angle
θ_p	angle between electron beam and surface of ground steel block
ν	Poisson's ratio
w_i	probability of the completion of stage i of the wear process

1. INTRODUCTION

Polymers are known for their excellent combination of properties, rather than an extreme of any single property. For example, no polymer is as strong as steel, as light in solid form as most woods, as elastic as soft rubber, nor as scratch resistant or transparent as glass. Yet, polymers are the only materials which can be simultaneously strong, light, flexible and transparent [1]^{*}. Typical polymer properties include high mechanical strength and rigidity, fatigue endurance, high resistance to moisture, excellent dimensional stability, ease of fabrication, resistance to repeated impacts, good electrical insulating characteristics, natural lubricity, noise and weight reduction and others. For these reasons, the polymer industry has seen a phenomenal growth over the past thirty-five years.

Polymers are used in a wide variety of engineering applications where high stresses are encountered. Some examples include drawer sliders, bearings in heart valves, gears and artificial bone joints. Aside from the frictional behavior of a polymer, its wear resistance is most important in determining its acceptance in industry. Thus, it is important to be able to predict polymer wear, under many adverse conditions, and hence arrive at the life expectancy of a given component.

The polymers used and discussed in this research are classified as linear high polymers. According to Steijn [2], the outstanding characteristic of a linear high polymer is its high molecular weight

*Numbers in brackets refer to similarly numbered references listed in Reference section.

and the end-to-end linkage of repeat units. Table 1 lists various linear high polymers along with their name abbreviation, repeat units, glass transition temperature (T_g) and crystalline melting point (T_m).

The performance of polymers in dry sliding contact is very difficult to predict. The wear resistance of the polymer is determined not only by its material properties, but also by external conditions such as load, speed and the roughness of the surface against which relative sliding occurs. In the initial stages of the wear of a polymer against a harder counterface, polymer transfers to the counterface. If the counterface is smooth, some polymers such as polytetrafluoroethylene (PTFE) and high density polyethylene (HDPE) transfer as continuous thin films via the adhesion mechanism [3]. If the counterface is rough, most polymers will transfer in discrete lumps via the abrasion mechanism [4-6]. As sliding continues other mechanisms such as fatigue may dominate the transfer process [5-6]. In addition to transfer to the counterface some polymers wear by roll formation [6]. The initial transfer process is often complicated by back transfer in which two or more wear mechanisms can be equally important.

In order to obtain a quantitative measure of the initial stages of polymer wear, a method capable of detecting very small quantities of transferred material is required. Quantitative wear data for polymers have been obtained by gravimetric methods, linear measurement of wear tracks, and measurements of dimensional changes of test specimens. There are inherent uncertainties in all of these techniques which have been dealt with in a variety of ways by different researchers in an

Table 1. Various Linear High Polymers With Name

Abbreviations, Repeat Units, Glass Transition

Temperature (T_g) And Crystalline Melting Point (T_m) [2].

Polymer (Name Abbreviation)	Repeat Unit	T_g (°C)	T_m (°C)
Polyhexamethylene adipamide (Nylon 66)	$\begin{array}{c} \text{H} & \text{O} \\ & \\ -\text{N}-\text{(CH}_2\text{)}_6-\text{N}-\text{C}-\text{(CH}_2\text{)}_4-\text{C}- \\ & \\ \text{H} & \text{O} \end{array}$	50	265
Polypropylene (PP)	$\begin{array}{c} \text{H} & \text{CH}_3 \\ & \\ -\text{C}-\text{C}- \\ & \\ \text{H} & \text{H} \end{array}$	-10, -18	176
Polyethylene (PE)	$\begin{array}{c} \text{H} & \text{H} \\ & \\ -\text{C}-\text{C}- \\ & \\ \text{H} & \text{H} \end{array}$	-120	137
Polytetrafluoroethylene (PTFE)	$\begin{array}{c} \text{F} & \text{F} \\ & \\ -\text{C}-\text{C}- \\ & \\ \text{F} & \text{F} \end{array}$	-50, 126	327
Polychlorotrifluoroethylene (PCTFE)	$\begin{array}{c} \text{Cl} & \text{F} \\ & \\ -\text{C}-\text{C}- \\ & \\ \text{F} & \text{F} \end{array}$	45	220
Polyvinylchloride (PVC)	$\begin{array}{c} \text{H} & \text{Cl} \\ & \\ -\text{C}-\text{C}- \\ & \\ \text{H} & \text{H} \end{array}$	87	212
Polystyrene (PS)	$\begin{array}{c} \text{H} & \text{C}_6\text{H}_5 \\ & \\ -\text{C}-\text{C}- \\ & \\ \text{H} & \text{H} \end{array}$	100, 105	240

Table 1. Various Linear High Polymers With Name

Abbreviations, Repeat Units, Glass Transition

Temperature (T_g) and Crystalline Melting Point (T_m) [2].

(Continued)

Polymer (Name Abbreviation)	Repeat Unit	T_g (°C)	T_m (°C)
Polyhexamethylene sebacamide (Nylon 6.10)	$\begin{array}{c} \text{H} \quad \text{O} \\ \quad \\ -\text{N}-\text{(CH}_2\text{)}_6-\text{N}-\text{C}-\text{(CH}_2\text{)}_8-\text{C}- \end{array}$	40	227
Polymethylmetha- crylate (PMM)	$\begin{array}{c} \text{H} \quad \text{CH}_3 \\ \quad \\ -\text{C}-\text{C}- \\ \quad \\ \text{H} \quad \text{COOCH}_3 \end{array}$	105	160
Polyisobutylene	$\begin{array}{c} \text{H} \quad \text{CH}_3 \\ \quad \\ -\text{C}-\text{C}- \\ \quad \\ \text{C} \quad \text{CH}_3 \end{array}$	-70,-60	128
Polyoxymethylene (POM)	$\begin{array}{c} \text{H} \\ \\ -\text{C}-\text{O}- \end{array}$	-50,-80	181
Polycaprolactam (Nylon 6)	$\begin{array}{c} \text{H} \quad \text{O} \\ \quad \\ -\text{N}-\text{(CH}_2\text{)}_5-\text{C}- \end{array}$	50	225
Polyisoprene	$\begin{array}{c} \text{H} \quad \text{H} \\ \quad \\ -\text{C}-\text{C}=\text{C}-\text{C}- \\ \quad \quad \quad \\ \text{C} \quad \text{CH}_3 \quad \text{H} \quad \text{H} \end{array}$	-73	28

effort to obtain accurate and repeatable wear data [7-13].

Radioactive tracer techniques which have been used extensively for metallic wear studies [14], have the capability of sensitivities on the order of 10^{-9} grams [15, p. 121]. These techniques have previously seen no application in polymer wear studies for some important reasons. Most engineering polymers are composed primarily of carbon, nitrogen, hydrogen, and oxygen. If isotopes of these elements are to be used as radioactive tracers in polymers, the isotopes must either be synthesized in the polymers or activated in the polymers by means of exposure to intense neutron flux. The former method requires producing polymers in special small batches in a facility licensed to handle the radioactive materials. The latter method is unsatisfactory because all four elements have relatively low atomic activation cross sections for thermal neutron capture. Therefore, they require long exposures to the neutron flux to obtain radiation intensities high enough to be detected. Sufficient irradiation causes cross linking or degradation of the polymer which can result in changes in the bulk material properties. These changes would be unacceptable for fundamental friction and wear research. In addition, the half lives of O^{19} and N^{16} are too short to be useful in wear studies.

However, some polymers such as PCTFE and PVC contain chlorine which can be activated to Cl^{38} which has a 37.2 min half life. The 37.2 min half life is long enough to run wear tests up to two hours duration and still have sufficient activity remaining that is many times the background radiation. This half life is also short enough

so that a 24 hr storage time is sufficient to permit the activity to decay to a non-hazardous level. The radiotracer technique has been demonstrated [16] to have a sensitivity of less than one microgram of transferred PCTFE and has the potential for use with doped and filled polymers.

When studying metal-metal wear phenomena, the initial surface finish is usually of little interest because the wear process is continually modifying the surface. However, when a polymer slides on a metal surface, the metal suffers relatively little change as the polymer is worn away and transfers to the metal. The metal finish is therefore one of the most important factors in the amount of polymer wear that occurs during the relative motion of the two materials.

The geometric description of a metal surface consists of the representation of the surface by one or more parameters. The fewer the parameters chosen to represent the surface, the greater is the loss of information about the surface. In most industrialized countries of the world, one or more surface roughness parameters have been designated as national standards. One such parameter, the arithmetic average roughness AA, a standard common to most industrialized countries is the only standard for geometric surface description in the USA.

Several events have occurred in recent years which have caused many engineers, scientists, and industries in USA to question the use of only one surface roughness parameter and one method, the stylus instrument, for measuring this parameter. The need for instruments with higher resolution than is possible with stylus instruments has

been recognized in the technology of electrodeposition [17,18] which demands high quality surface finish requirements. The availability of digital computers has encouraged engineers to develop programs to calculate several different surface parameters from digitalized profile data [18,19]. Engineers who had several parameters available then related the functions of surfaces to the parameters using mathematical models of the surface function [5,11,20] or by a linear discriminant analysis [21].

In parallel with the above events, the American National Standards Institute ANSI, Committee B46.1 Surface Texture is revising the standard. While the revised standard is still primarily concerned with the measurement of the arithmetic average roughness (now to be designated as R_a to conform with the designation of the other industrialized countries) by stylus instruments, an extensive appendix describing non-contacting surface characterization instruments and several other surface parameters is included. Reference 22 describes surface characterization parameters, some of which are included in Appendix C of B46.1, and discusses the current availability of instruments and services which can measure these parameters.

The purpose of this research is to determine the mechanical properties of polymers and the surface characterization parameters of ground steel surfaces that are important in influencing the wear of polymers. A major input to this research is observations of the wear process made in the scanning electron microscope both before, during and after wear experiments. Orthogonal cutting theory is modified to model the wear process. Correlations of experimental wear data with surface characterization data and model predictions are made.

2. LITERATURE SEARCH

2.1 Polymer Wear Theories

The four major types of wear most likely to occur in polymer-steel sliding are similar to the ones for metal-metal sliding [2]. These types are: (a) adhesive or sliding wear, (b) thermal and oxidative wear, (c) abrasive wear and (d) surface fatigue, corrosion, and cavitation. Although all of these types of wear are usually present, some are more predominant than others. Thermal wear, being the degradation of the polymer by frictional heating is usually associated with adhesive wear. In thermoplastics, thermal wear is indicated by excessive softening and in the thermosetting plastics it is indicated by charring of the polymer. The metallurgist, accustomed to the temperature and heat resistance of metals, regards thermal wear as the obvious limitation of a plastic bearing.

The ability of a material to deform and recover elastically or to deform plastically without breaking, determines whether or not abrasive wear will take place. Adhesive or sliding wear occurs when, due to the attractive forces between the molecules of the mating surfaces, small fragments are torn from the surfaces. Adhesive wear is generally the irreducible minimum of wear in plastics. In fatigue wear, a particle is detached after a sequence of repeated contacts occur over the same localized area. These repeated contacts usually involve cycles of compression and recovery, complicated by tensile stresses over the contact region arising from adhesion and tangential movements [4].

Archard and Hirst [23] ran wear experiments with polymer sliding on ground metal surfaces for PMM, PTFE, PE and several thermosets on a pin-ring machine in which the apparent area of contact was not a constant. However, they found the wear was linear with time and hence the wear rate was constant and independent of the apparent area of contact. They also found the wear rate was proportional to the load and expressed the wear as

$$V = kdW/p_m \quad (1)$$

where V is the total wear, d is the sliding distance, W is the load, p_m the flow pressure and k a constant called the wear coefficient. In this model it is assumed that the probability per unit encounter of a wear particle being produced is k . The actual area of contact (A_a) equals W/p_m [24], where p_m is constant for plastic deformation and equal to three times the yield strength (Y) of the softer material. Computed values of k were 2.5×10^{-5} for PTFE, 7×10^{-6} for PMM, 1.3×10^{-7} for PE, and from 0.3 to 7.5×10^{-6} for the thermosets tested. Steijn [2] states that the application of this simple wear model to complex industrial situations has not progressed very far, since the wear is proportional to the load only over a very limited range of load and sliding speed. Beyond this range the rapidly rising surface temperature invalidates the application of simple wear laws.

Rabinowicz [15, p. 168] derives a quantitative expression for abrasive wear in which a hard conical asperity is penetrating a softer material as shown in Fig. 1. A single asperity carrying a load W will penetrate a softer surface such that

$$W = p_m \cdot A_r = p_m \cdot \pi r^2 \quad (2)$$

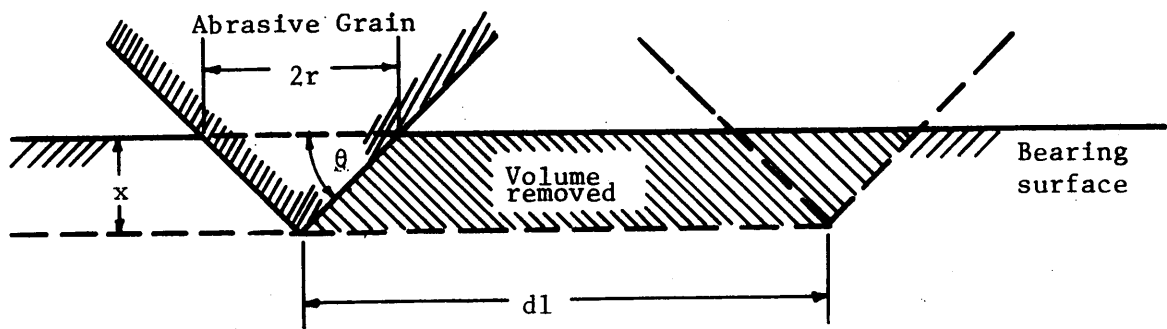


Figure 1. Abrasive Wear Model in which a cone removes material from a surface from Rabinowicz [15, p. 168].

where p_m is the flow pressure which equals the hardness of the softer surface.

The projected area of the cone in the vertical plane is πr^2 . Therefore, when the cone moves a distance dl , it will sweep out the volume dV equal to

$$dV = r \cdot \pi r^2 \cdot dl = \frac{r^2 \tan \theta \cdot dl}{\pi p_m} = \frac{W \cdot \tan \theta \cdot dl}{\pi p_m} \quad (3)$$

$$\frac{dV}{dl} = \frac{W \cdot \tan \theta}{\pi p_m} \quad (4)$$

Then if one adds the contributions of all the asperities

$$\frac{dV}{dl} = \frac{W_t \cdot \tan \bar{\theta}}{\pi p_m} \quad (5)$$

where $\tan \bar{\theta}$ is the average of the $\tan \theta$ values of all the individual cones and W_t is the total normal load.

Lancaster [5] discusses this model and states that Eq. 5 leads to

$$V = \frac{kWd}{p_m} \tan \bar{\theta} \quad (6)$$

where d is the total distance slid and k is a constant that expresses the fact that all the material involved in the deformation process is not removed as debris, some is simply deformed plastically.

Lancaster [4] shows that the volume of wear is proportional to the $\tan \bar{\theta}$ for soft metals but not for polymers. His results for an experiment where a hard conical indentor penetrates and ploughs a groove in a softer material are shown in Fig. 2. For tin the expected relationship (i.e., volume displaced is proportional to $\tan \bar{\theta}$) is true for all

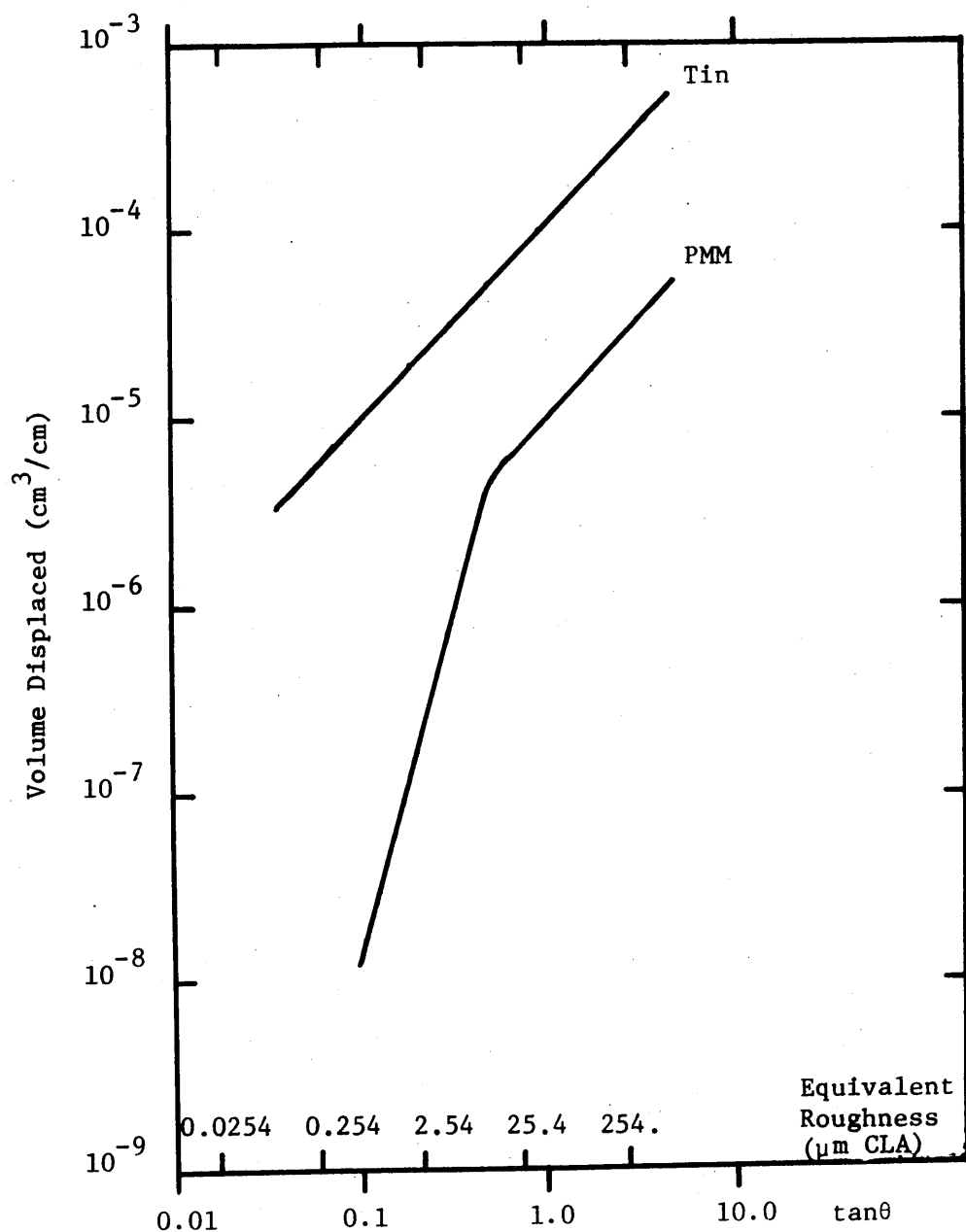


Figure 2. Relationship of volume displaced per unit sliding distance to base angle of the conical indenter from Lancaster [4].

angles of the cone but only holds for the polymer when the base angle θ , is very large. Lancaster states that since the elastic moduli of polymers are considerably lower than those of metals, it is reasonable to conclude that with polymers, plastic deformation only becomes the predominant mode of deformation when the indentor is very sharp. Elastic deformation is therefore going to play a much more important part in the abrasive wear processes of polymers than is the case for metals [4].

Lancaster concludes that during sliding against roughnesses commonly encountered in engineering practice, the deformation of polymers is partly elastic and partly plastic and the relative proportions will vary with the roughness. Two criteria are available to determine the point on the roughness scale at which plastic deformation begins. The Blok - Halliday criterion [25] states that the limiting slope of an asperity which can just be flattened by a rigid plane into the general plane of a surface is

$$\tan \theta_{\lim} = C \frac{H}{E} (1-\nu^2) \quad (7)$$

where H is the hardness of the material, E is Young's modulus and ν is Poisson's ratio. For the onset of plastic flow, $C=0.8$ and for full plasticity $C=2.0$. It is assumed that this criterion is equally applicable to the inverse case of a hard asperity penetrating a softer solid material. The second criterion, the "plasticity index" (I), introduced by Greenwood and Williamson [26], is

$$I = \frac{E}{H} \left(\frac{\sigma^{1/2}}{\beta} \right)^2 \quad (8)$$

where σ is the standard deviation of the asperity heights and β is

their average radius of curvature. Values of $(\sigma/\beta)^{1/2}$ for various surfaces can be obtained from computer analyses of profiles.

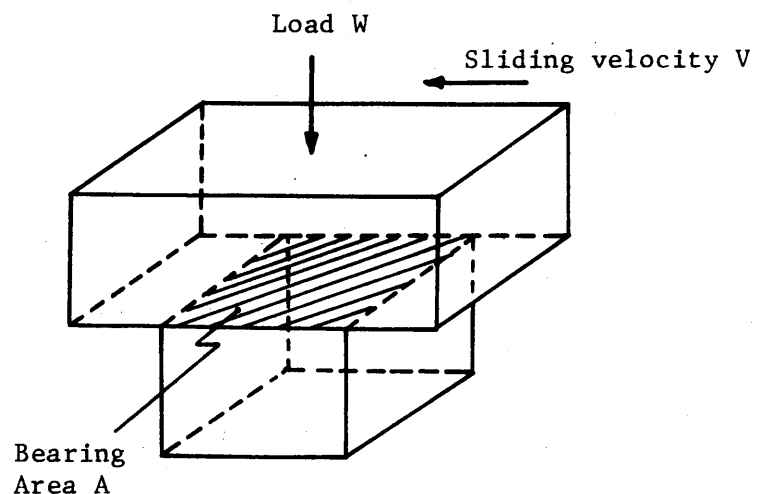
Lewis [27] states that the two most important criteria in the design of unlubricated plastic bearings, piston rings, and seals are Pv-limits and wear. Pv is the product of pressure (P) in N/m² and velocity (v) in m/sec. The Pv-limit of a given plastic in a given environment tells the designer the maximum values of pressure and velocity that the plastic will withstand in order to have sufficiently low wear or long life. According to Lewis, the wear rate of a plastic sliding against a steel surface is predictable if:

- "1.) The temperature rise due to frictional heating added to the ambient temperature, results in a surface temperature below the critical value associated with the plastic's Pv-limit.
- 2.) The mating surface is defined in terms of material, hardness and roughness.
- 3.) The environment is defined and free of contaminants."

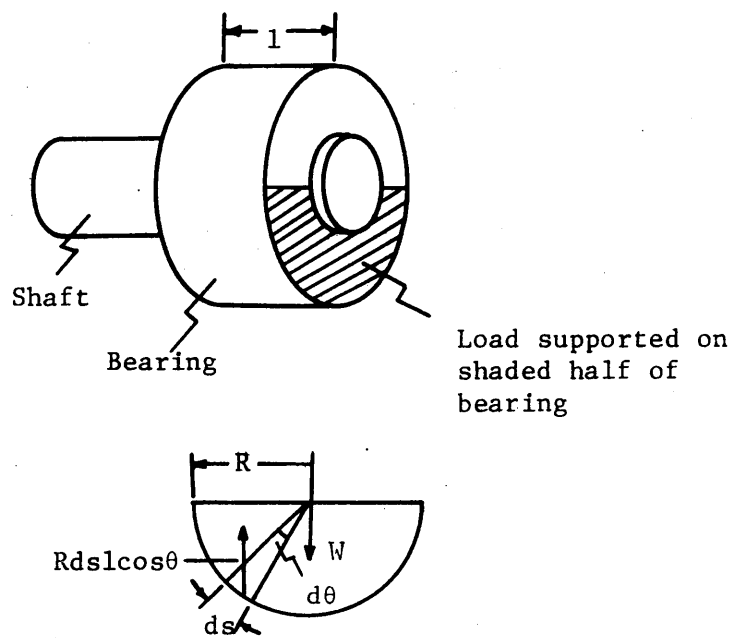
The Pv-factor, according to Halling [28] is based on the assumption that the wear rate is proportional to the rate of energy dissipation at the sliding interface. For a flat bearing surface of area A, as shown in Fig. 3a, the amount of energy dissipated on sliding a distance dx is given by $\mu W dx$, where μ is the coefficient of sliding friction and W is the normal load. The rate of energy dissipation is given by

$$\mu W \frac{dx}{dt} = \mu W v \quad (9)$$

where $v = \frac{dx}{dt}$ = sliding speed at the interface. If one assumes that



a) Flat bearing



b) Journal bearing

Figure 3. Schematic diagrams for derivation of Pv-factor from Halling [28].

the volume wear rate \dot{V} is proportional to the rate of dissipation then for constant μ

$$\dot{V} \propto Wv. \quad (10)$$

One is normally interested in the depth of wear or the rate of linear wear normal to the surface. This is simply \dot{V}/A and, therefore, the rate of linear wear is proportional to Wv/A which is equal to Pv . This same type equation is derived for a sleeve bearing as shown in Fig. 3b and the radial wear rate is again found to be proportional to μPv where P is the load per unit projected area.

For a certain life expectancy, it is possible to specify a certain Pv -factor which must not be exceeded. Criticism arises for the use of such a single factor because it assumes the same sensitivity of wear for changes of P and v . This is usually not the case and a more acceptable way is to give plots of wear rates on pressure velocity diagrams as shown in Fig. 4. The Pv -limit is that Pv factor at which the bearing fails rapidly due to melting or thermal decomposition. Halling also states that the steady state wear rate \dot{V} for a plastic bearing is proportional to the Pv -factor over much of the usable Pv -range. Hence, a wear coefficient K is defined where

$$\dot{V} = KPv. \quad (11)$$

It can be seen that if K can be calculated for one Pv -value then other Pv factors can be determined.

It should be noted that the Pv -limit of a plastic varies inversely with ambient temperature. This inverse relation is so because the Pv -limit is caused by the surface temperature of the plastic reaching or

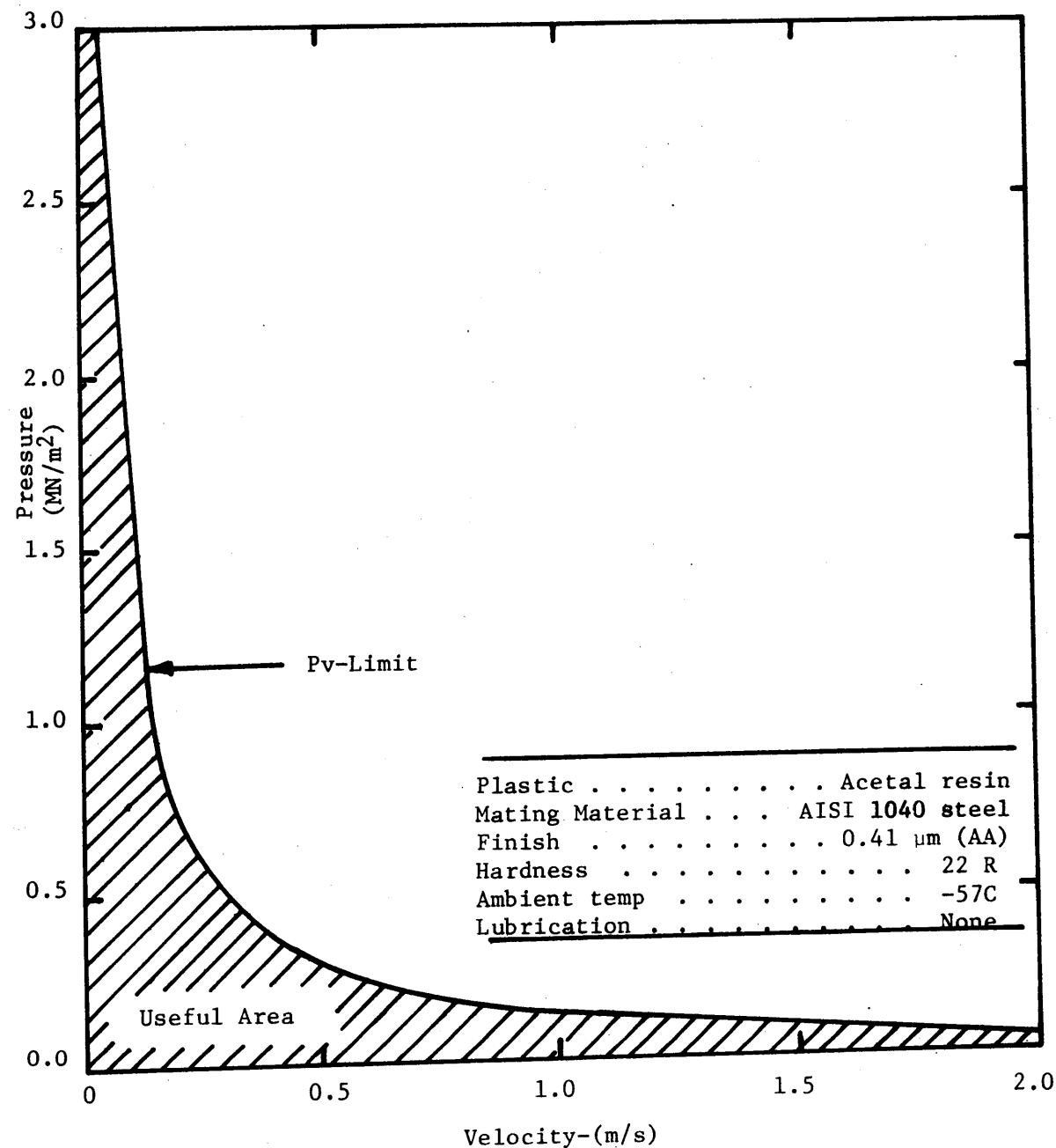


Figure 4. Example of a typical Pv-diagram from Lewis [27].

exceeding a critical value. Hence, the quantity of energy that can be added to the plastic without exceeding the critical temperature is inversely related to the ambient temperature of the plastic. Because heat transfer from the sliding interface limits the interface temperature, plastics with high thermal conductivities will have high Pv-limits.

In reference 29, wear is defined as the breakdown of a material on a friction surface. If wear is regarded as only a mechanical process, it is necessary to take into account not only the properties of the body subjected to wear but the wearing agent and its properties. Also, the thermal and mechanical properties of the surface layer are different from those of the rest of the wearing body. Further difficulty arises when predicting the wear of plastics because they cover a wide range of properties, rigid or soft, brittle or elastic, amorphous or crystalline.

Ratner, et al. [29] review the process of wear in stages and relate it to frictional and elastic strength characteristics as follows:

- "1.) First the two bodies approach each other; the establishment of contact is opposed by the hardness (H) of the polymer.
- 2.) One body slides over the other as a result of the traction force μ .
- 3.) Finally breakdown of the polymer occurs, the work of deformation, approximately equal to the product (or rather the integral) of strength σ and breaking elongation ϵ ."

Since these three processes occur in sequence, the wear V can be regarded as proportional to the probability ω_1 of the completion

of each stage, so that

$$V \sim w_1 w_2 w_3 \sim \frac{1}{H} \cdot \mu p \cdot \frac{1}{\sigma \epsilon} . \quad (12)$$

Hence, omitting the effect of pressure because of a concern only with the properties of the materials, Ratner obtains

$$V \sim \frac{\mu}{H \sigma \epsilon} \quad (13)$$

where V is the decrease in volume or dimensions of the body per unit distance traveled.

In reference 29, the relation of the breaking elongation ϵ to abrasive wear is noted. Wear occurs as a result of separation of particles which happens only when the elongation brought about by the abradant exceeds the breaking elongation of the material. In connection with the resistance to wear of a material, ϵ is related to hardness and strength as follows. If a body is rough, the amount of penetration of the abradant into the body is significantly affected by differences in hardness. Then for a smooth surface, the effect of hardness on penetration is much less. Two mechanical indices such as stress σ and hardness H are usually not enough to predict the complex wear phenomenon in plastics since the limiting deformability or breaking elongation varies considerably as illustrated in Figure 5.

Figure 6 shows the correlation between the wear resistance of various materials with the combination of mechanical properties shown in Eq. 13. For wear on an abrasive such as emery cloth, $\sigma \epsilon$ is replaced by the notched impact strength α , which is the work of

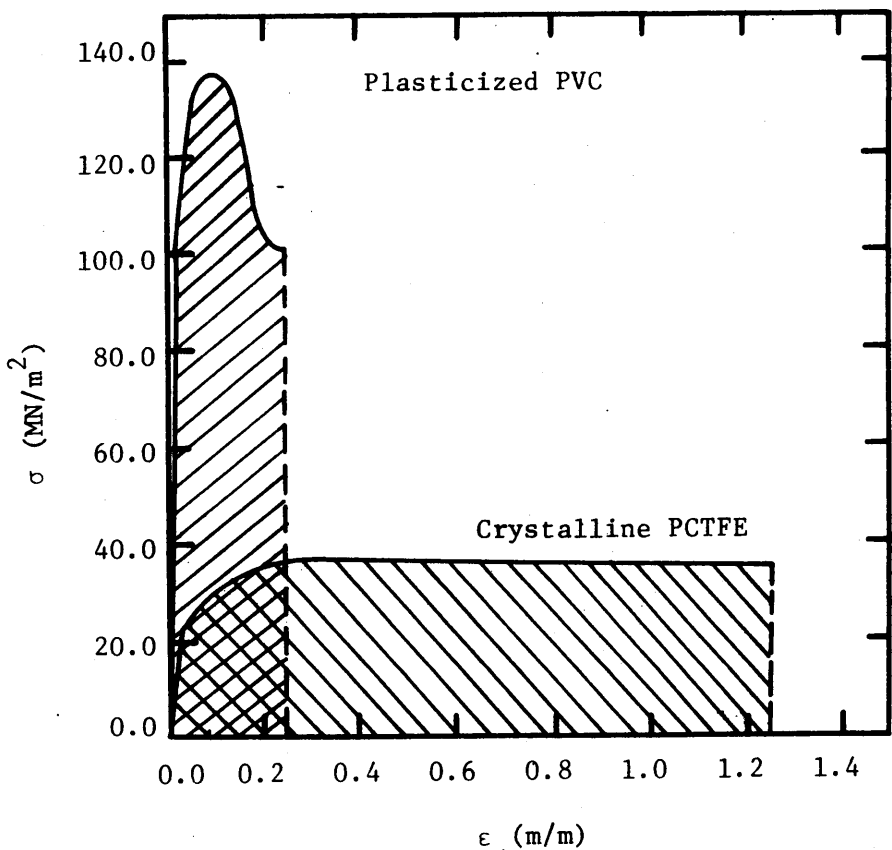


Figure 5. Approximate σ - ϵ curves for PVC and PCTFE.*

* Data for these curves taken from Table 2.

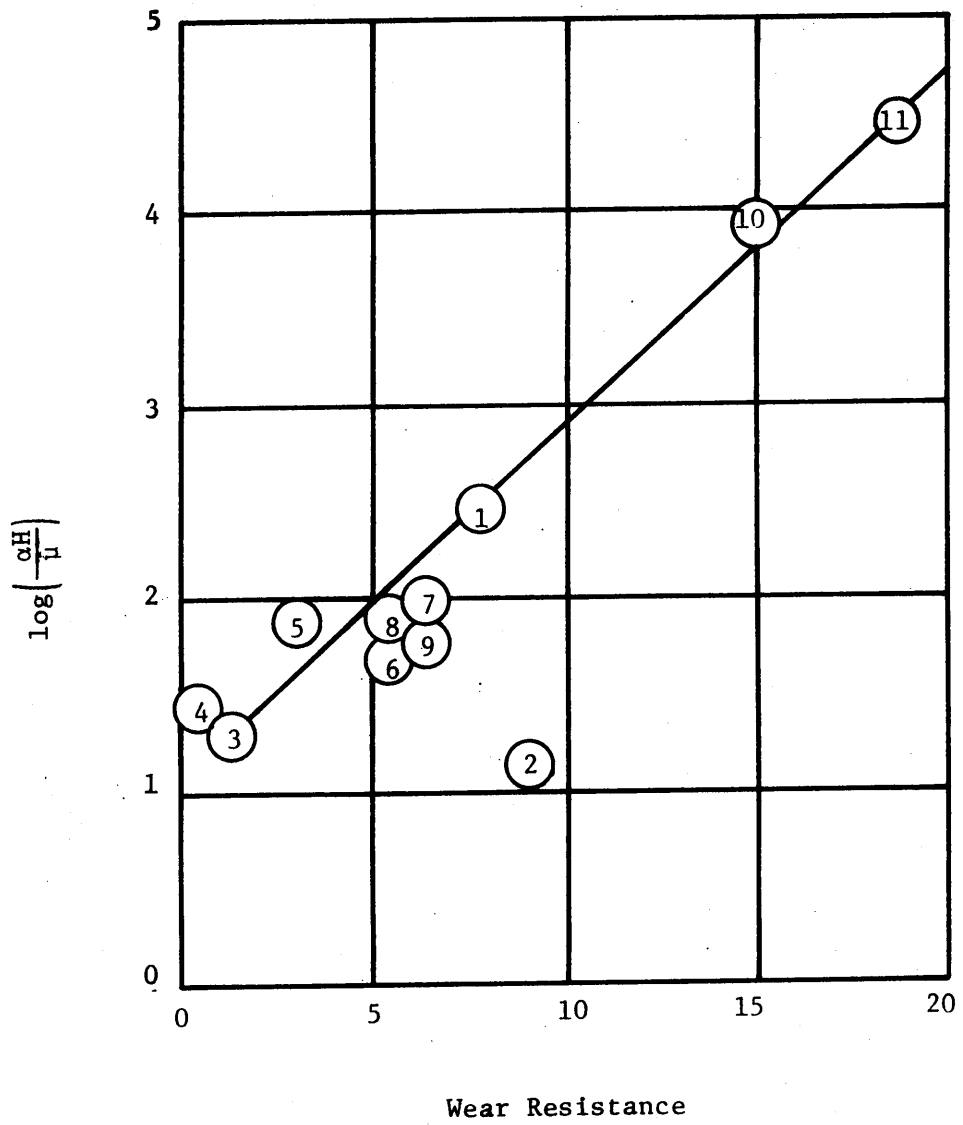


Figure 6. Dependence of wear resistance on other mechanical characteristics of plastics for wear on abrasive such as emery cloth from Ratner et al. [29].

1--PTFE; 2--PCTFE; 3--Polyamide-68; 4--Nylon-6;
5--1.p. polyethylene; 6--Rigid PVC; 7--FKP-1;
8--K-101-201; 9--K-17-81; 10--AG-4V; 11--AG-4S.

breakdown [29].

Pepper [30] studied the wear and transfer characteristics of PTFE, PVC and PCTFE sliding on clean metal in ultrahigh vacuum using Auger electron spectroscopy. From his results, he found the PTFE formed a continuous polymer film 2-4 atomic layers thick on the metal surface and the multiple traversals did not result in film buildup. However, when PVC and PCTFE slid on clean metal in ultrahigh vacuum, a polymer film was not developed on the surface. Instead a chemisorbed film of the polymer constituents appeared on the metal. Small fragments of metal were found embedded in the polymer specimens after sliding. Thus some shear is taking place in the metal and the situation is not simply one of interfacial polymer shear. An explanation of the lack of an adherent polymer film for the PVC and PCTFE was drawn from the results of Pooley and Tabor [31] who investigated PTFE, PVC and PCTFE sliding on glass in air. Their observations were the same as Pepper and explained in terms of the molecular profile of the polymer and the interfacial shear strength. Molecules with a very smooth molecular profile such as PTFE allow easy slippage of chains past one another. If the interfacial shear strength is great enough to anchor the chains, sliding draws the chains from the bulk of the polymer and a transfer film is established on the counterpart. Evidently, there is sufficient interfacial shear strength to anchor the PTFE chains on both metal in vacuum and glass in air. Interruption of the smoothness of the profile by the large chlorine atom (PVC and PCTFE) prohibits easy drawing of the

chains past one another. Evidently there is insufficient interfacial shear strength for both PVC and PCTFE on glass or metal to permit drawing of the polymer chains so that no transfer film is developed. The agreement in the experimental results implies that the general pattern of interfacial shear strength is maintained in going from sliding on glass in air to sliding on atomically clean metal in vacuum. Pepper thus feels that the mechanical interaction of polymers with solids are generally independent of the chemical constitution of the counterface.

2.2. Surface Characterization Parameters

In both industry and the laboratory a major concern is to be able to characterize surface finishes. This ability is needed in order to reproduce a given surface finish or for a way to simply describe a surface. Quantitative measures of the fine irregularities which are present on surfaces are called surface characterization parameters. An investigation of the literature shows two rapid historical increases in the number of parameters used. The first big increase was in 1929 with the development of the stylus instrument. By providing a profile of the surface, the stylus instrument made a big step in describing a surface finish. However, it was the availability of computers, especially minicomputers, that made the second big increase in the number of parameters and revolutionized the characterization of surfaces [18].

Many types of instruments and techniques are available for measuring surface roughness. Generally, these are divided into two major categories: the noncontacting methods and the contacting methods. The noncontacting methods category includes the following instruments and methods: optical section microscopy, optical scanning, optical reflectance measurement, double beam interferometry, multiple beam interferometry, differential interference contrast, the transmission electron microscope, the topografiner, the scanning electron microscope, and others. Several comparisons of these measuring systems are available in the literature [18,32,33,34] and will not be discussed in detail here. Under the contacting methods category, stylus instruments are generally the most used. Since the surface parameters used in this

research are calculated from profiles measured by a stylus instrument, this device is discussed.

Being known by such trade names as "Tallystep," "Micro-Topographs," "Talysurf," "Dektak," "Surfanalyzer," and "Proficorder," the stylus instrument employs a 1-15 μm diameter stylus. The stylus is mechanically traversed across the irregularities of a surface with a force of 5-250 mg. Vertical displacements of the stylus activate an electromechanical transducer, similar to a phonograph pickup, and the electrical output is amplified and either recorded on a strip chart, displayed on a meter, or stored in a computer memory. This type of instrument reveals considerable details for a large number of surfaces encountered in engineering applications but has the distinct characteristic of distorting the surface due to the high stress encountered at the stylus tip. Examples of surfaces requiring resolutions greater than those attained with a stylus instrument are given in reference 35.

The next question that often arises is how the stylus profile relates to the real surface being characterized. In the case of ground surfaces, two dimensional profiles taken both parallel and perpendicular to the grind can give a good representation of the surface being considered. However, for surfaces which have been bead blasted, for example, and have no distinct lay, it is necessary to take several successive parallel profiles and obtain a three dimensional characterization by putting successive profiles together. Due to the distortion of the surface caused by the stylus in a single traversal, the resulting deformation may affect the accuracy of succeeding traversals

and hence suggest a possible disadvantage of the stylus instrument. The scanning electron microscope, however, appears to have a large potential for three dimensional mapping of surfaces, due to the fact that it is non-contacting and its output is readily adaptable to computerization [36,37].

3. EXPERIMENTS

3.1 Wear Data

3.1.1 Apparatus

A pin-on-disk machine, shown in Fig. 7, was used to provide the relative motion between the polymer pin, A, and the steel disk, B. The polymer pin, A, was mounted in arm C, which pivoted vertically at D and horizontally at E. Horizontal motion of the beam was restrained by a cantilever beam, F, on which strain gauges, G, were mounted. The output of the strain gauges was plotted on an X-Y recorder and calibrated to read friction force. The normal load was applied by dead weight, H. The disk rotation was controlled by a variable speed transmission and the power was supplied by a 1/2 HP synchronous motor. The radius of the path of the pin on the disk was controlled by moving the pivot support, I, in the directions indicated.

The transfer of the polymer to the disk was measured by Neutron Activation Analysis (NAA), a technique which is described in reference 16. In these experiments, PCTFE and PVC were used because they contain chlorine which is suitable for NAA. However, the analysis of the amount of polymer transferred was performed differently from that described in reference 16. Instead of measuring the activity of the Cl³⁸ isotope through a window which spanned the two major energy peaks of gamma radiation, the activity of each peak was measured. The mass transferred was then calculated to be the average of the mass predicted by each energy peak.

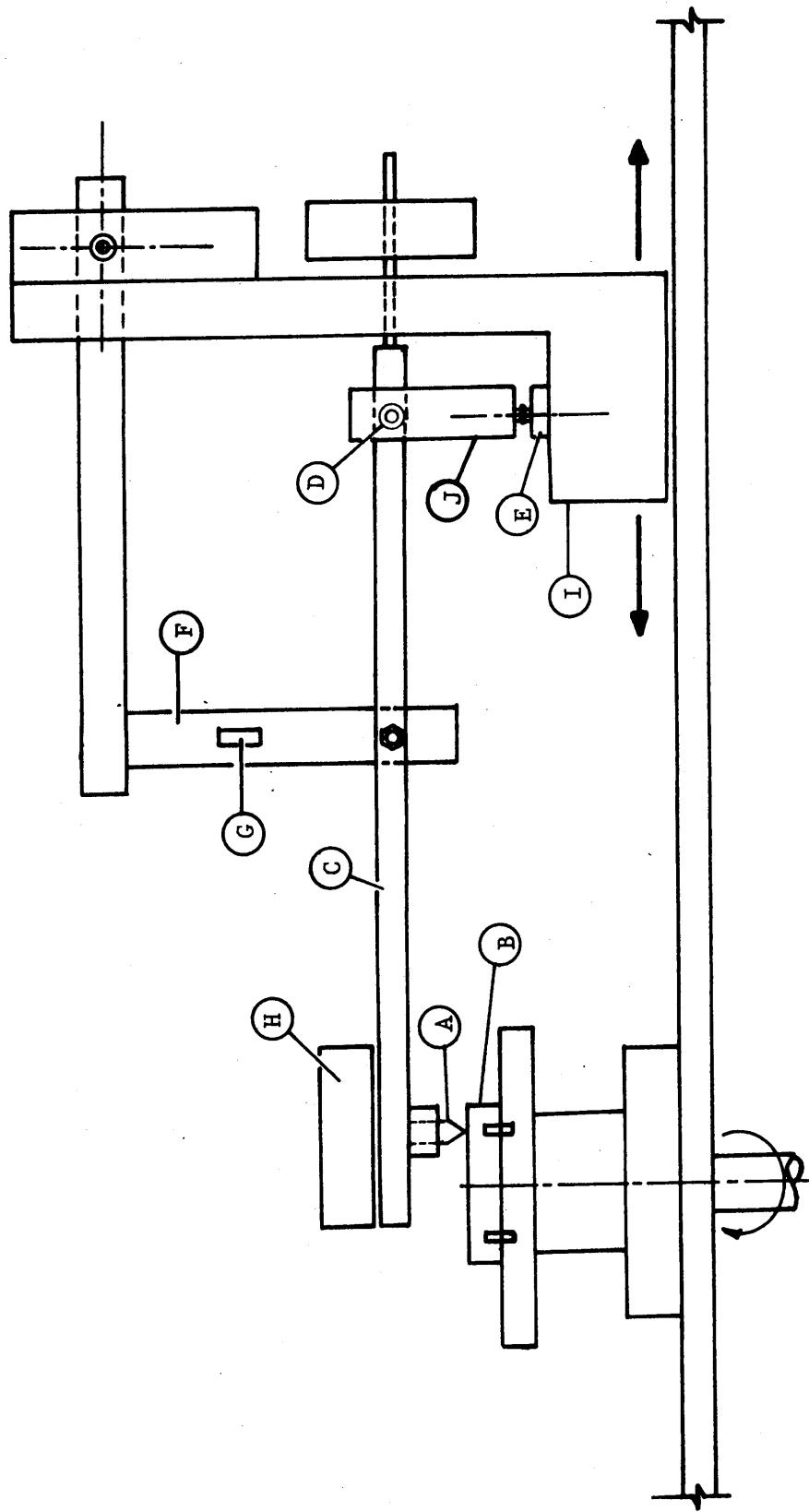


Figure 7. Pin-on-disk machine.

3.1.2. Experimental Materials

The PCTFE pins were prepared from 3.18 mm dia extruded rods. Two degrees of crystallinity were obtained by a procedure obtained from the manufacturer of the polymer [38]. The PCTFE rod was inserted in a quartz tube with a 3.18 mm inside dia, placed in a furnace, and heated to 218 C. Following a half hour at that temperature, one set of samples was removed from the furnace and quenched in water. These samples had a lower degree of crystallinity and were designated as amorphous. A second set of samples remained in the furnace while it cooled down to 100 C over a one hour period. These samples had a higher degree of crystallinity. The amorphous rods were not used for the results given in this dissertation; however, the effect of the degree of crystallinity of PCTFE on its transfer to steel surfaces has been investigated and is given in reference 39.

The plasticized PVC pins were prepared from 6.3 mm dia rods as obtained from the manufacturer. Material properties of the PVC were obtained from the stress-strain curves run by the author according to ASTM Standard D638 [40]. PCTFE properties were obtained from the manufacturer. These material properties are shown in Table 2. Both the PCTFE and PVC rods were cut to a length of 7.9 mm and turned to a conical shape with a 20° half angle on a lathe, washed in pentane, air dried and sealed in polyethylene vials. Pins were also produced with a 250,000 μm^2 circular area, by machining the point off the conical pin. This geometry causes less penetration of the polymer into the steel surface due to the increase in apparent area.

Table 2. Mechanical Property Data for Polymers.

	PCTFE ¹ 25 C 1.6 Caliper mm	PVC ² 25 C 5mm/min cross- head speed	Nylon 6-6 ³ Dry ⁴ Conditioned ⁵
Tensile Strength (MN/m ²)	35.85	102.38	86.9 59.3
Elongation to break (m/m)	1.25	0.263	0.90 2.40
Yield Point (MN/m ²)	36.54	136.86	- -
Yield Strength (0.2% Offset, MN/m ²)	23.10	103.42	86.9 59.3
Modulus of Elasticity (tension, GN/m ²)	1.31	3.94	- -
Energy to Rupture (tension, MNm/m ³)	41.82 ⁶	24.82 ⁷	78.2 ⁸ 142.3 ⁸

- 1) Reference 38.
- 2) Average value from 4 stress - strain curves
- 3) Reference 41.
- 4) Dry as molded.
- 5) Conditioned to 50% R.H.
- 6) Estimated from stress-strain curve reconstructed from above data.
- 7) Area under stress-strain curve.
- 8) Tensile strength times elongation to break.

The steel disks were machined from a 3.81 cm dia, 1018 cold rolled steel bar. One surface of the 6.3 mm thick disk was ground on a lathe such that the lay in the vicinity of the wear tracks was perpendicular to the sliding direction. The influence of the direction of the lay with respect to the sliding velocity vector on polymer transfer is also given in reference 39. After grinding, the disks were coated with oil to retard rusting. Just prior to testing, the disks were repeatedly flooded with methanol and wiped with a paper wiper. A final coating of methanol was allowed to evaporate from the disk prior to the start of a wear experiment.

3.1.3. Experimental Procedure

All experiments were run in laboratory air at an average temperature of 24 C and relative humidity of 60%. The PCTFE pins were irradiated in the reactor for 10 minutes while the PVC pins were irradiated for only 6 minutes. The 10 minute PCTFE irradiation time was determined as the best time that would increase wear measurement sensitivity, minimize radiation damage to the polymer and keep the radioactivity within the reactor room safety requirements [16]. Knowing the 10 minute irradiation time for PCTFE, 6 minutes for PVC was chosen because PCTFE contains approximately 60 percent as much Cl by weight per repeat unit as PVC. The 6 minute irradiation time thus resulted in approximately the same sensitivity for the PVC wear measurements as for the PCTFE measurements.

Wear measurements were obtained for both PVC and PCTFE on the same steel disk, with the same normal load and pin geometry so that differences in the wear due to only the polymer properties were obtained. One wear track consisted of five revolutions of the disk with the pivot support, I, being moved outward at the same time, thus creating a spiral track. A sliding speed of 0.935 cm/sec at the average radius of the spiral track was used. The spiral track allowed enough polymer to be deposited in order to obtain sensitive wear measurements, while still having only a single polymer pass at any point on the steel disk. A discussion of the amount of polymer required in order to reduce the error bars on the wear data is given in Appendix A.

After the irradiated polymer pin was worn on the steel disk, the

amount of activity of Cl³⁸ at energy peaks of 1642 and 2168 Kev was determined over a 30 minute counting interval. After counting, the deposited polymer was allowed to decay and then the other polymer five pass spiral track was run at another average radius. For disks where PVC was the first polymer deposited, the disks were washed in chloroform to remove the polymer and then PCTFE was run at the same radius. If, however, PCTFE was the first polymer deposited on the track, the PVC polymer track was run at another average radius because PCTFE is insoluble and cannot be removed from the surface. The wear data obtained was then normalized by dividing the mass transferred by the distance travelled.

3.1.4. Wear Data Results

Table 3 shows the results of PVC and PCTFE conical polymer pins run on steel disks 11 and 22 which were of different roughnesses. All the experiments were run at 1.96 N normal load with PVC and PCTFE each run on the same disk. As shown in Table 3, on disk 11 PVC has approximately 1.3 times more wear than PCTFE and on disk 22, PVC has approximately 2.6 times more wear than PCTFE. It is, therefore, evident that the PVC conical pins wore more than the PCTFE conical pins under the same loading and surface conditions.

Table 4 shows the results of PVC and PCTFE polymer pins having a $250,000 \mu\text{m}^2$ area run against five disks under two different loads. Disk 18 had a PVC polymer pin run against it with a 1.96 N load and the results show that it had the largest wear of all the other conditions. On disk 19 and 20 both PVC and PCTFE pins were run under a 0.98 N load. On disk 19 PVC wore 1.97 times more than PCTFE and on disk 20 PVC wore 2.12 times more than PCTFE. Thus, with the 0.98 N load, PVC wore more than PCTFE.

On disk 31 a 1.96 N load and 0.98 N load were applied to PCTFE and a 1.96 N load applied to PVC. For the 1.96 N load, PVC wore 1.2 times more than PCTFE. For the PCTFE and the two different loads, the 1.96 N load had 1.3 times more wear than the 0.98 N load. Thus, doubling the load did not double the wear.

On disk 33, a 1.96 N load was applied to PVC and PCTFE. In this case, however, the PVC wore only 0.68 times as much as the PCTFE. This is contrary to previous results on the other disks in which the PVC wore

Table 3. Wear Data for PVC and PCTFE Conical Polymer Pins Run on Steel Disks 11 and 12.

Disk No.	Load (N)	Polymer Pin	Average Radius (m)	No. of Revolutions Spiral Path	Distance Travelled (m)	Mass Transferred (10^9 Kg/m)
11	1.96	PCTFE	0.0143	5	0.4587	$0.1711 \pm 32.0\%^1$
11	1.96	PVC	0.0167	5	0.5244	$0.226 \pm 22.3\%$
22	1.96	PCTFE	0.0143	5	0.4587	$7.69 \pm 4.38\%$
22	1.96	PVC	0.0167	5	0.5244	$20.10 \pm 3.32\%$

¹ Percent Error, see Appendix A for discussion of error term.

Table 4. Wear Data for PVC and PCTFE Polymer Pins
Having a 250,000 μm^2 Circular Area.

Disk No.	Load (N)	Polymer Pin	Average Radius (m)	No. of Revolutions Spiral Path	Distance Travelled (m)	Mass Transferred (10^9 Kg/m)
18	1.96	PVC	0.0155	5	0.4885	$7.157 \pm 5.52\%$
19	0.98	PCTFE	0.0155	5	0.4855	$2.911 \pm 6.79\%$
19	0.98	PVC	0.0155	5	0.4855	$5.730 \pm 6.37\%$
20	0.98	PCTFE	0.0155	5	0.4855	$0.455 \pm 17.25\%$
20	0.98	PVC	0.0114	5	0.3593	$0.963 \pm 16.3\%$
31	1.96	PCTFE	0.0114	5	0.3593	$0.893 \pm 13.89\%$
31	0.98	PCTFE	0.0155	5	0.4855	$0.696 \pm 14.2\%$
31	1.96	PVC	0.0155	5	0.4855	$1.076 \pm 14.36\%$
33	1.96	PCTFE	0.0155	5	0.4855	$2.142 \pm 8.7\%$
33	1.96	PVC	0.0114	5	0.3593	$1.467 \pm 13.5\%$

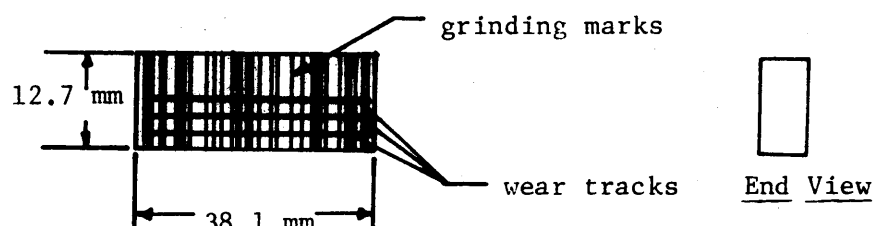
more than the PCTFE. Comparisons can also be made between different steel disks under the same loads with the same polymer pins. However, since the surface topography data is presented in a later section, comparisons between the wear on different disks will be made in the discussion section.

3.2 Shear Angle Data

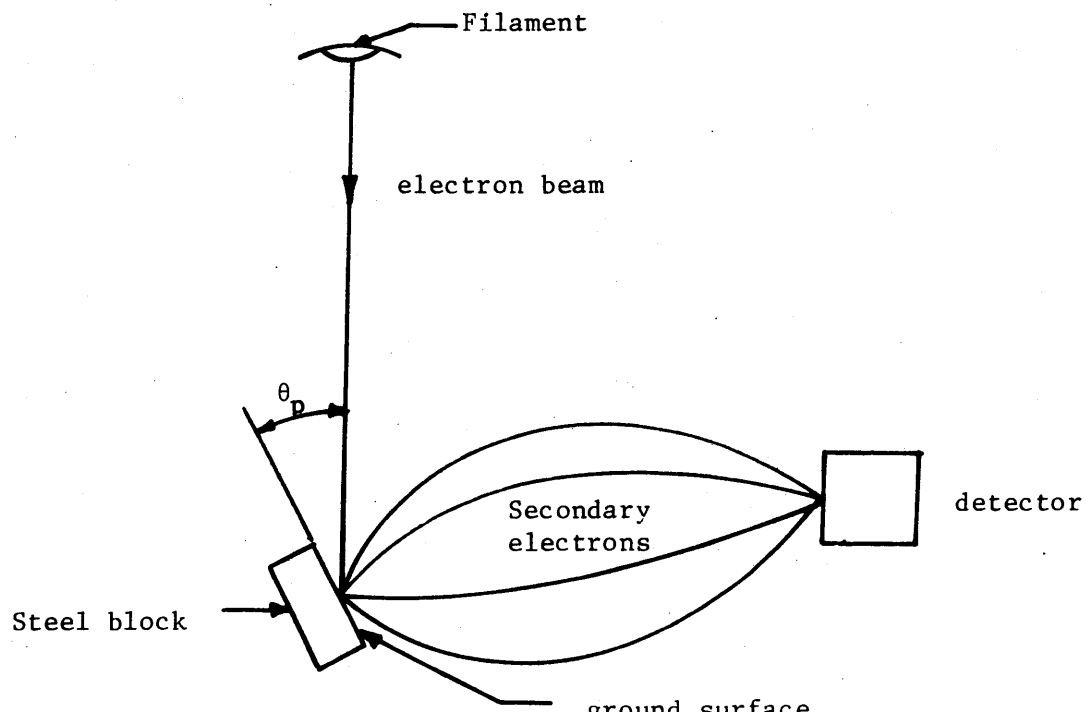
3.2.1. Apparatus

The pin-on-disk machine, shown in Fig. 7, was used to produce linear wear tracks on a 6.4 mm thick, 12.7 mm by 38.1 mm rectangular ground steel block. In order to produce the linear tracks, horizontal motion of arm C was prevented by making support J stationary and the pivot support I was then moved from left to right with the rotation motor turned off. This produced a linear track on the steel block as shown in Fig. 8a. Multiple tracks were obtained by allowing arm C to make a small horizontal motion on the shaft at pivot point D before before the next track was run.

Photographs of the polymer deposits were obtained in an AMR 900 scanning electron microscope (SEM). The plane of the ground surface of the block made an angle θ_p , with the electron beam as shown in Fig. 8b with the lay of the grind being parallel to the beam and the wear track perpendicular to the beam.



a) ground steel block



b) SEM configuration

Figure 8. a) A rectangular ground steel block with linear wear tracks.
b) The configuration of the steel block in the SEM.

3.2.2. Experimental Materials

Three polymers were used for the shear angle measurements. They were crystalline PCTFE, plasticized PVC and Nylon 6-6. The PCTFE and PVC were prepared just as for the wear data experiments. The Nylon 6-6 was also prepared in the same manner from a 3.18 mm dia extruded rod.

The steel blocks were made from a 6.4 mm thick 1018 cold rolled steel bar. After being cut to the dimensions shown in Fig. 8a, the blocks were surface ground with the lay running perpendicular to the longest dimension. After grinding, the blocks were coated with oil to retard rusting. Prior to running the wear experiment, the cleaning procedure discussed in section 3.1.2. was performed.

3.2.3. Experimental Procedures

All experiments were run in laboratory air at an average temperature of 24 C and relative humidity of 60%. The polymer pins were not irradiated as wear data was not required. Wear tracks were run in the pin-on-disk machine with the pivot support I moved by hand with a speed as close to the wear data conditions as possible. PVC, PCTFE and Nylon 6-6 wear tracks were run on the steel blocks for loads of 2.45N, 9.8N, and 14.7N. After running the wear experiment the steel block was placed in the stage of the SEM and photographs were taken.

Nineteen degrees was chosen for θ_p as a compromise between the ability to measure observable differences in the polymer angles and still obtain good photographs with the entire field of view focused. Smaller angles prohibited complete focusing due to the large depth of field required and larger angles made the angle of the polymer deposit appear smaller and hence more difficult to measure.

After taking a series of photographs of the wear tracks, the angles between the polymer deposits and the steel surfaces were measured. Corrections for the fact that the angle between the disk surface and the electron beam were not zero was made by the following equation:

$$\phi = \tan^{-1} \left(\frac{\tan \theta_m}{\cos \theta_p} \right) \quad (14)$$

where

ϕ = real angle of the deposited polymer

θ_m = measured angle of the deposited polymer

θ_p = angle between the disk surface and the electron beam.

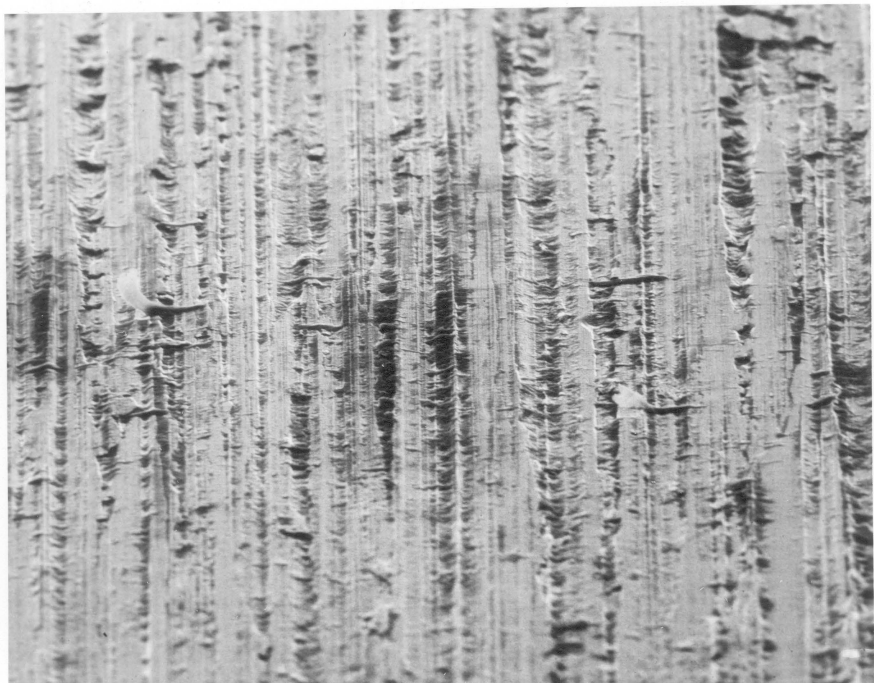
This equation is derived in Appendix B.

3.2.4. Shear Angle Results

Figure 9 is a photograph of a Nylon 6-6 wear track at a magnification of 375X. One notices from this photograph the dark polymer deposits at discrete and continuous sites on the leading side of the steel asperities. Figure 10 is the same track at 1500X illustrating two large grinding scratches with polymer deposited against them. Figures 11 and 12 are again the same wear track at 3750X with each scratch shown in a different photograph. Typical angles of the deposited polymer are shown as they were measured from the photograph and then corrected by Eq. 14 for the tilt of the steel disk.

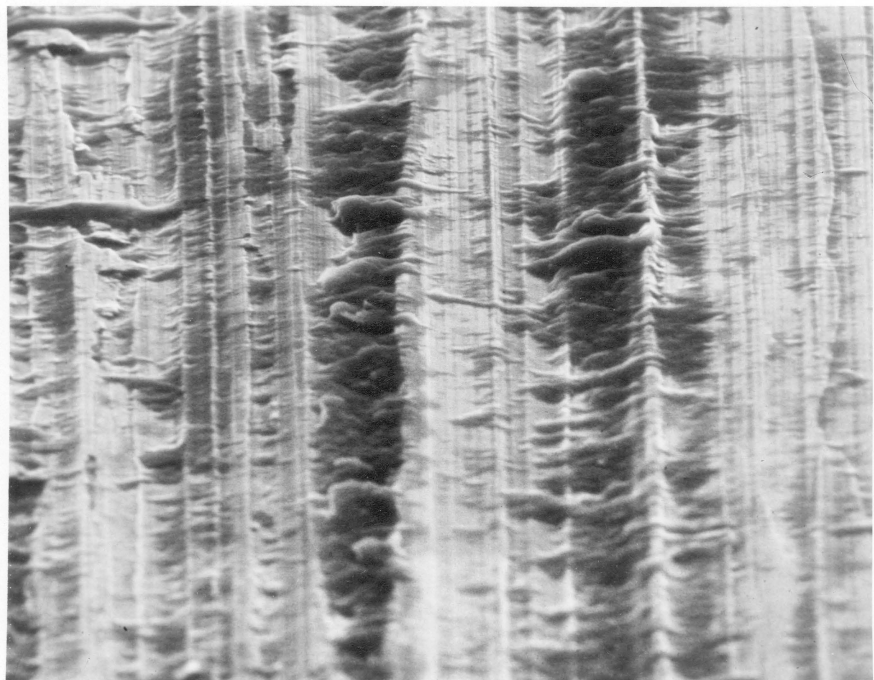
There are many variations in the way the polymer is deposited on the steel disks and several examples are given with illustrations as to how measurement of the angles was made before presenting the actual data. Figure 13 is an excellent example of three continuous PVC deposits along the leading edge of three steel asperities. One notes how very little polymer is deposited on the trailing side of the asperity on the right. Fig. 14 shows PVC again under the same loading conditions as Fig. 13 but instead of being deposited continuously along the asperities, the polymer is in discrete lumps. In this case, the angle measurements are made as shown. One also notes that the steeper asperities tend to have steeper polymer deposits.

Figure 15 is an example of a PVC wear track with a 2.45N load. In this case, there is more polymer on the trailing side of the asperity. It appears as though it flowed over the top of the asperity and was then deposited on the trailing side. The deposits on the trailing

100 μm

Polymer Travel

Figure 9. Conical Nylon 6-6 pin run on rectangular block 4, 14.7 N load, 1 Pass, 5/21/76.



[20 μm] Polymer Travel 

Figure 10. Conical Nylon 6-6 pin run on rectangular block 4, 14.7 N load, 1 Pass, 5/21/76.

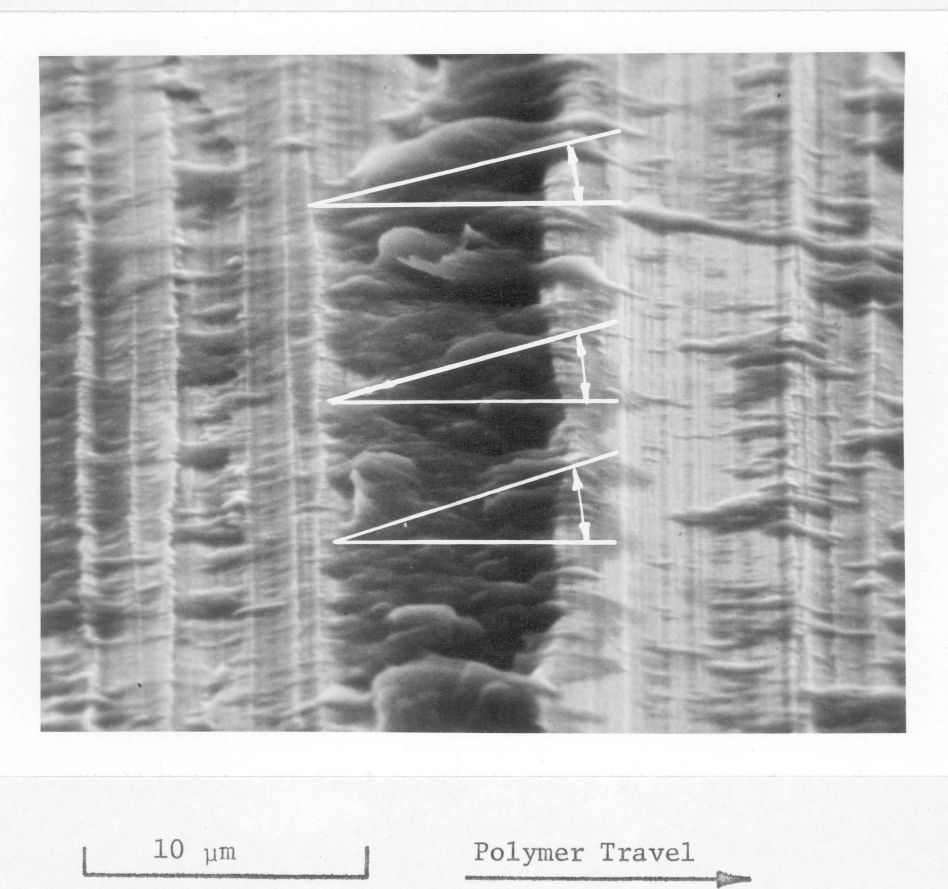
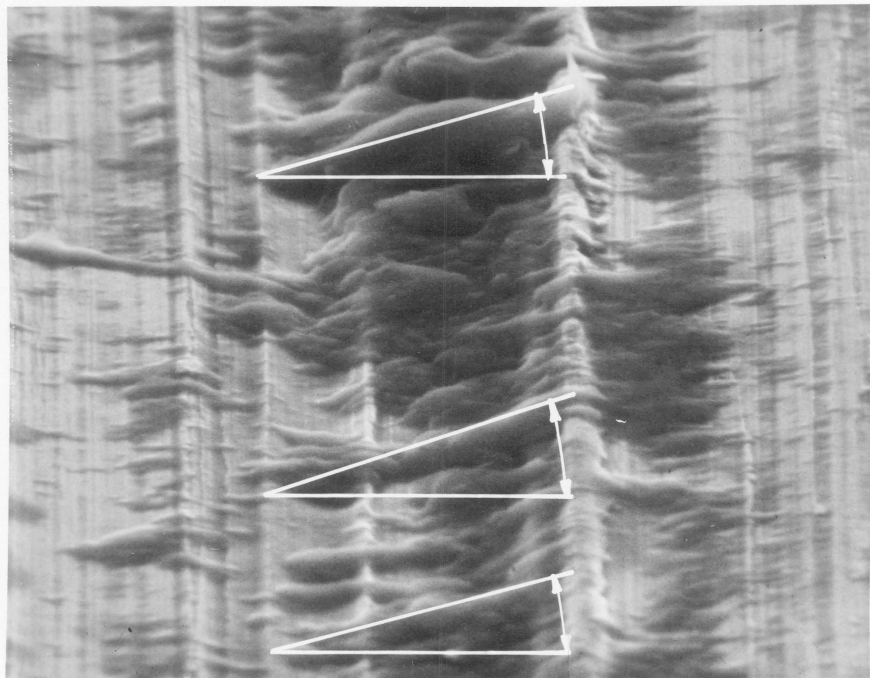


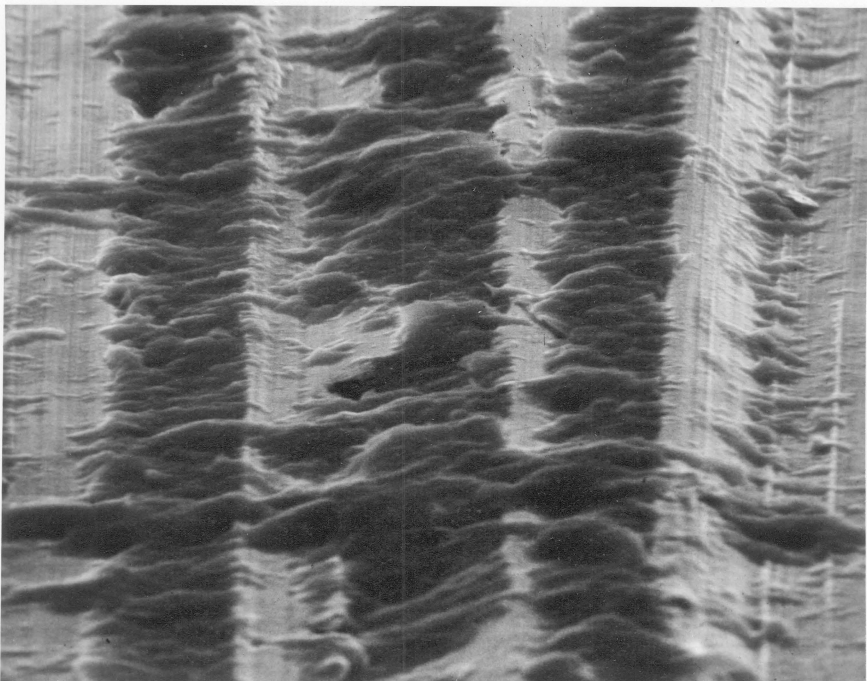
Figure 11. Conical Nylon 6-6 pin run on rectangular block 4, 14.7 N load, 1 Pass, 5/21/76.

10 μm

Polymer Travel



Figure 12. Conical Nylon 6-6 pin run on rectangular block 4, 14.7 N load, 1 Pass, 5/21/76.



20 μm

Polymer Travel \rightarrow

Figure 13. Conical PVC pin run on rectangular block 5, 9.8 N load, 1 Pass, 6/3/76.

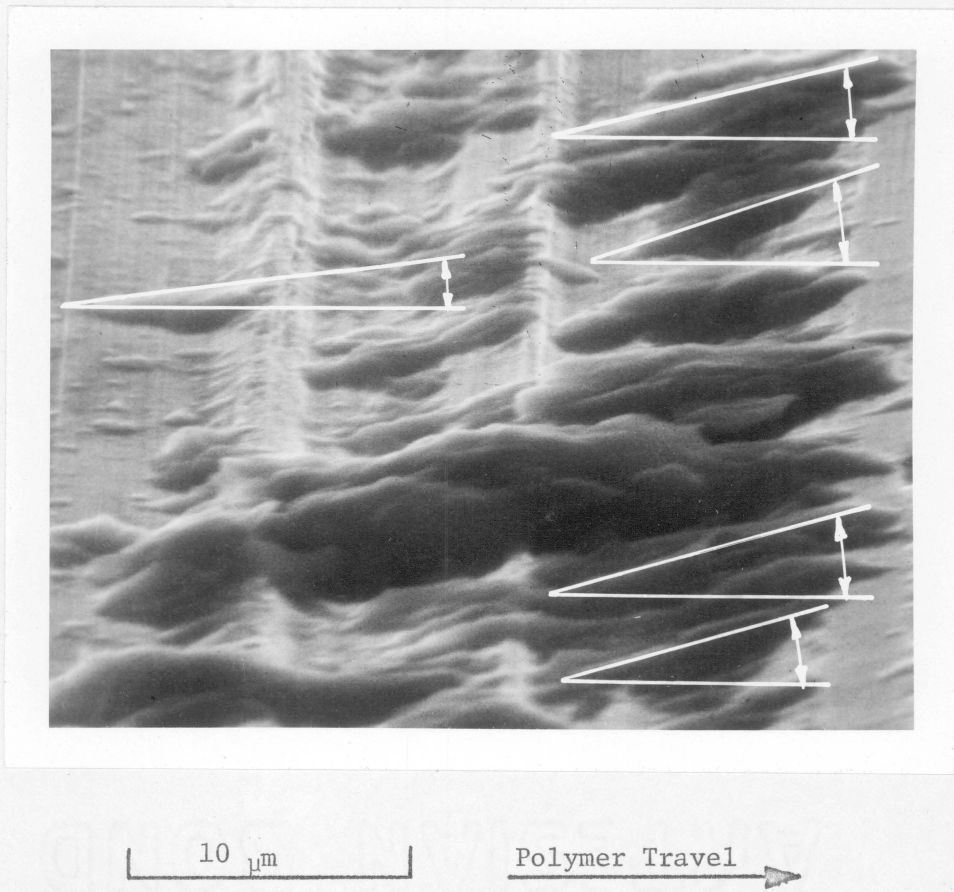
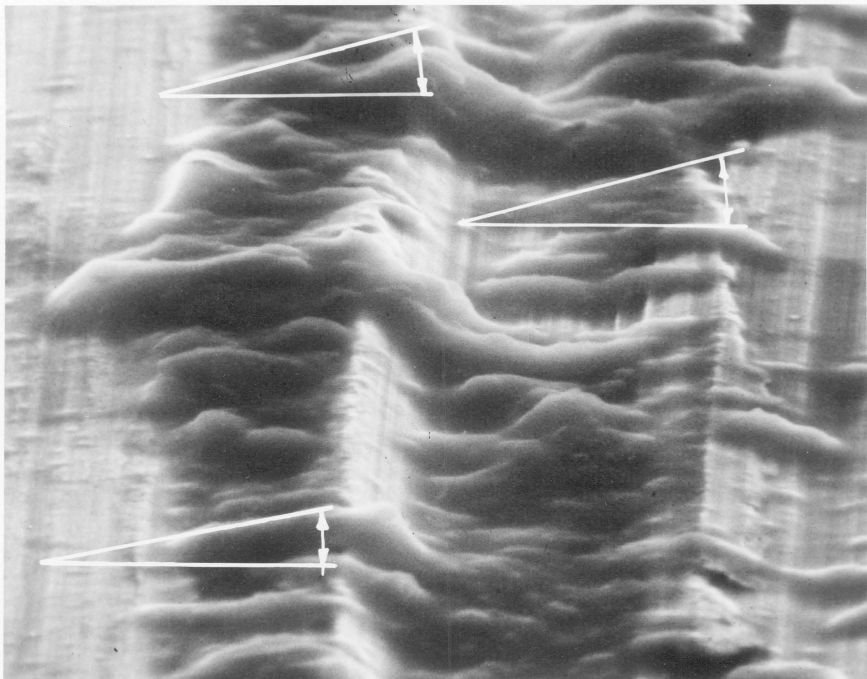


Figure 14. Conical PVC pin run on rectangular block 5, 9.8 N load, 1 Pass, 6/3/76.



10 μm

Polymer Travel

Figure 15. Conical PVC pin run on rectangular block 7, 2.45 N load, 1 Pass, 6/8/76.

side appear to be more numerous on the lighter loaded tracks. Figure 16 shows a steel surface having an anomaly in the grinding scratch and the polymer deposit at an approximately constant angle along the anomaly and the asperity on the leading side. Figure 17 illustrates an asperity with a large flat on it and another anomaly along the leading side. Again, the polymer is deposited in an approximately constant angle on the leading side.

Figure 18 is a PVC wear track where the PVC pin had a $250,000 \mu\text{m}^2$ area rather than a conical point. In this photograph the fuzziness is due to very small amounts of polymer. One notes that the polymer is still shearing off along the edge of the asperity at an angle and apparently filling in the space between the bottom of the pin and the steel surface.

The original data for the shear angles, ϕ for polymers PVC, PCTFE, and Nylon 6-6, is given in Appendix B. After being corrected for the tilt of the photograph, the data was analyzed and the minimum and maximum values of ϕ , along with the means and standard deviations shown in Table 5 were obtained. In Table 5, n is the number of observations, $\bar{\phi}$ is the average shear angle and S is the standard deviation. Having this data, a 2 way ANOVA was performed to determine whether the means were statistically different for each polymer and independent of the load. The ANOVA was performed using adjusted sums of squares to correct for the unequal numbers of observations per load - polymer block. The significance-level for each source of variation is indicated in Table 6 under the heading Prob >F. The ANOVA indicates the

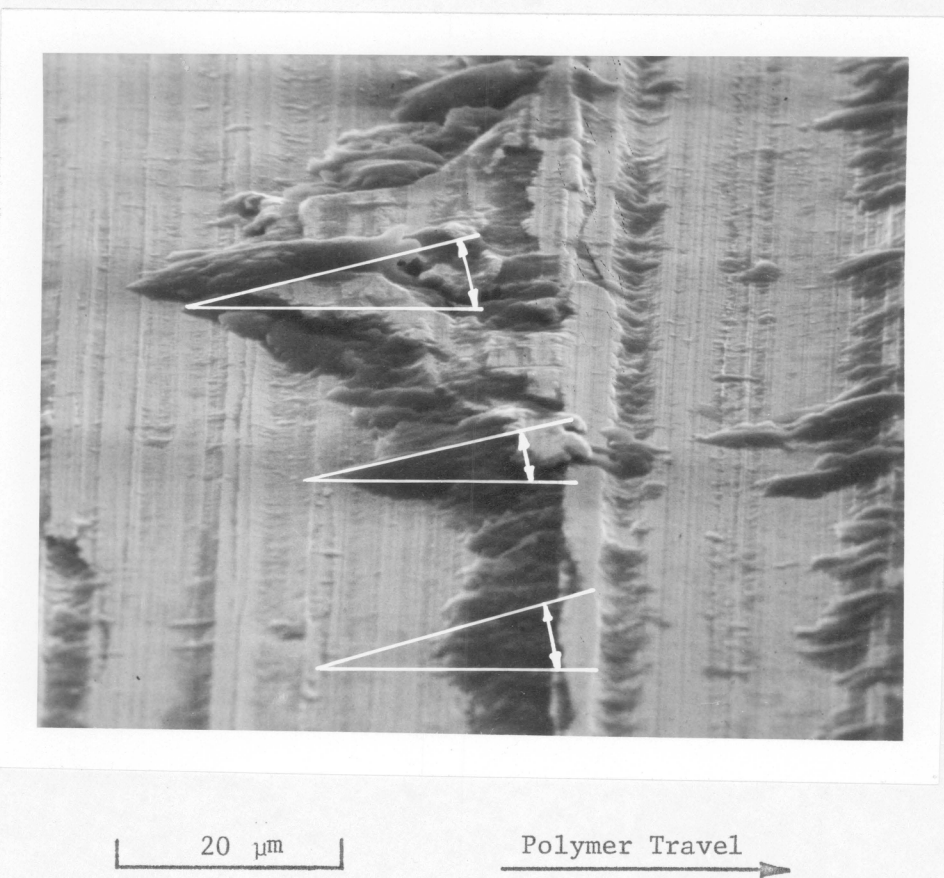


Figure 16. Conical PCTFE pin run on rectangular block 3, 14.7 N load, 1 Pass, 5/19/76.

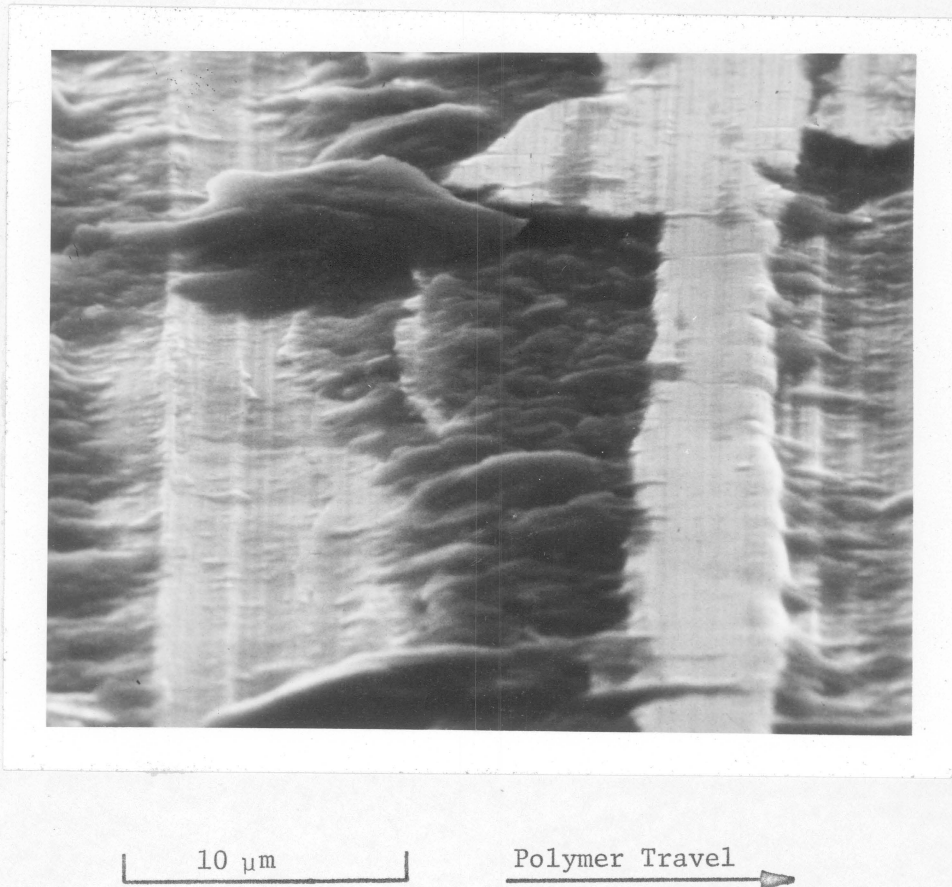


Figure 17. Conical PCTFE pin run on rectangular block 3, 14.7 N load, 1 Pass, 5/19/76.

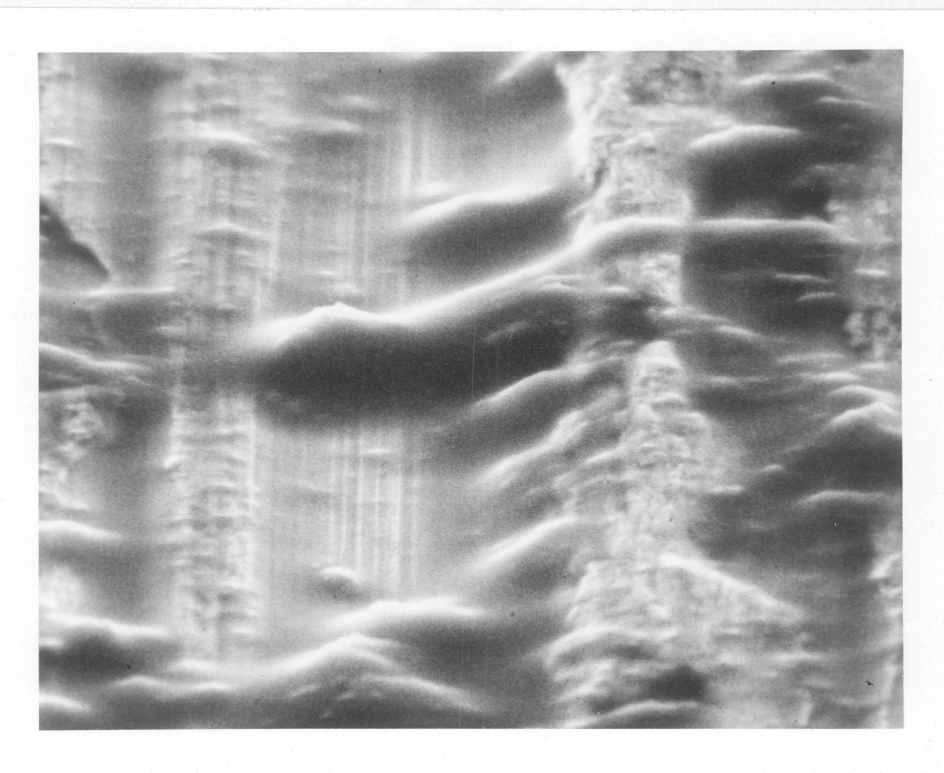


Figure 18. PVC pin with $250,000 \mu\text{m}^2$ area run
on rectangular block 6, 9.8 N load,
1 Pass, 6/10/76.

Table 5. Shear Angle Measurements.

		Load (N)		
		2.45	9.80	14.70
PVC	n	99	84	106
	ϕ min	2.1	3.6	2.6
	Φ	11.9	10.9	9.8
	ϕ max	19.9	24.2	34.7
Polymer PCTFE	S	3.8	4.3	4.4
	n	49	60	46
	ϕ min	6.9	6.9	6.3
	Φ	13.3	12.4	12.1
Nylon 6-6	ϕ max	26.3	17.9	16.6
	S	3.5	2.5	2.7
	n	56	64	128
	ϕ min	7.8	9.5	7.2
Nylon 6-6	Φ	18.6	19.0	19.0
	ϕ max	32.9	34.0	46.6
	S	5.0	5.1	5.6

Table 6. Two Way Analysis of Variance Table.

Source of Variation	Degrees of Freedom	Adjusted Sums of Squares	F Value	Prob > F
Load	2	112.76	2.94	0.0520
Polymer	2	112.81	211.39	0.0001
Load • Polymer	4	157.17	2.05	0.0850
Error	678	13,010.36		
Total	686	22,332.51		

possibility of an interaction between load and polymer since the significance-level is 0.085. A significant interaction indicates that the difference in the load means is not constant for the three polymers. Thus, a test on load means averaged across polymers could be misleading. A one-way ANOVA for each polymer is thus more appropriate.

In Fig. 19, the average shear angle Φ is plotted as a function of load for the three different polymers. If there is no interaction, the three lines should be parallel; however, they are not. Therefore, interaction is again indicated. From Fig. 19 one could conclude that Φ for Nylon 6-6, PVC and PCTFE are different, and that Φ is a constant for the three polymers independent of the load.

Tables 7, 8 and 9 are one-way analyses of variance for each of the three loads as a function of polymer. In each case the significance level is 0.0001. Therefore, one rejects the null hypothesis, that the shear angle means are equal among the polymers for each load.

The F test performed in the previous paragraph rejected the null hypothesis that the shear angle means were all equal, but it did not tell which means were significantly different from each other. Therefore, Duncan's multiple range test as extended by Kramer [42], for unequal numbers of replications, was used to determine which means are significantly different. In Duncan's test for an unequal number of replications, the difference between any two ranked means \bar{X}_b and \bar{X}_c is significant, if $(\bar{X}_b - \bar{X}_c) \frac{2n_b n_c}{n_b + n_c}$ exceeds a shortest significant range (R_p), where

$$R_p = S \cdot Z_{p, n_2} \quad (15)$$

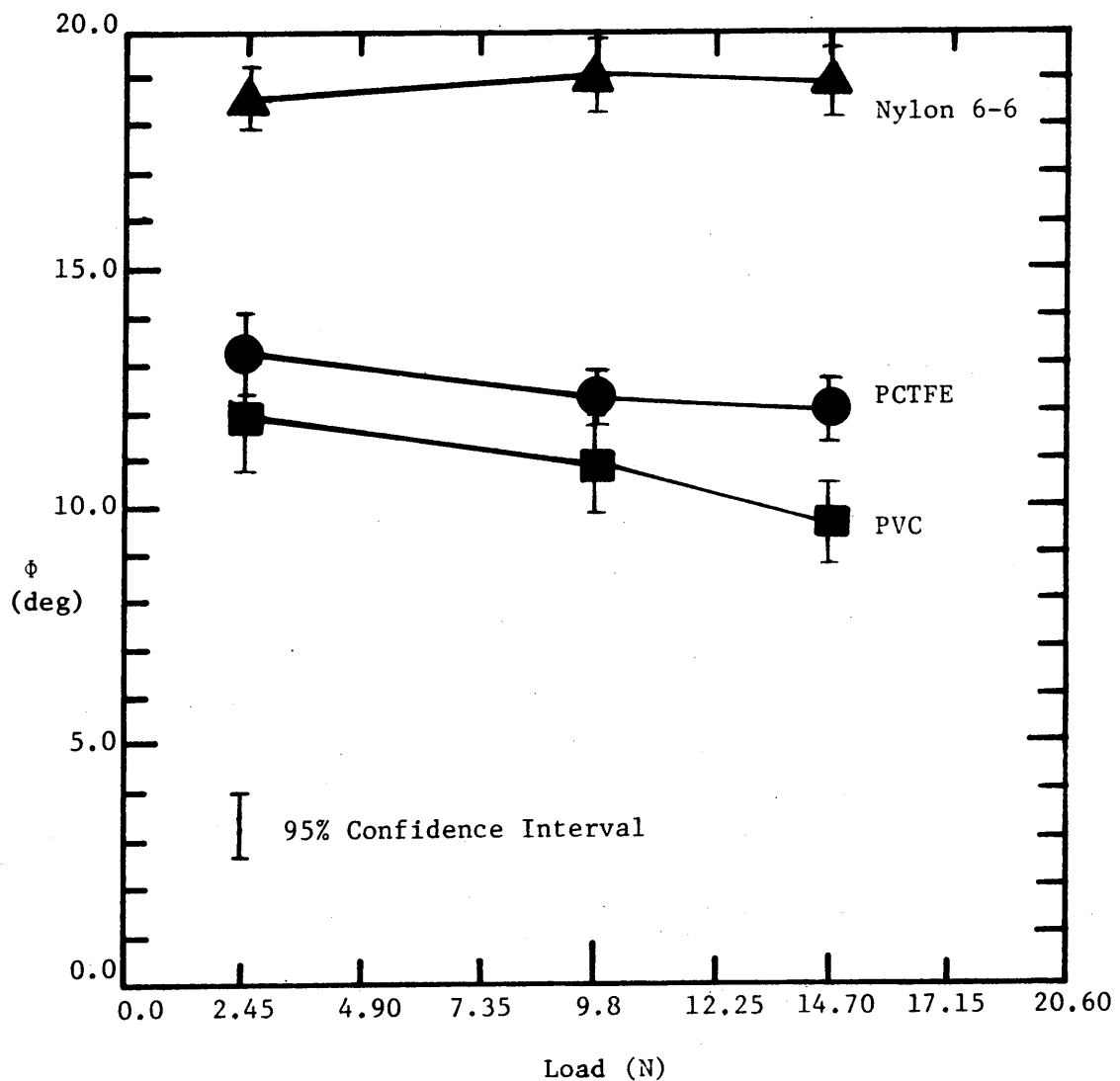


Figure 19. Plot of ϕ as a Function of Load
for Nylon 6-6, PCTFE, and PVC.

Table 7. Shear Angle Means and One Way Analysis
of Variance Table for 2.45N Load.

Shear Angle Means

Polymer	n	Φ
PVC	99	11.9
PCTFE	49	13.3
Nylon 6-6	56	18.6
<hr/>		
Overall mean		14.1

ANOVA TABLE

Source of Variation	Degrees of Freedom	Sums of Squares	Mean Square	F	Prob > F
Polymer	2	1619.13	809.56	48.33	0.0001
Error	201	3366.84	16.75		
Total	203	4885.97	24.56		

**Table 8. Shear Angle Means and One Way Analysis
of Variance Table for 9.80N Load.**

Shear Angle Means

<u>Polymer</u>	<u>n</u>	ϕ
PVC	84	10.9
PCTFE	60	12.4
Nylon 6-6	64	19.0
<hr/>		
Overall mean		13.9

ANOVA TABLE

<u>Source of Variation</u>	<u>Degree of Freedom</u>	<u>Sums of Squares</u>	<u>Mean Square</u>	F	Prob > F
Polymer	2	2559.71	1279.86	75.12	0.0001
Error	205	3492.89	17.04		
Total	207	6052.61	29.24		

Table 9. Shear Angle Means and One Way Analysis
of Variance Table for 14.70N Load.

<u>Shear Angle Means</u>		
Polymer	n	Φ
PVC	106	9.8
PCTFE	46	12.1
Nylon 6-6	128	19.0

Overall mean		14.4

ANOVA TABLE

Source of Variation	Degrees of Freedom	Sums of Squares	Mean Square	F	Prob > F
Polymer	2	5138.78	2569.39	113.78	0.0001
Error	277	6255.33	33.58		
Total	279	11394.11	40.84		

In Eq. 15, $p = 1, 2, \dots, t$, is the number of means concerned, S is the root mean square error, n_2 is the degrees of freedom of the root mean square error, and Z_{p,n_2} is obtained from a table of significant studentized ranges which Duncan has tabulated for both the 5% and 1% test [43].

Table 10 shows Duncan's test for the three loads. Any two means not underscored by the same line are significantly different. As seen in Tables 10b and 10c, there is a significant difference between the average shear angles for all three polymers at loads of 9.8N and 14.7N. However, in Table 10a, one observes that the average shear angles for PVC and PCTFE are not significantly different for a load of 2.45N. At the 2.45N load, the average shear angle for PCTFE and PVC are, however, significantly different from those of Nylon 6-6.

Tables 11, 12 and 13 are one-way analyses of variance for each of the three polymers as a function of load. In Table 11, the significance level for PCTFE is 0.0924, which is small enough to indicate the possibility of differences in ϕ for the different loads. However, since one would make an error 9.24 times out of 100 if the null hypothesis (that the load dependent means were equal) were rejected, it is concluded that the means are not significantly different.

In Table 12 the significance-level for Nylon 6-6 is 0.8713 and one accepts the null hypothesis that the means for the three different loads are equal. In Table 13, however, the significance-level is 0.002. Therefore, one rejects the null hypothesis for PVC that the shear angle means for the three different loads are equal.

Table 10. Duncan's Test for Loads of 2.45, 9.8 and 14.7N.

Shear angle means ranked in order (smallest to largest) and number of replications for:

a) 2.45N Load

<u>Polymer</u>	<u>PVC</u>	<u>PCTFE</u>	<u>Nylon 6-6</u>
Φ	11.9	13.3	18.6
N	<u>99</u>	<u>49</u>	56
			—

b) 9.8N Load

<u>Polymer</u>	<u>PVC</u>	<u>PCTFE</u>	<u>Nylon 6-6</u>
Φ	10.9	12.4	19.0
N	<u>84</u>	60	64
		—	—

c) 14.7N Load

<u>Polymer</u>	<u>PVC</u>	<u>PCTFE</u>	<u>Nylon 6-6</u>
Φ	9.8	12.1	19.0
N	<u>106</u>	46	128
		—	—

Table 11. Shear Angle Means and One Way Analysis
of Variance Table for PCTFE.

Shear Angle Means

Load (N)	n	Φ
14.7	46	12.1
9.8	60	12.4
2.45	49	13.3

Overall mean		12.6

ANOVA TABLE

Source of Variation	Degrees of Freedom	Sums of Squares	Mean Square	F	Prob > F
Load	2	40.37	20.19	2.40	0.0924
Error	152	1280.36	8.42		
Total	154	1320.74	8.58		

Table 12. Shear Angle Means and One Way Analysis
of Variance Table for Nylon 6-6.

Shear Angle Means

Load (N)	n	Φ
2.45	56	18.57
14.7	128	18.95
9.8	64	19.04
<hr/>		
Overall mean		18.9

ANOVA TABLE

Source of Variation	Degree of Freedom	Sums of Squares	Mean Square	F	Prob > F
Load	2	7.77	3.89	0.14	0.8713
Error	245	6893.85	28.14		
Total	247	6901.62	27.94		

**Table 13. Shear Angle Means and One Way Analysis
of Variance Table for PVC.**

Shear Angle Means

Load (N)	n	Φ
14.7	106	9.8
9.8	84	10.9
2.45	99	11.9
<hr/>		
Overall mean		10.8

ANOVA TABLE

Source of Variation	Degrees of Freedom	Sums of Squares	Mean Square	F	Prob > F
Load	2	227.59	113.80	6.59	0.0020
Error	286	4940.85	17.28		
Total	288	5168.44	17.95		

Table 15 shows Duncan's Test for PVC. As seen in this table, there is no significant difference between the 9.8N load and the 14.7N or the 2.45N load at the $\alpha=0.05$ level. However, there is a significant difference at the $\alpha=0.05$ level between the 14.7N and the 2.45N load. The author has no explanation at this time for the significant difference between these two loads and why it only occurs for PVC. Since PVC is the only polymer that is load dependent and this load dependence is only for the extreme range of 2.45-14.7N, the overall shear angle means shown in Tables 11, 12 and 13 will be used to compare the three polymers. Thus, $\Phi_{PVC} = 10.8$ deg; $\Phi_{PCTFE} = 12.6$ deg; and $\Phi_{Nylon\ 6-6} = 18.9$ deg.

Table 14. Duncan's Test for PVC.

Shear angle means ranked in order (smallest to largest) and number of replications

Load	14.7N	9.8N	2.45N
ϕ	9.8	10.9	11.9
n	106	84	99

3.3. Surface Topography Data

3.3.1. Apparatus, Materials, Procedure

The topography of the steel disks were characterized by Calspan Corporation in Buffalo, New York. Stylus traces were run in a straight line for a total length of 4.76 mm. Disks 11 and 22 were traced four times, each trace being ninety degrees apart and tangent to a circle having a 14.27 mm radius. Disks 18, 19, 20, 31, and 33 were traced four times with two of the traces at a radius of 14.27 mm, each ninety degrees apart and the other two traces at a radius of 16.89 mm, each ninety degrees apart. All of the above traces were run with the profilometer in the roughness mode having a 762 μm waviness filter.

Rectangular block 5 used in the shear angle measurements was also characterized. On this block two 6.35 mm traces were made perpendicular to the grind direction over the same surface. One trace was made with the profilometer in the roughness mode and the other trace was made with the profilometer in the profile mode. The roughness mode had the 762 μm waviness filter while the profile mode had no filter.

From the stylus traces, digitized output was obtained giving relative heights of the profile at equal horizontal increments. The digitized data was then used in a computer program to obtain statistical surface characterization parameters.

3.3.2. Surface Characterization Results

Tables 15 and 16 show the surface topography data for disks 11 and 22. All of the parameters are calculated from stylus traces at a 14.27 mm radius with four values given, each ninety degrees apart, and listed as bottom, right side, top, and left side. An overall average value is also given. The values for the peak and valley are only relative for a given trace and thus it is not correct to compare these values for different traces. The peak-to-valley height is, however, an absolute value and may be compared for the various traces. One should note, however, that the peak-to-valley height given in the overall average column is not an average but is the maximum height of those for the four traces.

The slope at a given point (I) was calculated as

$$\text{Slope } (I) = \frac{Y(I+1)-Y(I-1)}{2 \cdot Dx} \quad (16)$$

where $Y(I+1)$ and $Y(I-1)$ are the profile heights on either side of the point I and Dx is the horizontal spacing between two points. When a peak or valley was encountered, the slope at I was calculated as

$$\text{Slope } (I) = 1/2 \left| \frac{Y(I-1)-Y(I)}{Dx} + \frac{Y(I+1)-Y(I)}{Dx} \right| \quad (17)$$

This gives a slope equal to the average of the slopes on either side of the peak or valley. The profile average slope shown in the tables was calculated by summing the absolute values of all the slopes and dividing by the number of points.

The correlation length (L) was determined as the distance a profile must be shifted for the autocorrelation function to drop to

Table 15. Surface Topography Data for Disk 11.

	Radius (14.27 mm)			Overall Average
	Bottom	Right Side	Top	
1) Peak (μm)	4.56	4.40	4.52	4.34
2) Valley (μm)	3.39	3.36	3.47	3.33
3) Peak-to-Valley (μm)	1.17	1.04	1.05	1.01
4) Profile Avg. Slope	0.0081	0.0068	0.0072	0.0068
5) L (μm)	7.16	10.57	23.34	19.45
6) R_a (μm)	0.11	0.08	0.10	0.09
7) $L \times R_a$ (μm) ²	1.89	0.85	2.33	1.75
8) RMS (μm)	0.16	0.13	0.15	0.12
				0.14

Table 16. Surface Topography Data for Disk 22.

	Radius (14.27 mm)			Overall Average
	Bottom	Right Side	Top	
1) Peak (μm)	21.06	18.14	18.42	18.35
2) Valley (μm)	14.06	14.57	14.25	14.30
3) Peak-to-Valley (μm)	7.00	3.57	4.17	4.05
4) Profile Avg. Slope	0.0264	0.0218	0.0225	0.0229
5) L (μm)	24.11	30.43	22.96	23.70
6) R_a (μm)	0.41	0.32	0.32	0.33
7) $L \times R_a$ (μm) ²	9.89	9.74	7.35	7.82
8) RMS (μm)	0.58	0.39	0.45	0.44
				0.47

10% of its zero shift value. The arithmetic average (R_a), root mean square (RMS) and product of correlation length and arithmetic average ($L \times R_a$) are also given.

Tables 17-21 are for disks 18, 19, 20, 31 and 33, all of which had polymer pins with a $250,000 \mu\text{m}^2$ area worn against them. For these disks, two traces were run at two radii and are listed as inside radius, bottom and right side and outside radius, bottom and right side. Averages for each radius as well as an overall average for the four radii are given.

For the polymer pins run on disks 18, 19, 30, 31 and 33, the apparent area was $250,000 \mu\text{m}^2$ and the real area required to support the normal load was assumed to be

$$A_r = \frac{W_t}{p_m} \quad (18)$$

where p_m is the flow pressure of the polymer, equal to $3 \cdot Y$ where Y is the yield strength of the polymer [24]. Therefore, using the yield strength of PVC and PCTFE from Table 2, the percent of the apparent area required to support loads of 0.98 and 1.96N are given in Table 22. Knowing these values, the relative height at which a given polymer will be supported is determined from the bearing area curve and is shown in Tables 17-21 for PVC and PCTFE. This value is listed as the bearing height (B_{ht}). A typical bearing area curve is shown in the discussion of results. Average slope values were then obtained for the parts of the profile above the bearing height. The absolute penetration for the two polymers was calculated as the peak minus the bearing height for the given polymer and this is also

Table 17. Surface Topography Data for Steel Disk 18.

	Inside Radius (14.2 mm)			Outside Radius (16.9 mm)			Overall Average
	Bottom	Right Side	Average	Bottom	Right Side	Average	
1. Peak (μm)	10.54	8.80	-	8.92	9.90	-	-
2. Valley (μm)	6.76	6.88	-	6.95	6.06	-	-
3. Peak-to-Valley (μm)	3.78	1.92	3.78	1.97	3.84	3.84	3.84
4. Profile Avg. Slope	0.0287	0.0267	0.0277	0.0249	0.0259	0.0254	0.0266
5. PCTFE Bht (μm)	-	-	-	-	-	-	-
6. Avg. Slope above PCTFE Bht	-	-	-	-	-	-	-
7. PVC Bht (μm)	8.60	8.49	8.54	8.45	8.28	8.37	8.45
8. Avg. Slope above PVC Bht	0.0840	0.0436	0.0638	0.0617	0.0733	0.0675	0.0656
9. PCTFE Penetration 1-5 (μm)	-	-	-	-	-	-	-
10. PVC Penetration 1-7 (μm)	1.94	0.31	1.13	0.47	1.62	1.05	1.09
11. L (μm)	16.3	15.8	16.1	17.2	15.5	16.4	16.3
12. R_a (μm)	0.27	0.26	0.26	0.25	0.26	0.26	0.26
13. RMS (μm)	0.36	0.34	0.35	0.34	0.35	0.34	0.35

Table 18. Surface Topography Data for Steel Disk 19.

	Inside Bottom	Radius (14.2 mm) Right Side	Outside Bottom	Radius (16.9 mm) Right Side	Overall Average
1. Peak (μm)	9.59	10.92	—	15.62	10.65
2. Valley (μm)	6.26	5.52	—	0.0	5.39
3. Peak-to-Valley (μm)	3.33	5.40	5.40	15.62	5.26
4. Profile Avg. Slope	0.0294	0.0329	0.0312	0.0334	0.0344
5. PCTFE Bht (μm)	8.51	8.63	—	8.57	8.75
6. Avg. Slope above PCTFE Bht	0.0686	0.0913	0.0800	0.1163	0.1069
7. PVC Bht (μm)	9.19	9.57	—	9.46	9.77
8. Avg. Slope above PVC Bht	0.0603	0.1292	0.0947	0.2830	0.1349
9. PCTFE Penetration 1-5 (μm)	1.08	2.29	1.69	7.05	1.90
10. PVC Penetration 1-7 (μm)	0.40	1.35	0.88	6.16	0.88
11. L (μm)	31.2	24.0	27.6	21.0	27.7
12. R_a (μm)	0.32	0.43	0.38	0.36	0.49
13. RMS (μm)	0.43	0.64	0.51	1.05	0.72
14. Skewness	0.1687	0.3553	0.2620	0.0781	0.1903
15. Kurtosis	4.0438	5.5765	4.8102	4.8653	4.4132
					4.6393
					4.7247

Table 19. Surface Topography Data for Steel Disk 20.

	Inside Bottom	Radius (14.2 mm) Right Side	Average	Outside Bottom	Right Side	Radius (16.9 mm) Average	Overall Average
1. Peak (μm)	8.86	9.02	-	8.96	9.21	-	-
2. Valley (μm)	6.35	6.21	-	6.38	6.24	-	-
3. Peak-to-Valley (μm)	2.51	2.81	2.81	2.58	2.97	2.97	2.97
4. Profile Avg. Slope	0.0366	0.0346	0.0356	0.0319	0.0301	0.0310	0.0333
5. PCTFE Bht (μm)	8.48	8.46	-	8.44	8.41	-	-
6. Avg. Slope above PCTFE Bht	0.0523	0.0529	0.0526	0.0544	0.0586	0.0565	0.0546
7. PVC Bht (μm)	8.66	8.74	-	8.66	8.64	-	-
8. Avg. Slope above PVC Bht	0.0782	0.0458	0.0620	0.0629	0.0855	0.0742	0.0681
9. PCTFE Penetration 1-5 (μm)	0.38	0.56	0.47	0.52	0.80	0.66	0.57
10. PVC Penetration 1-7 (μm)	0.20	0.28	0.24	0.30	0.57	0.44	0.34
11. L (μm)	14.6	14.1	14.3	15.8	13.7	14.8	14.6
12. R_a (μm)	0.43	0.43	0.43	0.39	0.34	0.37	0.40
13. RMS (μm)	0.53	0.54	0.53	0.50	0.46	0.48	0.51
14. Skewness	-0.5684	-0.5244	-0.5464	-0.5115	-0.6959	-0.6037	-0.5750
15. Kurtosis	2.4620	2.5846	2.5233	2.7702	3.1651	2.9677	2.7455

Table 20. Surface Topography Data for Steel Disk 31.

	Inside Bottom	Radius (14.2 mm) Right Side	Radius (14.2 mm) Average	Outside Bottom	Radius (16.9 mm) Right Side	Radius (16.9 mm) Average	Overall Average
1. Peak (μm)	8.64	8.61	-	8.99	8.55	-	-
2. Valley (μm)	6.49	6.73	-	6.54	6.52	-	-
3. Peak-to-Valley (μm)	2.15	1.88	2.15	2.45	2.03	2.45	2.45
4. Profile Avg. Slope	0.0226	0.0233	0.0230	0.0226	0.0220	0.0223	0.0226
5. PCTFE Bht (μm)	8.12	8.13	-	8.13	8.10	-	-
6. Avg. Slope above PCTFE Bht	0.0391	0.0351	0.0371	0.0348	0.0403	0.0376	0.0373
7. PVC Bht (μm)	8.33	8.32	-	8.32	8.31	-	-
8. Avg. Slope above PVC Bht	0.0473	0.0438	0.0456	0.0486	0.0422	0.0454	0.0455
9. PCTFE Penetration 1-5 (μm)	0.52	0.48	0.50	0.86	0.45	0.65	0.58
10. PVC Penetration 1-7 (μm)	0.31	0.29	0.30	0.67	0.24	0.46	0.38
11. L (μm)	21.7	22.4	22.1	20.9	20.8	20.9	21.5
12. R_a (μm)	0.24	0.26	0.25	0.25	0.25	0.25	0.25
13. RMS (μm)	0.30	0.32	0.31	0.31	0.31	0.31	0.31
14. Skewness	-0.0881	-0.1883	-0.1382	-0.1827	-0.3211	-0.2519	-0.1950
15. Kurtosis	2.8796	2.6191	2.749	3.1474	2.7376	2.9425	2.8459

Table 21. Surface Topography Data for Steel Disk 33.

	Inside Bottom	Radius (14.2 mm)			Outside		Radius (16.9 mm)		Overall Average
		Right Side	Average	Bottom	Right Side	Average	Right Side	Average	
1. Peak (μm)	9.20	9.02	-	9.21	9.07	-	-	-	-
2. Valley (μm)	6.25	6.15	-	6.34	6.19	-	-	-	-
3. Peak-to-Valley (μm)	2.94	2.87	2.94	2.87	2.88	2.88	2.88	2.94	2.94
4. Profile Avg. Slope	0.0383	0.0375	0.0379	0.0394	0.0365	0.0379	0.0379	0.0379	0.0379
5. PCTFE Bht (μm)	8.37	8.35	-	8.36	8.35	-	-	-	-
6. Avg. Slope above PCTFE Bht	0.0513	0.0581	0.0547	0.0576	0.0522	0.0549	0.0549	0.0548	0.0548
7. PVC Bht (μm)	8.68	8.66	-	8.75	8.68	-	-	-	-
8. Avg. Slope above PVC Bht	0.0706	0.0561	0.0634	0.0719	0.0614	0.0667	0.0667	0.0650	0.0650
9. PCTFE Penetration 1-5 (μm)	0.83	0.67	0.75	0.85	0.72	0.79	0.79	0.77	0.77
10. PVC Penetration 1-7 (μm)	0.52	0.36	0.44	0.46	0.39	0.43	0.43	0.43	0.43
11. L (μm)	19.9	18.9	19.4	21.8	20.3	21.1	21.1	20.3	20.3
12. R_a (μm)	0.42	0.42	0.42	0.45	0.41	0.43	0.43	0.43	0.43
13. RMS (μm)	0.53	-	0.53	0.56	0.53	0.55	0.55	0.54	0.54
14. Skewness	-0.3172	-0.5680	-0.4426	-0.2356	-0.5622	-0.3989	-0.3989	-0.4208	-0.4208
15. Kurtosis	2.819	2.9881	2.9034	2.8057	3.1897	2.9977	2.9977	2.9506	2.9506

Table 22. Percent Area Required to Support a Given Normal Load for Different Polymers According to the Disk Worn On.

		$\% \text{ Area} = A_r/A_a$	
Disk No	Load (N)	Polymer	
		PVC	PCTFE
18	1.96	0.0252	---
19	0.98	0.0126	0.0566
20	0.98	0.0126	0.0566
31	1.96	0.0252	0.1130
31	0.98	---	0.0566
33	1.96	0.0252	0.1130

tabulated. Values for the skewness and kurtosis were calculated and are tabulated for some of the disks as shown.

Table 23 is for rectangular block 5. On this block two profile traces were run perpendicular to the grind over the same surface, one in the roughness mode, having a 762 μm waviness filter and the other in the profile mode having no filter. The maximum slope value for the profile is given. The maximum asperity base angle equal to the arctangent of the maximum slope is also given.

**Table 23. Surface Topography Data
for Rectangular Block 5.**

	Roughness Mode (762 μm Waviness filter)	Profile Mode (No Filter)
1 Peak (μm)	9.76	17.73
2 Valley (μm)	6.59	11.65
3 Peak-Valley (μm)	3.17	6.08
4 Profile Avg Slope	0.0318	0.0519
5 Maximum Slope	0.3002	0.4551
6 Maximum Base Angle (deg)	16.7	24.5
7 L (μm)	22.24	--
8 Ra (μm)	0.32	0.82
9 RMS (μm)	0.43	0.88

4. DISCUSSION OF RESULTS

4.1. Single Point Orthogonal Cutting Theory

The consideration and determination of factors important in a wear model, consistent with the wear and shear angle data already presented, are the major efforts of this research. From the SEM observations of wear tracks, one observes that polymer deposits are distributed in discrete sites rather than continuous films. It is, therefore, apparent that some of the steel asperities are removing material and some are not. It is also apparent, due to the differences in the amount of polymer deposited at these discrete sites, that some asperities are removing more material than others. A typical two dimensional stylus profile of a ground steel surface is shown in Fig. 20. From this profile and the SEM observations, two important questions must be answered in order to construct a wear model:

- 1) Which of the steel asperities are going to remove material?
- 2) How much material will they remove?

It is noted that the process of the cutting or machining of metals is related to the polymer wear mechanism, where the cutting tool and the steel asperity are analogous. Therefore, in order to answer the above questions and develop a wear model, a modification to orthogonal cutting theory is made. Before discussing the model, a brief review of orthogonal cutting theory must be presented.

Orthogonal cutting is said to occur when the cutting edge of a

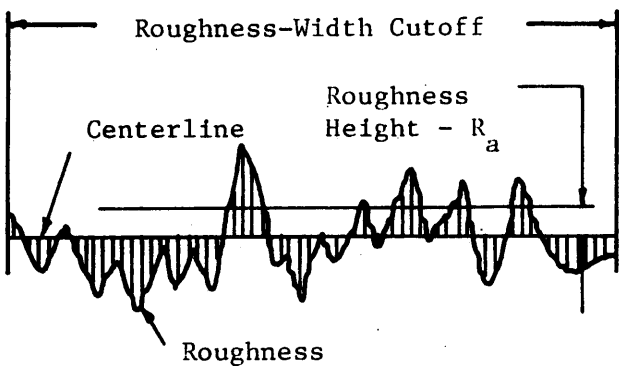


Figure 20. A typical stylus profile of a ground steel surface.

tool is a straight line perpendicular to the direction of motion of the tool [44]. The forward face of the tool is usually considered to be a plane surface and the angle which this plane surface makes with the normal to the newly formed metal surface is called the rake angle (α). All of the forces of an orthogonal cutting system lie in a plane and may be represented as shown in Fig. 21. This figure illustrates a positive rake angle, but the mathematics applies to both positive and negative rake angles if the appropriate sign is attached to α .

The tool is driven through the work-piece with a horizontal force F_c and a vertical force F_v giving a resultant force vector R , which forms the diameter of the force circle. The chip in escaping exerts a friction force F along the tool surface and a normal force N perpendicular to the surface.

The relative magnitudes of F and N are determined by the coefficient of friction μ according to the usual relation

$$\mu = \tan \tau = F/N \quad (19)$$

The forces on the shear plane consist of a compressive force F_N and a shearing force F_S . The shear plane of area A_S is the plane in which the shear stress

$$S_S = F_S / A_S \quad (20)$$

is a maximum.

The model is based on the assumption that all the material in the path of the tool is removed as a chip. The work-piece shears along a narrow zone which is the plane of maximum stress leading from the

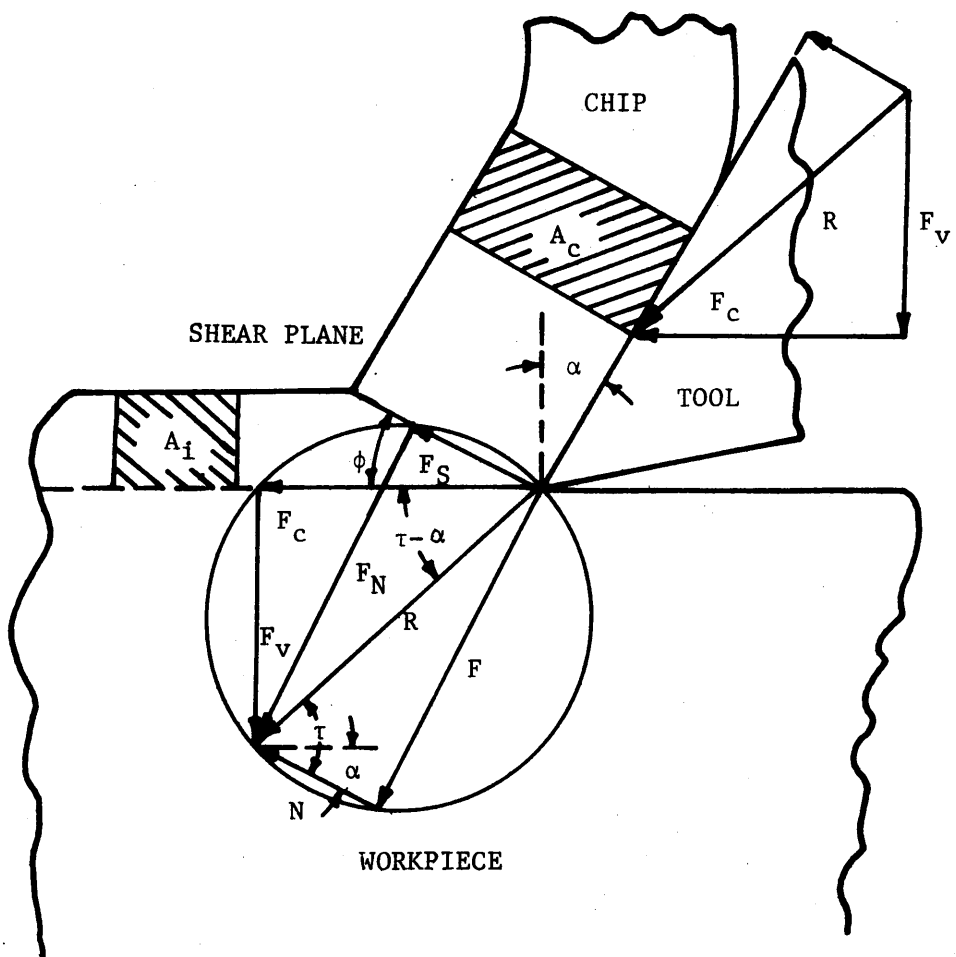


Figure 21. Force Diagram Showing Geometric Relationships Between Forces At Tool Point When No Built-Up Edge Exists [44].

tip of the tool to the surface of the workpiece and forming an angle ϕ with the direction of tool travel. Assuming a constant shear strength for the material being cut, invariant with respect to ϕ and solving for the plane in which the shear stress is a maximum, Ernst and Merchant [45] define the location of the shear plane ϕ as

$$\phi = 45^\circ + \frac{\alpha}{2} - \frac{\tau}{2} \quad (21)$$

Therefore, the shear plane angle is defined by the rake angle and the coefficient of friction between the tool and chip. The shear stress on the shear plane has a value equal to

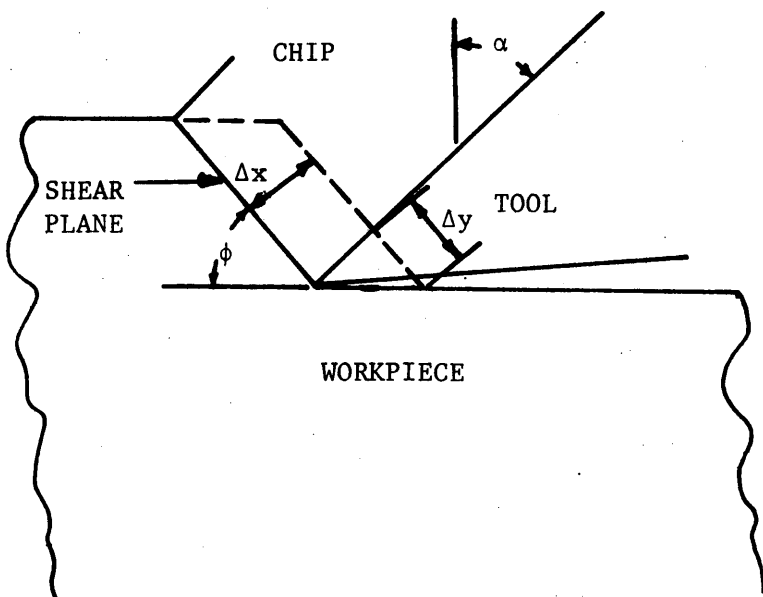
$$S_S = \frac{R \cos (\phi + \tau - \alpha)}{A_i / \sin \phi} \quad (22)$$

Kobayashi and Thomsen [46] define the shear strain (γ_S) in metal cutting as shown in Fig. 22a. In the case shown

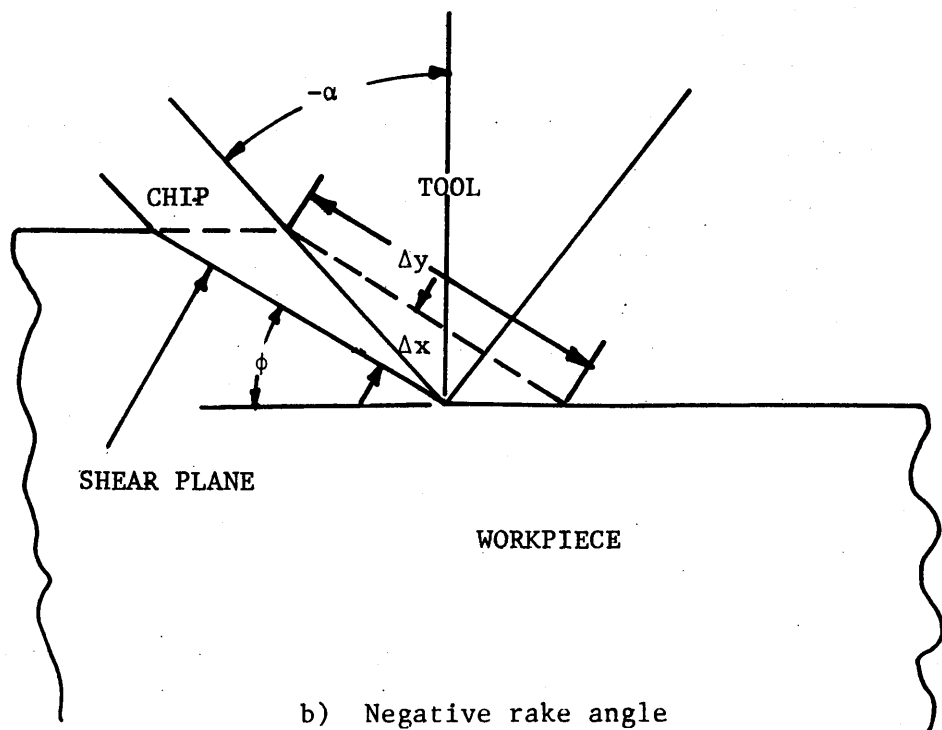
$$\gamma_S = \lim_{\Delta x \rightarrow 0} \frac{\Delta y}{\Delta x} = \cot (\phi) + \tan (\phi - \alpha). \quad (23)$$

The shear strain defined by Eq. 23 is a measure of large plastic shear deformation and also holds for negative rake angles as shown in Fig. 22b.

In reference 47, Merchant finds that the constant shear strength assumption is a poor approximation in the case of the cutting of a polycrystalline metal. The reason for this is that the shear strength is influenced by a number of different quantities. The most important are temperature, rate of shear, shearing strain (plastic) and the



a) Positive rake angle



b) Negative rake angle

Figure 22. Shearing Process on the shear plane [46].

stress acting normal to the plane of shear. Merchant concludes that of the above quantities, the normal or compressive stress existing on the potential shear planes ahead of the cutting edge is the only one which is active in influencing the shear strength when the metal is merely stressed and has not yet started to undergo plastic strain. He concluded that temperature, rate of shear, and shearing strain should all be secondary in their influence on the shear angle, compared to the compressive stress on the shear plane.

According to Merchant, the shear strength of a polycrystalline metal has been quite extensively investigated and for conditions closely duplicating those in metal cutting the relationship between shear strength and normal stress is approximately linear. Therefore, the shear strength of the metal (S'_S) can be defined as

$$S'_S = S'_0 + kS_N \quad (24)$$

where S'_0 is the shear strength of the metal under zero compressive stress, S_N is the normal stress, and k is the slope of the shear strength versus compressive stress curve. S'_0 is approximately equal to one-half the tensile strength of the metal at high values of strain.

By assuming Eq. 24 is true, Merchant again solves for the plane of maximum shear stress. In this case Eq. 21 becomes

$$\phi = \frac{C + \alpha - \tau}{2} \quad (25)$$

where

$$C = \operatorname{arccot}(k) \quad (26)$$

The shear stress on the shear plane is then equal to

$$S_S = \frac{F_c}{A_1} \left(\frac{1}{\cot \phi + \tan (C-\phi)} \right). \quad (27)$$

4.2. Types of Penetration

In order to develop a wear model, assumptions have to be made regarding the type of deformation that the polymer pin is undergoing. Figure 23 illustrates gross amounts of plastic deformation occurring to an originally conical polymer pin due to the application of only a normal load. From this type of observation, one assumes that gross plastic deformation and flowing of the tip of the pin occur until the polymer completely fills the "valleys" of the ground steel surface. It is assumed that the polymer flowing occurs until the projected area of the pin is equal to W_t / p_m where W_t is the normal load and p_m is the flow pressure of the polymer [24]. In the case where the "valleys" of the ground steel surface are completely filled, the apparent and real areas of contact are approximately equal. This case is defined as full penetration.

The material which flows and deforms on the tip of the pin can be modeled as a cylindrical shape as shown in Fig. 24. As material is removed from the pin, full penetration is assumed to occur until the cylindrical portion of height h_o has worn away. Beyond this point, the pin area (apparent area) is greater than the real area required to support the load. This condition is defined as partial penetration. Partial and full penetration are illustrated in Fig. 25.

Knowing the real area of the polymer pin and the type of penetration that is occurring, the orthogonal cutting theory can be modified for polymer wear. This is done for a single pass where full and partial penetration occur.

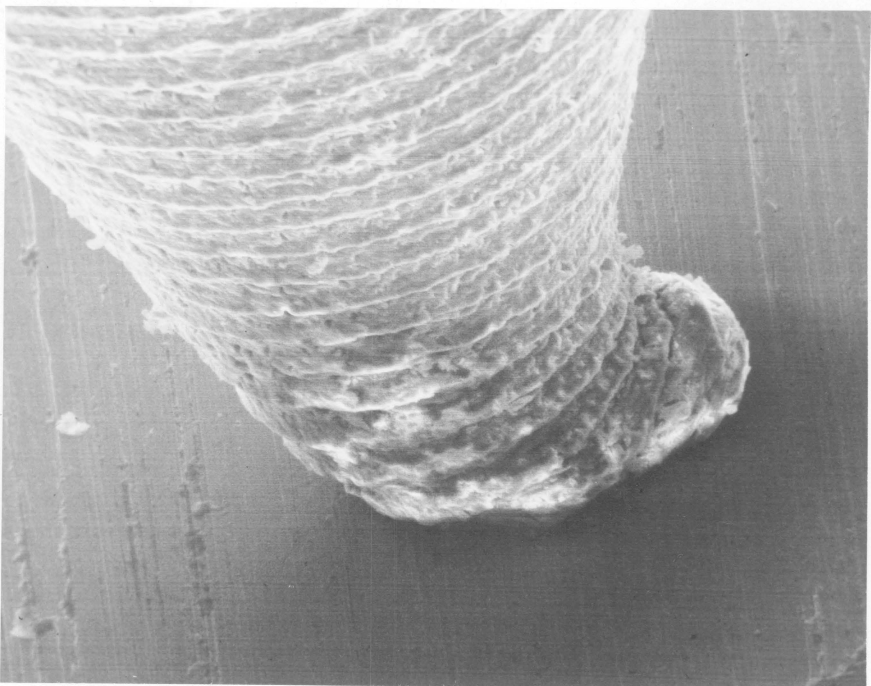


Figure 23. Conical PCTFE pin loaded normal to a ground steel surface.

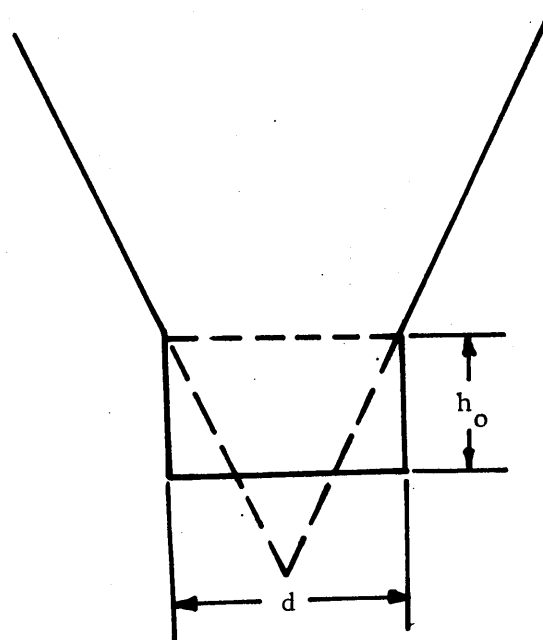


Figure 24. Original Deformation of Conical Polymer Pin.

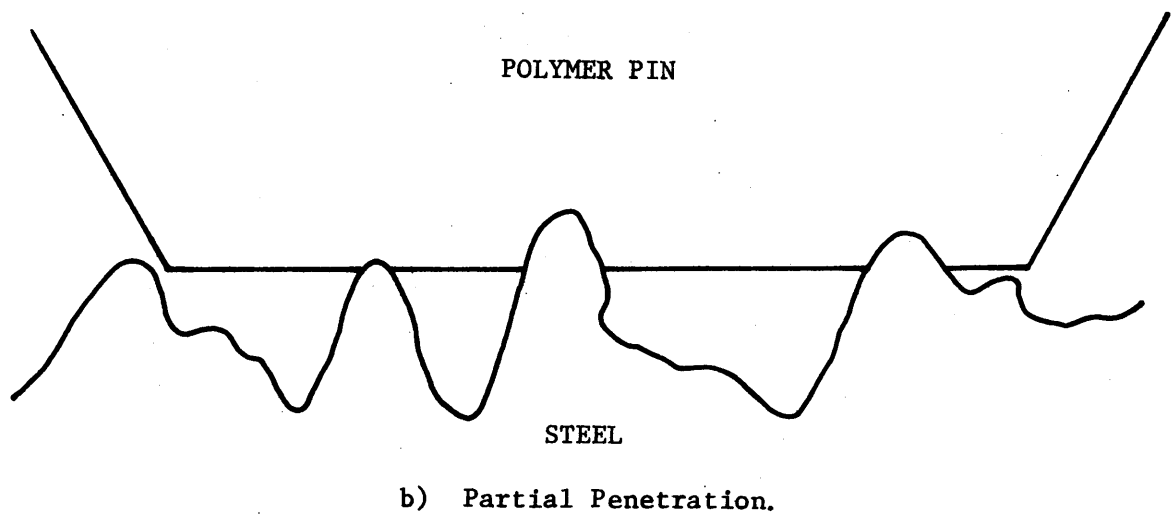
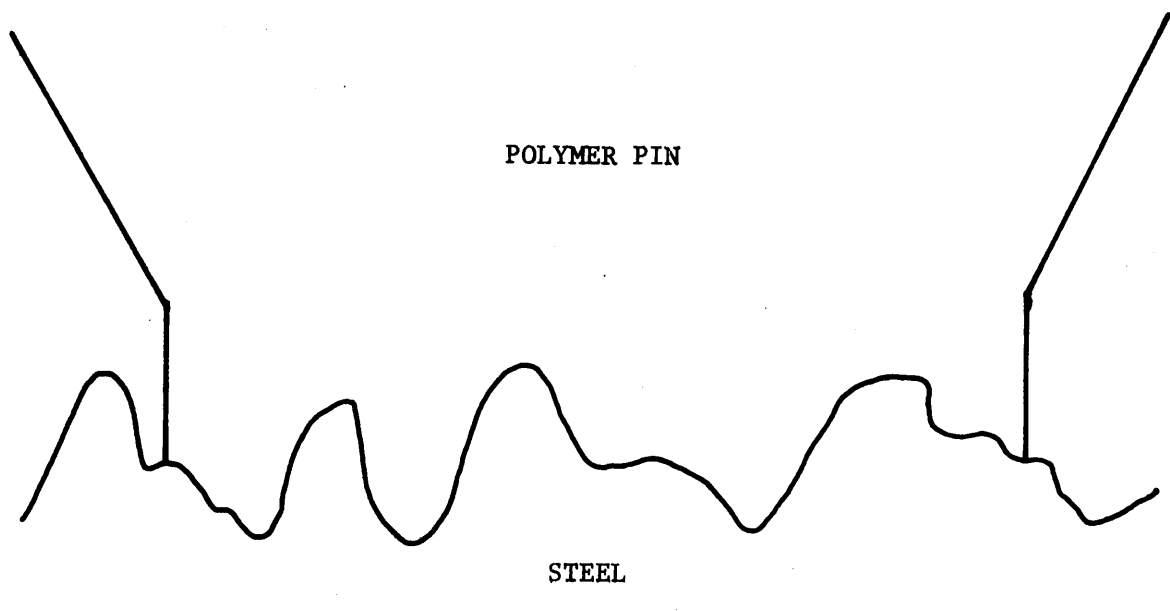


Figure 25. Examples of full and partial penetration

4.2.1. Full Penetration

Figure 26 illustrates the forces acting on a single steel asperity with full penetration under the application of normal (W) and tangential (F) loads. Lines BC and CD denote the steel asperity. Under static conditions the polymer and steel make contact on the surface ABCDE. When a tangential force (F) is applied to the asperity as shown in Fig. 26, the polymer no longer contacts the steel along CDE, where E is determined by the viscoelastic properties of the polymer, the rate of tangential loading and the rate of wear. In the orthogonal cutting theory, as previously discussed, shear occurs along a shear plane AC making an angle ϕ with the horizontal. The chip is free to move along the steel surface BC. However, in this single asperity wear model, the "chip", or polymer deposit, is not free to move along the steel asperity face due to the steel surface AB. Therefore, there can be no friction force between the steel asperity and the polymer deposit along BC and hence τ must equal zero. The only way τ can equal zero is for the resultant R to be perpendicular to the cutting side of the steel asperity BC. The amount of normal load (W) supported by the asperity is

$$W = \frac{A_i \cdot \tan (-\alpha)}{A_r} \cdot W_t \quad (28)$$

where \overline{BC} is the length of side BC, A_i is the cross sectional area of the polymer as shown in Fig. 26, W_t is the total normal load and A_r is the real area of contact of the entire polymer pin.

Knowing the direction of R, the magnitude and direction of W , and the direction of the friction force F, the magnitude of R and F

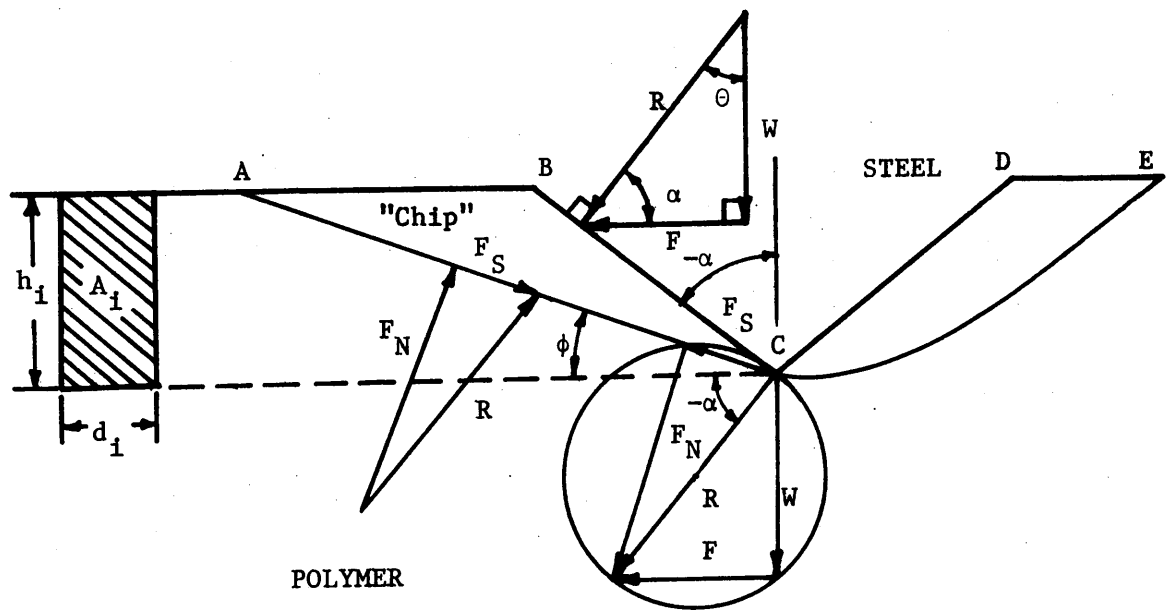


Figure 26. Forces acting on a single steel asperity.

can be determined. As shown in Fig. 26, the angle between R and W is defined as θ , where $\theta - \alpha = 90^\circ$. Therefore

$$R = W / \cos \theta \quad (29)$$

and

$$F = W \cdot \tan \theta. \quad (30)$$

Because the average shear angle for Nylon 6-6, PVC and PCTFE, as determined in Section 3.2.4. are different, it appears that some mechanical property or properties of the polymers must influence ϕ . Therefore, the polymer wear model must include polymer mechanical properties. If the constant shear strength assumption is made for the polymers, the shear angle ϕ is a function of only the asperity angle ($-\alpha$) according to Eq. 21. However, if one assumes that the shear strength of the polymer is a linear function of the normal stress, then Eq. 25 predicts that ϕ changes not only with $-\alpha$ but also with k , a property of the polymer. Therefore, the shear strength of the polymer is assumed to be a linear function of the normal load as described in Eq. 24 for the wear model. With $\tau = 0$, Eq. 25 becomes

$$\phi = \frac{C + \alpha}{2} \quad (31)$$

In order to determine the shear stress on this plane, which is the maximum shear stress in the polymer, F_c/A_i needs to be determined so that Eq. 27 can be evaluated. Referring to Fig. 26

$$F_c = \frac{W}{\tan(-\alpha)} \quad (32)$$

and from Eq. 28

$$W = \frac{A_i \tan(-\alpha)}{A_r} \cdot w_t \quad (33)$$

Assuming

$$W_t = A_r p_m \quad (34)$$

then

$$F_c = \frac{A_i \tan(-\alpha) A_r p_m}{A_r \tan(-\alpha)} \quad (35)$$

or

$$\frac{F_c}{A_i} = p_m \quad (36)$$

Therefore, the maximum shear stress in the polymer occurs along an angle ϕ with the direction of horizontal pin travel and is

$$S_S = \frac{p_m}{\cot \phi + \tan(C-\phi)} \quad (37)$$

It is assumed that the relative motion between the slider and the surface will produce sufficient strain to cause rupture if the maximum stress exceeds the shear strength. Therefore, rupture or shear will occur if the shear stress (S_S) is equal to or greater than the shear strength (S'_S) of the polymer. Substituting Eq. 31 into Eq. 27 and setting $S_S \geq S'_S$, then those asperities that have values of α which satisfy the following

$$\frac{S'_S}{p_m} \leq \frac{1}{\cot \frac{(C+\alpha)}{2} + \tan \frac{(C-\alpha)}{2}} \quad (38)$$

will produce wear.

Figure 27 is a plot of S_S/p_m versus α for various values of k . On this graph, the values of S'_S/p_m are shown for PVC and PCTFE. These values are calculated by assuming S'_S is equal to one half the tensile strength of the polymer and p_m is equal to three times the yield strength of the polymer. Tabulated values of the tensile and yield

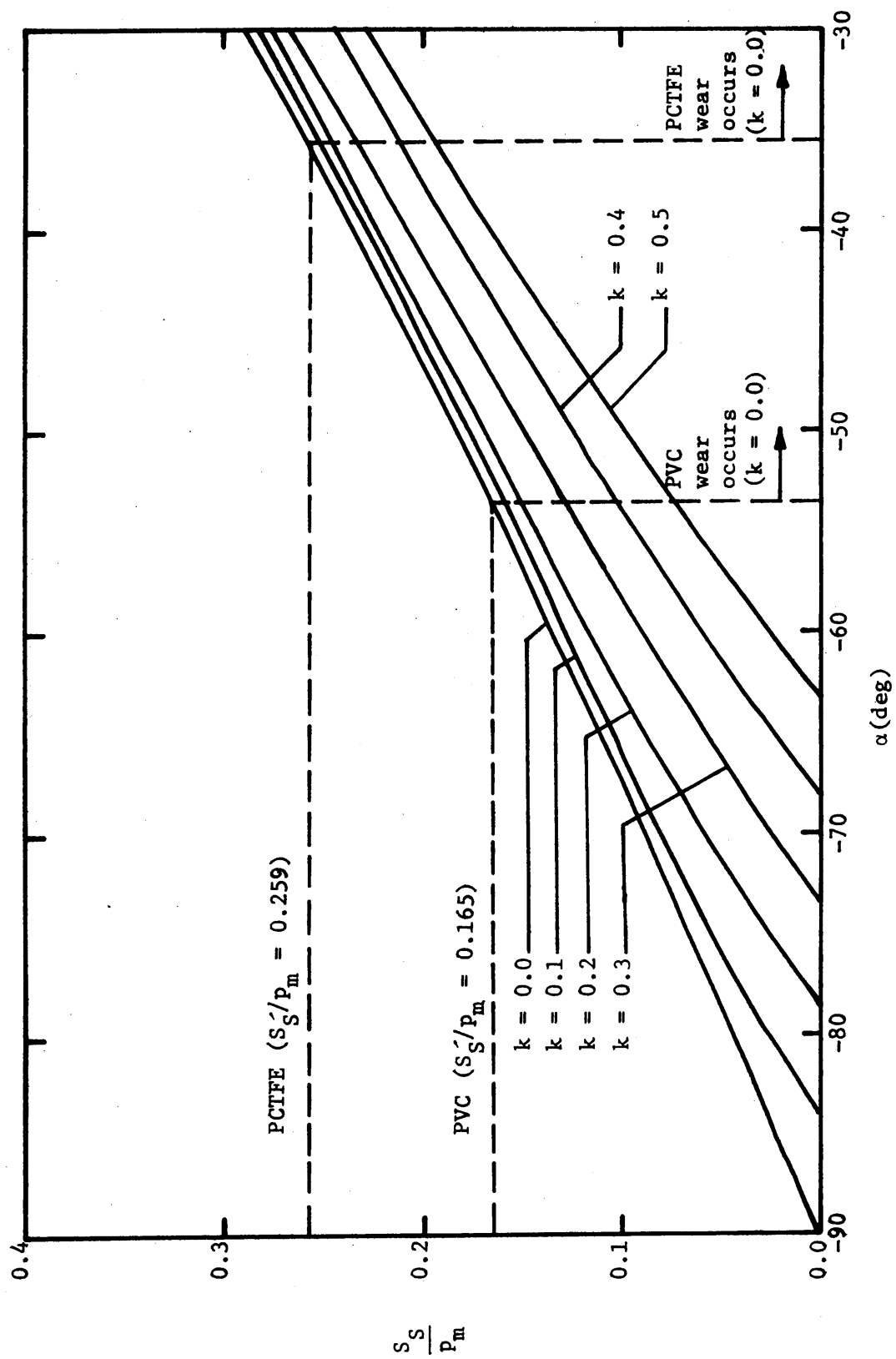


Figure 27. S'_S/P_m versus α for different values of k .

strength are obtained from Table 2. For a given value of k , one notes in Fig. 27 that PVC will shear for values of α which are more negative than the values of α for which PCTFE will shear. For example, if $k=0$ for both polymers, PVC will shear for angles ϕ greater than -53.5 deg whereas PCTFE must have asperity angles greater than -35.2 deg before shear will occur. This means that if $k=0$ for both polymers, asperities with angles α between -53.5 deg and -35.2 deg will produce wear on PVC and will not produce wear on PCTFE. Thus, PVC should wear more than PCTFE. It should also be noted in Fig. 27 that as k increases, the asperities must become sharper (α becomes less negative) in order to produce stresses in the polymer that are large enough to exceed the shear strength of the polymer.

Figure 28 is a plot of ϕ versus k for various values of α . The average shear angles measured from the profiles are also shown. One notes from this plot that for a given asperity angle, the average shear angles measured imply different values of k for the three different polymers. For example, if $\alpha_{avg} = -50$ deg, $k_{PVC} = 0.328$, $k_{PCTFE} = 0.264$, and $k_{Nylon\ 6-6} = 0.040$. This shows that k_{PVC} is greater than k_{PCTFE} . From Fig. 27 for these values of k , asperities with rake angles less than -46 deg will remove PVC and those with rake angles less than -33 deg will remove PCTFE. For sliding on the same surface there are more asperities with rake angles less than -46 deg than with rake angles less than -36 deg. Hence, more asperities should remove more PVC.

Figure 28 also indicates that for a given asperity angle α , if

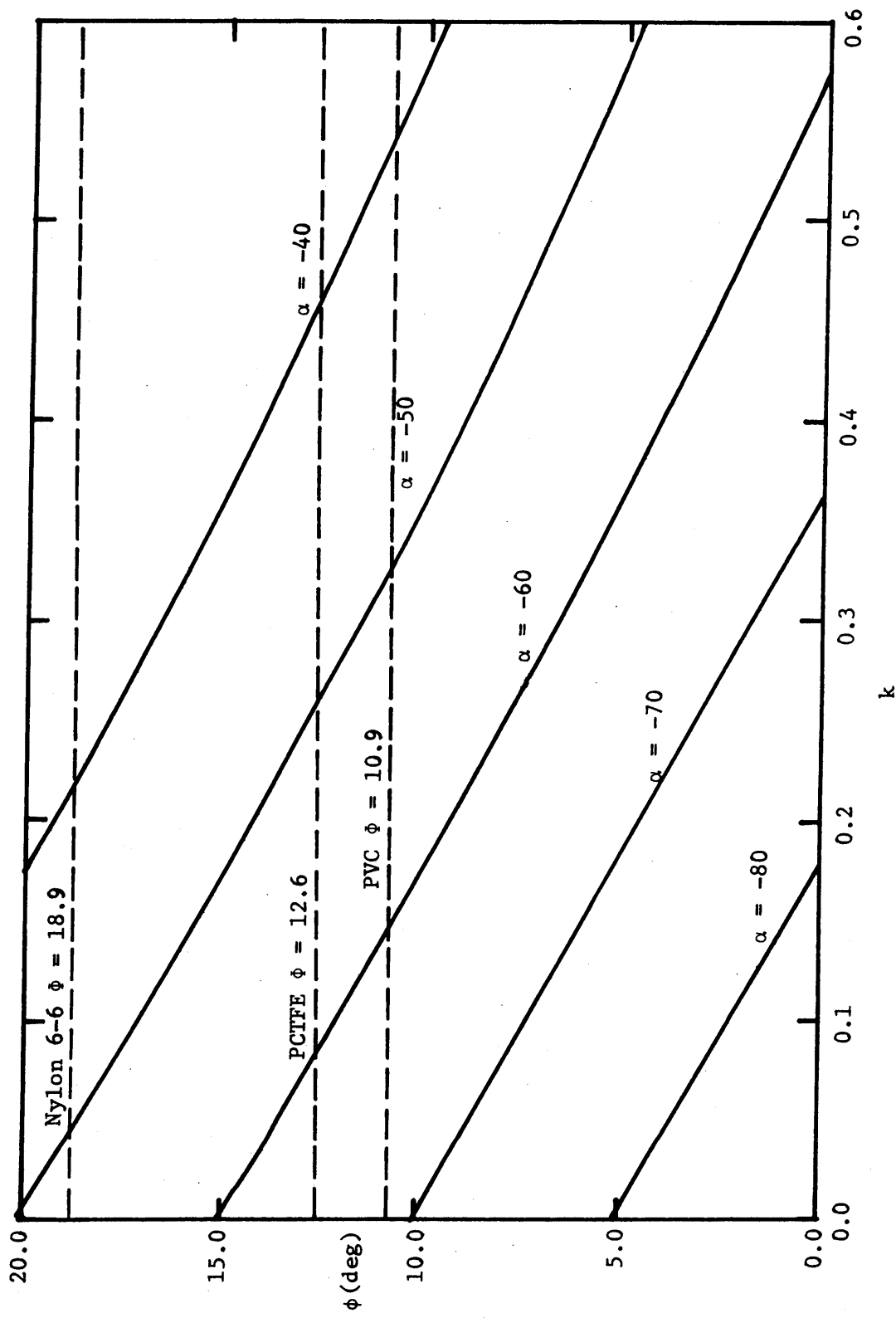


Figure 28. Plot of ϕ versus k for various values of α .

PCTFE and PVC are being removed, PVC will have a shear angle (ϕ_{PVC}) less than the shear angle for PCTFE (ϕ_{PCTFE}). As seen in Fig. 29, the volume removed by a given asperity per unit depth is the area between the profile and the shear plane angle. Thus, PVC will again wear more than PCTFE with the cross hatched area indicating the difference in the amounts of wear.

One also notes from Table 5 on the shear angle data that the minimum average shear angles also correlate with the energy to rupture of the polymers. If for the three polymers one calculates the overall minimum shear angle averages, one obtains the following: 2.8 deg for PVC, 6.7 deg for PCTFE, and 8.2 deg for Nylon 6-6. These correspond to the energy to rupture values of 24.82 MNm/m^3 for PVC, 41.82 MNm/m^3 for PCTFE, and 142.3 MNm/m^3 for Nylon 6-6. Thus, this is another indicator that there is a minimum asperity angle beyond which the product of stress times strain attained in the polymer is not high enough to produce fracture. If one assumes that the stresses must reach the yield point of the polymer and then enough strain will be supplied to produce fracture, the above angles do not exactly correlate. This lack of correlation is because the yield strength of PVC is higher than that of Nylon 6-6, yet Nylon 6-6 has the larger minimum angle. Thus, a determination of which criteria should be used to predict fracture must be made in order to predict the wear correctly.

Comparing the wear and surface topography data to this model, several conclusions are made. From Table 3 one observes that PVC does wear more than PCTFE for both disks 11 and 22. Thus, a correlation

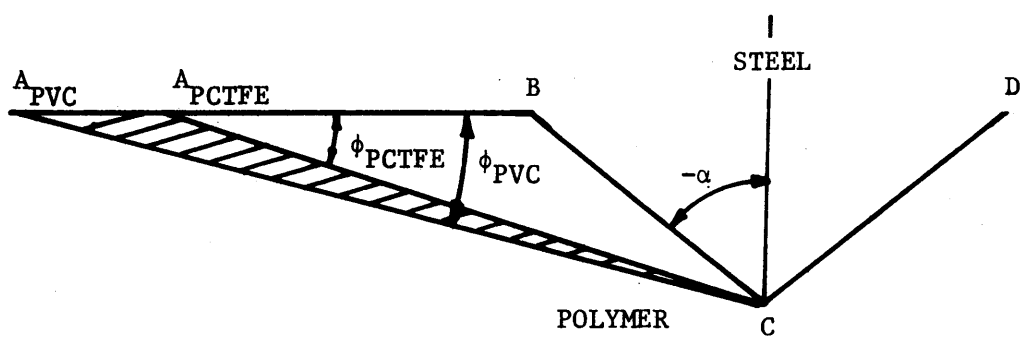


Figure 29. Volume of material removed by a given asperity for PVC and PCTFE.

between the wear and S'/p_m and $1/ER$ of the polymers appears to occur. From Table 2, $ER_{PVC} = 24.82 \text{ MNm/m}^3$ and $ER_{PCTFE} = 41.82 \text{ MNm/m}^3$ and the ratio of $1/ER_{PVC}/1/ER_{PCTFE} = 1.68$. From Table 3 on disk 11, PVC wears 1.3 times more than PCTFE and on disk 22 PVC wears 2.6 times more than PCTFE. Thus, the energy to rupture ratio is between the wear ratios for the two disks. It appears then that the surface topography must also affect the wear.

From Tables 15 and 16 one observes that the maximum peak-to-valley height for disk 22 is $7.00 \mu\text{m}$ whereas for disk 11 it is only $1.17 \mu\text{m}$. Thus, more wear should occur on disk 22. This does occur. One also notes that the average profile slope for disk 22 is 0.0234 and on disk 11 the slope is only 0.0072. This implies sharper asperities and higher stresses in the polymer for disk 22 than 11, according to Fig. 27, and hence more wear should again occur on disk 22. It was shown in reference 20 that the product of the correlation length L times the arithmetic average R_a correlated with the wear on a given surface. One observes in Tables 15 and 16 that for disk 22 $L \times R_a$ is $8.60 \mu\text{m}^2$ and for disk 11 it is $1.76 \mu\text{m}^2$. Thus, disk 22 should again have more wear. One also notes that the RMS values of 0.47 and 0.14 for disks 22 and 11, respectively, also correlate with the wear.

In Table 23 the data for rectangular block 5 is given. This is one of the blocks that the shear angle measurements were made on. It is interesting to note the differences in the parameters given for the profile mode and the roughness mode. One notes that every

parameter listed is larger for the profile mode. This emphasizes, once again, the problems involved in making sure that the surface data obtained is representative of the surface. From the profile mode data one notes that the maximum asperity base angle is 24.5 deg, hence the measured average angles Φ could indeed have been measured from this surface. This, however, points out a problem with the modified orthogonal cutting theory model. According to Fig. 27, in order for shear to occur for PVC with $k=0$, the maximum base angle $(90 + \alpha)$ must be greater than or equal to 36.5 deg. However, on rectangular disk 5, the maximum angle over the distance traced is 24.5 deg. Therefore, the model must be incorrect since wear did occur on disk 5. There are several assumptions that are made in the model that might be wrong and should be investigated in future work. One notes in Fig. 27 that if S'_S/p_m for each polymer were lower, wear would occur for shallower asperities. This means that S'_S should be smaller and/or p_m should be larger. Therefore, the value of S'_S equal to one-half the tensile strength of the polymer might be too large and hence should be investigated for varying strain rates. Also the flow pressure of the polymer probably varies as a function of asperity angle and might not be a constant equal to $3Y$ as shown and assumed for metals in reference 24. This again needs to be investigated for varying strain rates. It is obvious that the assumption of constant shear strength is incorrect since the shear angle data is different for different polymers. However, the linear assumption with respect to normal load as assumed for metals might not be correct. This,

needs to be investigated also, as no work in this area is available to the author's knowledge.

In reference 48, Rao, et al. ran some cutting tests on Delrin and Zytel plastics and found that indeed the coefficient of friction between the tool and the chip was approximately zero. Thus, the author feels that assuming $\tau=0$ when the chip cannot move is correct.

One also notes that the average profile slope on block 5 in the roughness mode is 0.0318 and on disk 22 is 0.0234. Thus, the maximum base angle for disk 22 is probably much less than the maximum base angle of 16.7 deg observed on block 5. But wear does occur on disk 22 and this again points out the problem with the S'_s/p_m value used in the model.

4.2.2. Partial Penetration

For partial penetration, the assumption of $\tau=0$ as made for the full penetration case is still assumed since Rao, et al. [48] observed a coefficient of friction approaching zero in the cutting of Delrin and Zytel plastics. If $\tau=0$, then the same model used in the full penetration case can be assumed, except that the chip is free to move. Equation 38 and Fig. 27 are still correct for determining the relative magnitudes of asperity slopes that will remove material for the different polymers. Thus, from Fig. 27 one suspects that more asperities will remove PVC than PCTFE.

In comparing the wear data given in Table 24 for disks 19, 20 and 31 for polymers PVC and PCTFE, one notes that PVC wears more than PCTFE. However, for disk 33, PCTFE wears more than PVC. Thus, surface parameters must also be affecting the wear.

Figure 30 is the upper portion of the bearing area curves for disks 18, 19, 20, 31 and 33 with the data being obtained from the bottom inside stylus traces. The bearing areas required to support PVC and PCTFE under both the 0.98 and the 1.96N loads are shown. Knowing these areas, the depths of polymer penetration into the steel surfaces can be determined for each. By comparing the depths of penetration with the wear and plotting wear versus depth of penetration as shown in Fig. 31, several interesting conclusions are made.

First, the PVC data appears in general to have more wear than

Table 24. Summary of Wear and Bottom Inside Profile Data for Disks 18, 19, 20, 31, and 33.

Disk	Load (N)	Polymer	Depth (μm)	Slope	Wear (10^9 Kg/m)
18	1.96	PVC	1.94	0.084	7.16
19	0.98	PCTFE	1.08	0.069	2.91
19	0.98	PVC	0.40	0.060	5.73
20	0.98	PCTFE	0.38	0.052	0.46
20	0.98	PVC	0.20	0.078	0.96
31	1.96	PCTFE	0.52	0.039	0.89
31	1.96	PVC	0.31	0.047	1.08
31	0.98	PCTFE	0.42	--	0.70
33	1.96	PCTFE	0.83	0.051	2.14
33	1.96	PVC	0.52	0.071	1.47

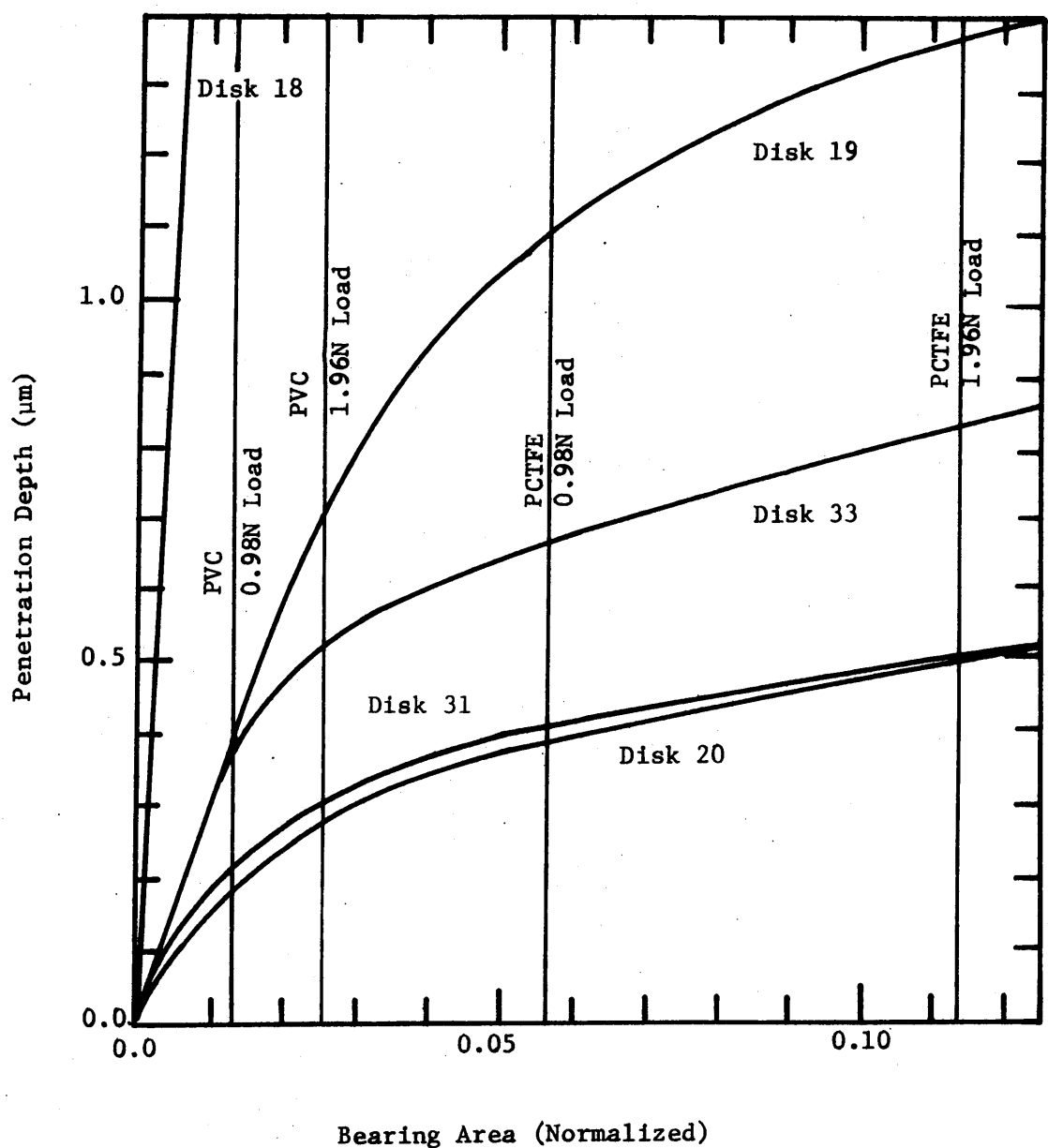


Figure 30. Upper portion of bearing area curve for disks 18, 19, 20, 31 and 33.

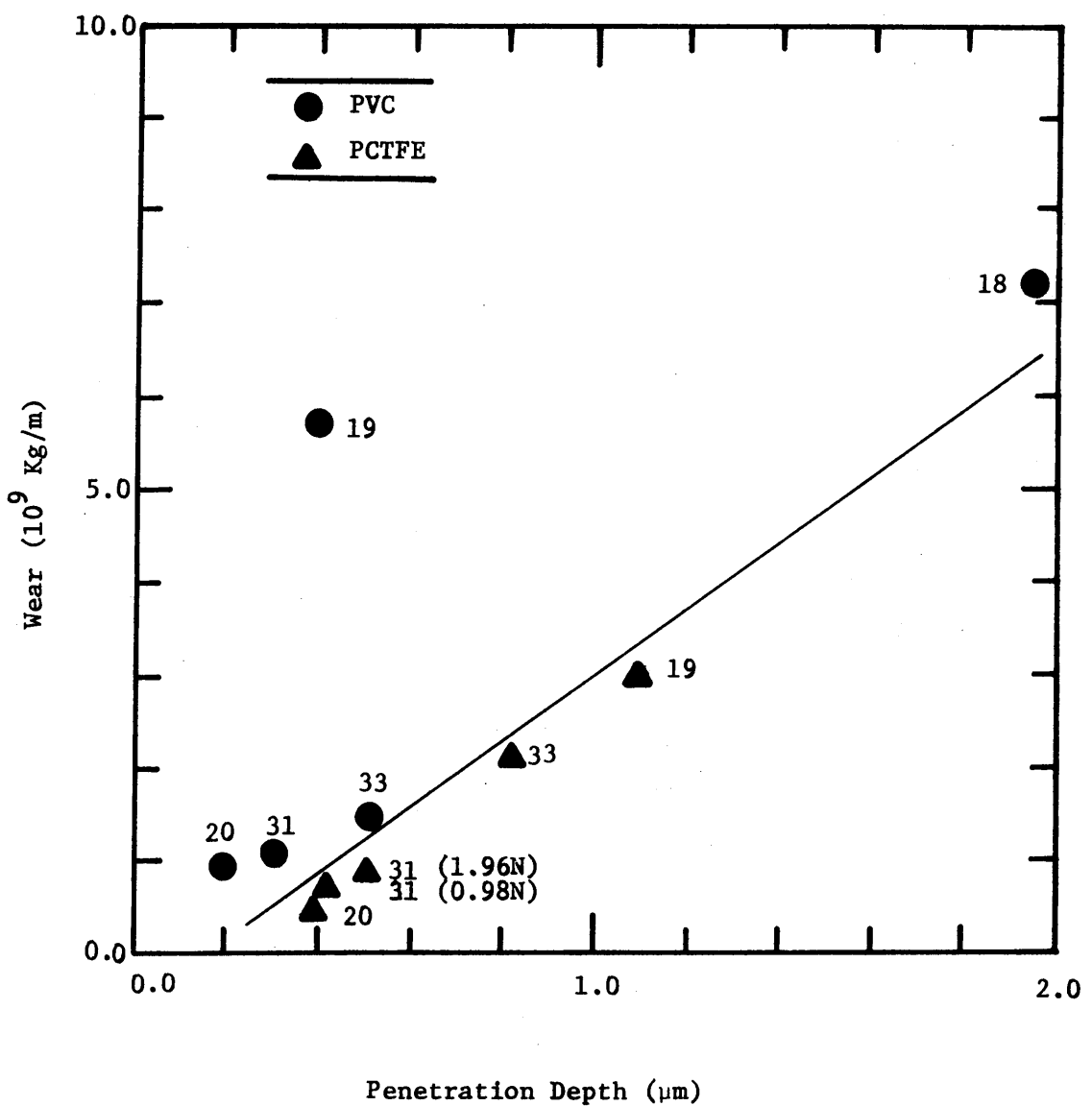


Figure 31. Wear versus penetration depth for disks 18, 19, 20, 31 and 33.

the PCTFE data as noted by the points above and below the solid line drawn on the graph. Secondly, at the same depth of penetration PVC appears to have more wear than PCTFE (e.g. compare wear for disk 31 (1.96N load) with wear for disk 33). This is expected from the model and the shear angle data since at the same depth more asperities should be removing PVC. Also, asperities removing both PVC and PCTFE will remove more PVC since the shear angle is smaller for the PVC.

One notes from Fig. 31 for the PVC data that there appears to be a lot of scatter. This is explained by the fact that the depth of penetration is defined from the highest peak on the stylus trace. Thus, if the surface has a peak much higher than the peak shown in the area traced, the wear on the disk will be more than the predicted wear. This appears to be the case for disk 19 since the data given in Table 18 indicates an outlying point that would increase the wear. This point, however, is on the bottom outside trace rather than the bottom inside trace used in Fig. 31 and hence the penetration depth plotted is actually less than the total surface penetration. This is another reason that one must be sure that the surface data is indicative of the entire surface being characterized.

For the PCTFE pins, the wear always increases as the depth increases for the different steel disks. Thus, the depth of penetration appears to be a good parameter for indicating the amount of wear that will occur since it includes both mechanical properties of the polymer and surface properties of the steel disk. Factors such as the flow pressure (p_m) used to determine the real area of contact

and hence the penetration depth of the polymer needs to be investigated along with more experiments of different polymers to determine if indeed the depth of penetration is indicative of the wear of a given polymer.

Table 25 shows the average slope data for disks 19, 20, 31 and 33. The overall average slope of the profile and the average slopes above the PVC and PCTFE bearing heights are also given. One notes that the average slope increases when going from the PCTFE bearing height to the PVC bearing height. Thus, with the average slopes being greater, higher stresses are predicted and thus more asperities should remove PVC rather than PCTFE. It should be noted that defining the slope of a real asperity rather than the slope of a wedge as is done in the previous model is going to be most important in the wear process. For a real asperity, the slope usually changes between any two points. This is indicated by the differences in the averages shown for the parts of the profile above the bearing height in Table 25. Curvature of the asperity peak is also probably a most important parameter since the sharpness of the peak will determine the magnitude of the stress in the polymer. Due to the magnitude of the shear angles measured on the rectangular disks and the smallness of the average slope values reported for block 5, it is the author's feeling that average profile slopes are not going to be very useful in predicting polymer wear. It also appears to be the upper portion of the profile that is important in determining when wear occurs.

Table 25. Average Slope Data for
Disks 19, 20, 31 and 33.

Disk	Overall Average	Average Above PCTFE Bht	Average Above PVC Bht
19	0.0325	0.0958	0.1518
20	0.0333	0.0546	0.0681
31	0.0226	0.0373	0.0455
33	0.0379	0.0548	0.0650

5. CONCLUSIONS AND RECOMMENDATIONS

For polymers PVC, PCTFE, and Nylon 6-6 wear occurs in discrete sites rather than continuous films. At these discrete sites the polymer shears at an angle which is dependent on the mechanical properties of the polymer and on the asperity angle. There appears to be a minimum shear angle for each polymer beyond which no wear occurs. This angle correlates with the energy to rupture of the polymer.

Orthogonal cutting theory can be modified to predict a shear angle which is dependent on both the asperity angle and the polymer properties, if it is assumed that the shear strength of the polymer is a linear function of the normal load. The modified theory requires, however, that material removing asperities have slopes much larger than those actually measured on the steel surfaces investigated. Thus, assumptions made in the model regarding the shear strength and the flow pressure of the polymer might be incorrect and should be investigated in future research.

In the model given it is assumed that the coefficient of friction between the asperity and the chip is zero, since the chip cannot move. However, as seen in Fig. 32, no mention was made of the forces acting along the surface AB. In this case AB supports part of the normal load W' , and F'_f is the force which opposes the tendency for the polymer to slide from C to B as in metal cutting theory. An investigation of the effect of these forces should also be made in future research.

The shear strength of the polymer as a function of normal load must also be determined. It was shown that when the normal

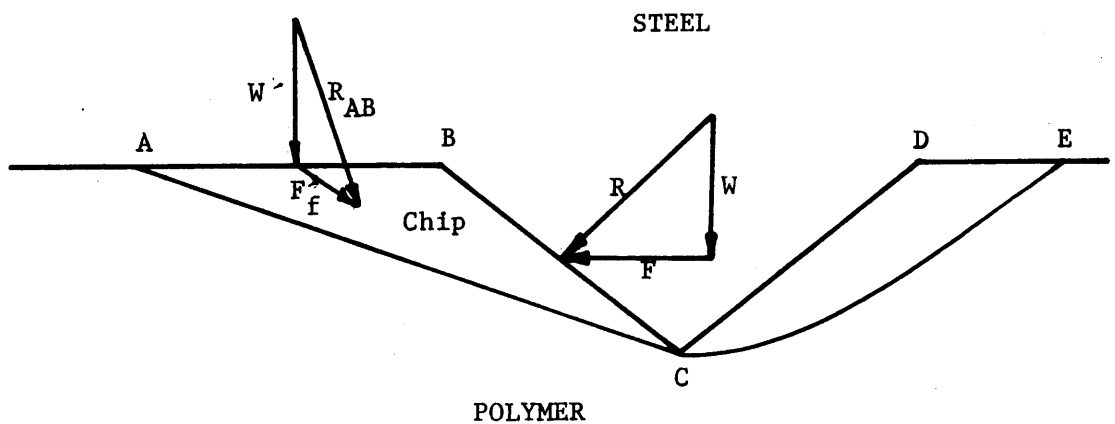


Figure 32. Additional forces that might be acting on the steel asperity and polymer chip.

load had no effect on the shear strength, the shear angle was only a function of the asperity angle. However, when it was assumed that the shear strength was a linear function of the asperity angle, the model predicted much larger asperity slopes that would produce wear, than those at which wear actually occurred. Thus, experimental verification of the effect of normal load on the shear strength of polymers would be most helpful.

In the wear model a parameter was needed to estimate when the polymer will fracture. The energy to rupture was investigated along with S'_S/p_m . Correlations were shown for both of these, however, more work needs to be done in this area. For instance, if S'_S/p_m is to be used, better estimates of S'_S and p_m need to be made. Experimental work needs to be done to determine if p_m is actually equal to $3Y$ for the polymer and if so, is p_m a constant independent of the asperity angle. Also, is one-half the tensile strength of the polymer a good estimate for S'_S .

The steel surface roughness is very important in determining the wear of the polymers. For the full penetration case, the peak to valley heights, arithmetic average (R_a), correlation length times arithmetic average, and average profile slopes all tend to correlate with the wear. The factor S'_S/p_m and $1/ER$ for the different polymers also correlates with the wear.

One must be careful to make sure that the calculated surface profile statistics are indicative of the surface being characterized. It was shown that surface parameters calculated from traces of the same

surface, one trace having a 762 μm waviness filter and one having no filter made quite a difference in the surface data reported. The data calculated from the trace with no filter was larger than that calculated from the trace with the filter. Thus, when a filter is used it should be made small enough to include wavelengths comparable to the dimensions of the apparent area of the polymer pin in the direction of sliding.

In the partial penetration case, the amount of wear appears to be discriminated by the depth of penetration of the polymer into the steel surface. The depth of penetration appears to be a good parameter for indicating the amount of wear since it includes both mechanical properties of the polymer and surface properties of the steel disk. Factors such as the flow pressure (p_m) used to determine the real area of contact and hence the penetration depth of the polymer, need to be investigated along with more experiments of different polymers to determine if indeed the depth of penetration is indicative of the wear.

Although the depth of penetration appears to be important, other parameters such as the reciprocal mean peak curvature need to be investigated in order to completely describe the wear process. This type of parameter will have much to do with the magnitude of the stresses occurring in the polymer and hence the amount of wear that occurs. A definition of the asperity slope that is important in the wear process will eventually have to be made, since the slope of an

asperity usually changes between any two points on a real surface.

The wedge type asperity model in which the slope is a constant is greatly oversimplified.

Concluding, correlations have been made between the amount of wear, and the polymer and surface properties involved. An attempt has been made to modify orthogonal cutting theory into a wear model, however, properties of the polymer need to be investigated further in order to be able to completely predict polymer wear. Along with further development of the model, more data on the shear angle, and also wear and surface characterization data, will be an asset in this endeavor. Extension of the NAA technique to more polymers will also be helpful.

6. REFERENCES

1. Dourlet, E. F., "Selecting Plastics," Machine Design, Plastics/Elastomers Reference Issue, 1971, pp. 1-4.
2. Steijn, R. P., "Friction and Wear of Plastics," Metals Engineering Quarterly, American Society for Metals, May, 1967, pp. 9-21.
3. Briscoe, B. J., C. M. Pooley, and D. Tabor, "Friction and Transfer of Some Polymers in Unlubricated Sliding," Advances in Polymer Friction and Wear, L. H. Lee, Ed., Volume 5A, Plenum Press, New York, 1974, p. 191.
4. Lancaster, J. K., "Abrasive Wear of Polymers," Wear, 14, 1969, p. 223.
5. Lancaster, J. K., "Basic Mechanisms of Friction and Wear of Polymers," Plastics and Polymers, 41, 1973, p. 297.
6. Lee, L. H., "Effect of Surface Energetics on Polymer Friction and Wear," Advances in Polymer Friction and Wear, L. H. Lee, Ed., Volume 5A, Plenum Press, New York, 1974, p. 31.
7. Dowson, D., J. R. Atkinson, and K. Brown, "The Wear of High Molecular Weight Polyethylene with Particular Reference to its Use in Artificial Human Joints," Advances in Polymer Friction and Wear, L. H. Lee, Ed., Volume 5B, Plenum Press, New York, 1974, p. 533.
8. Lancaster, J. K., "Relationships Between the Wear of Polymers and Their Mechanical Properties," Proc. Instn. Mech. Engrs., 183, 3P, January, 1969, pp. 98-106.
9. Bayer, R. G., W. C. Clinton, C. W. Nelson, and R. A. Schumacker, "Engineering Model for Wear," Wear, 5, 1962, p. 378.
10. Clinton, W. C., T. C. Ku, and R. A. Schumacker, "Extension of the Engineering Model for Wear to Plastics, Sintered Metals and Platings," Wear, 1, 354, 1964.
11. Hollander, A. E. and J. K. Lancaster, "An Application of Topographical Analysis to the Wear of Polymers," Wear, 25, January, 1973, pp. 155-170.

REFERENCES (cont'd)

12. Steijn, R. P., "Sliding Experiments with Polytetrafluoroethylene," ASLE Transactions, 11, 1968, pp. 235-247.
13. Pooley, C. M. and D. Tabor. "Friction and Molecular Structure: The Behavior of Some Thermoplastics," Proc. Royal Soc. London, 329, 1972, pp. 251-274.
14. Lancaster, J. K., "A Review of Radio-Active Tracer Applications in Friction, Lubrication, and Wear," Royal Aircraft Establishment, Tech. Note CPM64, March, 1964.
15. Rabinowicz, E., Friction and Wear of Materials, John Wiley and Sons, New York, 1965.
16. Eiss, N. S. Jr., S. D. Doolittle and J. H. Warren, "An Application of Neutron Activation Analysis to the Measurement of the Wear of Polymers, Wear, 38, No. 4, 1976, pp. 127-143.
17. Young, R. D., "Surface Microtopography," Physics Today, 24, Nov. 1971, pp. 42-49.
18. Young, R. D. and E. C. Teague, "The Measurement and Characterization of Surface Finish," Properties of Electrodeposits, Their Measurement and Significance, Chapter 2, pp. 22-49.
19. Thomas, T. R., "Recent Advances in the Measurement and Analysis of Surface Microgeometry," Wear, 33, 1975, pp. 205-233.
20. Eiss, N. S. Jr., and J. H. Warren, "The Effect of Surface Finish on the Friction and Wear of PCTFE Plastic on Mild Steel," Society of Manufacturing Engineers, Paper No. IQ75-125, April, 1975.
21. Thomas, T. R., C. F. Holmes, H. T. McAdams, and J. C. Bernard, "Surface Features Influencing the Effectiveness of Lip Seals: A Pattern Recognition Approach," Society of Manufacturing Engineers, Paper No. IQ75-128, April, 1975.
22. Eiss, N. S. Jr., and J. H. Warren, "Current Advances in Surface Characterization," to be presented at the 2nd ASME Design Technology Transfer Conference, Montreal, Canada, Sept. 27-30, 1976.
23. Archard, J. F. and W. Hirst, "The Wear of Metals under Unlubricated Conditions," Proc. Royal Soc. London, Vol. A, 236, 1956, p. 397.

REFERENCES (cont'd)

24. Bowden, F. P. and D. Tabor, The Friction and Lubrication of Solids, Part I, Oxford University Press, Ely House, London, 1950, pp. 10-14.
25. Halliday, J. S., "Surface Examination by Reflection Electron Microscopy," Proceedings of the Institute of Mechanical Engineers, London, 169, 1955, p. 777.
26. Greenwood, J. A. and J. P. B. Williamson, "Contact of Nominally Flat Surfaces," Proc. Royal Soc. London, Sec. A, 295, 1966, p. 300.
27. Lewis, R. B., "Predicting the Wear of Sliding Plastic Surfaces," Mechanical Engineering, October, 1964, pp. 32-35.
28. Halling, J., Ed., Principles of Tribology, The Macmillan Press, LTD., London, 1975, pp. 140-145.
29. Ratner, S. B., I. I. Farberova, O. V. Radyukevich, E. G. Lur'e, "Connection Between Wear Resistance of Plastics and Other Mechanical Properties," Soviet Plastics, 1964, (Plast. Massy, 1963), No. 7, 37, pp. 145-160.
30. Pepper, S. V., "Auger Analysis of Films," Journal of Applied Physics, Vol. 45, No. 7, July, 1974, pp. 2947-2956.
31. Pooley, C. N. and D. Tabor, "Friction and Molecular Structure: The Behavior of Some Thermoplastics," Proc. Royal Soc. London, Sec. A, 329, 1972, p. 251.
32. Quinn, T. F. J., The Application of Modern Physical Techniques to Tribology, Van Nostrand Reinhold Company, London, England, 1971, pp. 1-253.
33. Torgusen, S. J. E., "On-Line Statistical Analysis of Surface Roughness by Means of a Small Digital Computer," Technical Univ. of Norway, Trendheim, June, 1969.
34. The American Society of Mechanical Engineers, "Surface Texture (ASA B46.1 - 1962)," United Engineering Center, 345 East 47th Street, New York 17, New York.
35. Young, R. D., "The Role of NBS in the U. S. National Measurement System for Surface Finish," submitted to Members of Committee S-CIRP, May, 1974.

REFERENCES (cont'd)

36. McAdams, H. T., "Quantitative Physio-Geometric Approach to Surface Integrity," Presented at 1974 SESA Meeting, Detroit, Michigan, May 14-17, 1974.
37. McAdams, H. T., "Scanning Electron Microscope and the Computer: New Tools for Surface Metrology," Modern Machine Shop, June, 1974, pp. 82-91.
38. 3M Company, "Physical Properties of Kel-F81 Plastic," Technical Information Bulletin, August 1, 1961.
39. Eiss, N. S. Jr., J. H. Warren and T. F. J. Quinn, "On the Influence of the Degree of Crystallinity of PCTFE on its Transfer to Steel Surface of Different Roughnesses, to be presented at the Leeds-Lyon Symposium on the Friction and Wear of Non Metallic Materials, September 7-10, 1976, Leeds, England.
40. American Society for Testing Metals, Annual Book of ASTM Standards, Part 27, Plastics-General Method of Testing, Nomenclature, Easton, Maryland, 1973, pp. 186-193.
41. "Materials Selector 75," Materials Engineering, Vol. 80, No. 4, September, 1974, p. 186.
42. Kramer, C. Y., "Extension of Multiple Range Tests to Group Means with Unequal Numbers of Replications," Biometrics, 12, September, 1956, pp. 307-310.
43. Duncan, D. B., "Multiple Range and Multiple F tests," Biometrics, 11, March, 1955, pp. 1-42.
44. Mohun, W. A., "Grinding with Abrasive Disks, Part 3 - Attritious Camber, Glazing and Rate of Cut," Trans. ASME, Journal of Engineering for Industry, November, 1962, pp. 451-465.
45. Ernst, H. and M. E. Merchant, "Chip Formation, Friction and Finish," Surface Treatment of Metals, American Society for Metals, Cleveland, Ohio, 1941, pp. 299-378.
46. Kobayashi, S. and E. G. Thomsen, "Metal Cutting Analysis -1, Re-Evaluation and New Method of Presentation of Theories," Trans. ASME, Series B, Journal of Engineering for Industry, February, 1962, pp. 63-70.

REFERENCES (cont'd)

47. Merchant, M. E., "Mechanics of the Metal Cutting Process. II. Plasticity Conditions in Orthogonal Cutting," Journal of Applied Physics, 16, June, 1945, pp. 318-324.
48. Rao, U. M., J. D. Cumming, and E. G. Thomsen, "Some Observations on the Mechanics of Orthogonal Cutting of Delrin and Zytel Plastics," Trans. ASME, Journal of Engineering for Industry, 86, May 2, 1964, pp. 117-121.

7. APPENDIX A: WEAR MEASUREMENT SENSITIVITY

WEAR MEASUREMENT SENSITIVITY

Assuming a Poisson's distribution, the error associated with a given energy peak is

$$\text{Error} = \sqrt{\frac{\text{Area}}{\text{Area}}} \quad (\text{A1})$$

where area = area of the energy peak.

If as shown in Fig. A1 a given background (Bg) is associated with the peak area, then the error is

$$\text{Error} = \sqrt{\frac{\text{Area} + \text{Bg}}{\text{Area}}} \quad (\text{A2})$$

For a given area of 20 counts, Eq. A1 indicates an error of 22.4%, while for a given area of 200 counts, the error is only 7.1%. But if a constant background of 10 counts is associated with both areas, then Eq. A2 indicates an error of 27.4% for the 20 count area and an error of only 7.2% for the 200 count area. It is, therefore, apparent that the larger the peak area, the smaller the percent error will be for a given background.

The equation used to determine the amount of wear, by measuring the activity of the two major energy peaks of gamma radiation from Cl^{38} , is

$$\mu\text{gm} = \frac{\text{Area} \cdot \lambda \cdot 10^6 \cdot 120 \cdot (t_e/t_c)}{\text{SA} \cdot \text{wt} \cdot (1-e^{-\lambda t_a}) \cdot e^{-\lambda t_w} \cdot \text{flux} \cdot (1-e^{-\lambda t_c})} \quad (\text{A3})$$

where

μgm = micrograms of polymer wear

Area = area of energy peak
 = $2.50663 * \text{peak height} * \text{Gaussian peak width}$

λ = decay constant
 = $\ln 2.0 / \text{material half life}$

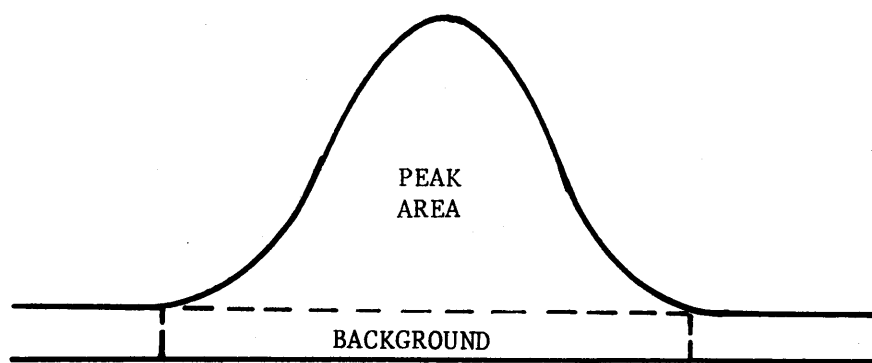


Figure A1. Illustration of energy peak with background for gamma radiation.

120 = normalization constant for reactor flux, where
 flux flux = 1.2×10^{12} neutrons/cm² sec

t_e = elapsed real world time during counting process

t_c = specified counting time

SA = specific activity

wt = 1.00000 for wear measurements

t_a = activation time

t_w = wait time (sample out of reactor until count starts).

Since the micrograms of wear is a constant for a given steel disk being counted, it is desirable to rewrite Eq. A3 as

$$\text{Area} = \frac{\mu\text{gm} \cdot \text{SA} \cdot \text{wt} \cdot (1-e^{-\lambda t_a}) \cdot e^{-\lambda t_w} \cdot \text{Flux} \cdot (1-e^{-\lambda t_c})}{\lambda \cdot 10^6 \cdot 120 \cdot (t_e/t_c)} \quad (\text{A4})$$

so that the factors which influence the size of the peak area can be investigated. By examining the equation term by term, one notes that μgm , SA, wt, flux, and λ are all constant. The term t_e/t_c is also fairly constant. Therefore, the terms which affect the area are $(1-e^{-\lambda t_a})$, $e^{-\lambda t_w}$, and $(1-e^{-\lambda t_c})$, all of which are in the numerator. The term $(1-e^{-\lambda t_a})$ increases as t_a increases. Therefore, an increase in the activation time will increase the peak area. For the term $e^{-\lambda t_w}$, one notes that as t_w gets larger, $e^{-\lambda t_w}$ gets smaller and, hence, the shorter the wait time, the larger the peak area. Finally, one notes that $(1-e^{-\lambda t_c})$ gets larger as t_c gets larger and hence an increase in the elapsed counting time increases the area. Therefore in order to have the largest area, one prefers as large an activation

and counting time as possible, with a small wait time in between.

8. APPENDIX B: SHEAR ANGLE MEASUREMENT

SHEAR ANGLE MEASUREMENT

Figure Bla illustrates the end and side views of a steel asperity with polymer shearing at an angle ϕ . Figure Blb illustrates the same asperity as it is seen in the SEM when titled at an angle of θ_p as shown. In this case, θ_m is the angle measured in the photographs. However, ϕ as shown in Fig. Bla is the angle that is required. It is known that

$$\tan \phi = \frac{L}{y} \quad (B1)$$

and

$$\tan \theta_m = \frac{L \cos \theta_p}{y} \quad (B2)$$

Therefore

$$\tan \theta_m = \tan \phi \cos \theta_p \quad (B3)$$

and hence the shear angle is

$$\phi = \tan^{-1} \left(\frac{\tan \theta_m}{\cos \theta_p} \right) \quad (B4)$$

Equation B4 is then used to determine the real shear angle from the measured angle as reported in the following tables.

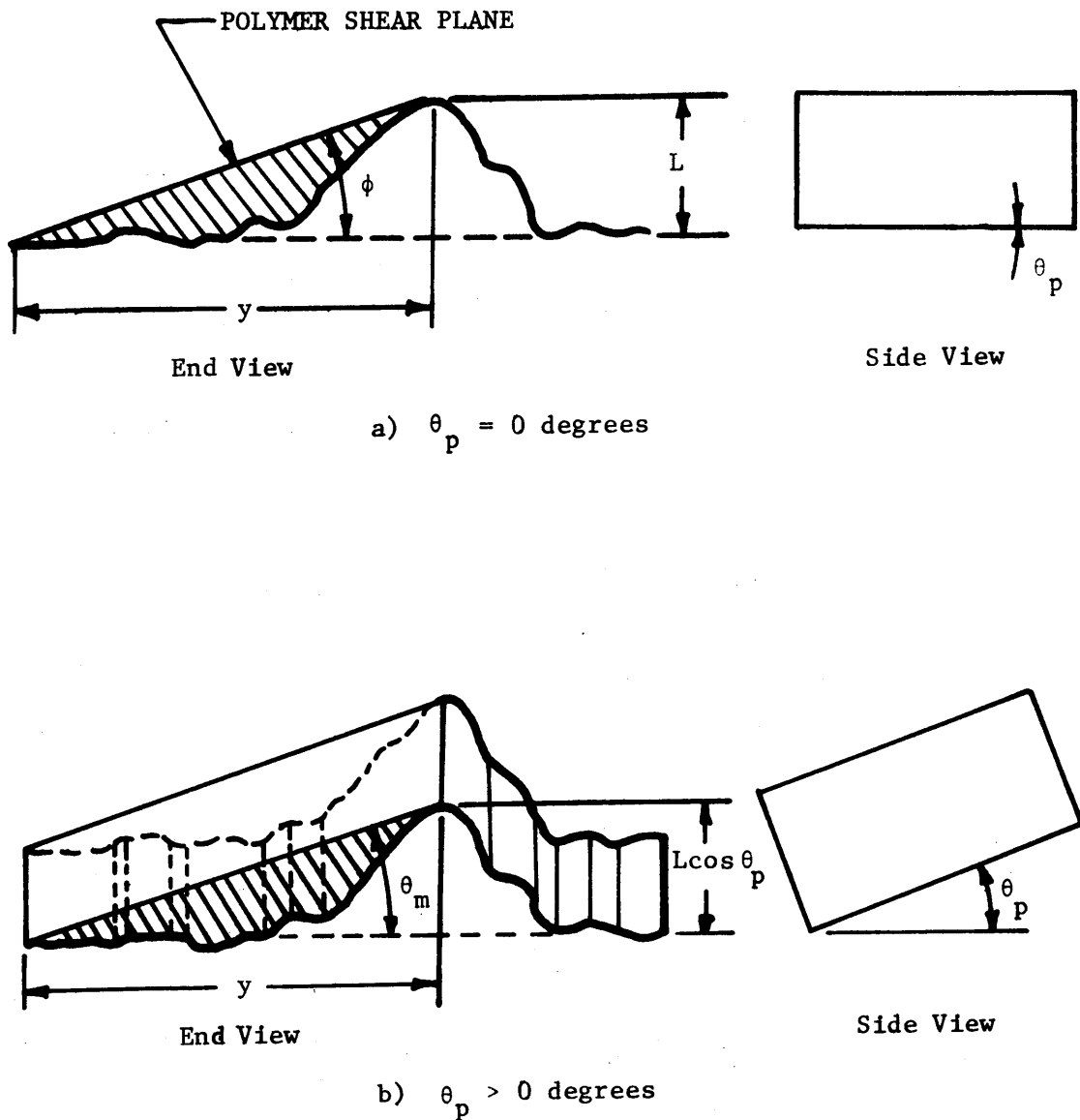


Figure B1. Illustration of polymer shear angle as measured.

POLYMER = PCTFE

LOAD = 14.7 N

DATE = 05/13/76

PHOTO NO.	PHOTO ANGLE (DEG.)	MEASURED ANGLE (DEG.)	REAL ANGLE (DEG.)
1	5.0	13.5	13.5
6	5.0	12.0	12.0
6	5.0	13.0	13.0
8	12.0	12.0	12.3
9	5.0	9.5	9.5
10	5.0	13.5	13.5
11	5.0	12.5	12.5
13	12.0	10.5	10.7
14	12.0	16.0	16.3
15	12.0	10.5	10.7
15	12.0	13.0	13.3
16	19.0	14.5	15.3
17	19.0	12.0	12.7

POLYMER = PCTFE

LOAD = 14.7 N

DATE = 05/19/76

PHOTO NO.	PHOTO ANGLE (DEG.)	MEASURED ANGLE (DEG.)	REAL ANGLE (DEG.)
1	19.0	13.8	14.6
2	26.0	15.0	15.5
3	26.0	12.0	13.3
4	26.0	9.0	10.0
4	26.0	14.0	15.5
5	19.0	8.5	9.0
5	19.0	12.5	13.2
6	19.0	11.0	11.6
6	19.0	15.0	15.8
7	19.0	13.5	14.2
8	19.0	15.5	16.3
9	19.0	9.5	10.0
10	19.0	8.0	8.5
11	19.0	14.3	15.1
12	19.0	7.0	7.4
12	19.0	8.0	8.5
13	19.0	10.0	10.5
14	19.0	8.5	9.0
14	19.0	8.0	8.5
15	19.0	11.5	12.1
15	19.0	10.5	11.1
16	19.0	8.0	8.5
17	19.0	10.0	10.6
18	19.0	10.2	10.8
19	19.0	11.6	12.2
19	19.0	12.0	12.7
20	19.0	6.0	6.3
21	19.0	11.0	11.6
22	19.0	8.0	8.5
23	19.0	11.0	11.6
24	19.0	14.5	15.3
24	19.0	13.0	13.7
24	19.0	15.5	16.3

POLYMER = NYLON 6-6

LOAD = 14.7 N

DATE = 05/21/76

PHOTO NO.	PHOTO ANGLE (DEG.)	MEASURED ANGLE (DEG.)	REAL ANGLE (DEG.)
1	19.0	10.0	10.6
3	19.0	13.0	13.7
3	19.0	14.5	15.3
4	19.0	14.5	15.3
5	19.0	14.0	14.8
5	19.0	14.5	15.3
5	19.0	19.0	20.0
5	19.0	21.5	22.6
6	19.0	18.0	19.0
6	19.0	18.5	19.5
6	19.0	18.5	19.5
7	19.0	16.5	17.4
7	19.0	11.0	11.6
8	19.0	16.0	16.9
8	19.0	26.0	27.3
9	19.0	15.0	15.8
9	19.0	16.0	16.9
10	19.0	26.0	27.3
10	19.0	22.5	23.7
10	19.0	19.0	20.0
10	19.0	20.0	21.1
11	19.0	13.0	13.7
11	19.0	12.0	12.7
11	19.0	14.4	15.2
12	19.0	21.0	22.1
12	19.0	16.5	17.4
12	19.0	11.0	11.6
13	19.0	14.0	14.8
13	19.0	14.5	15.3
14	19.0	18.0	19.0
14	19.0	18.0	19.0
17	19.0	10.0	10.6
18	19.0	15.0	15.8
18	19.0	13.0	13.7
18	19.0	12.5	13.2

NYLON 6-6 14.7 N 05/21/76 (CONTINUED)

PHOTO NO.	PHOTO ANGLE (DEG.)	MEASURED ANGLE (DEG.)	REAL ANGLE (DEG.)
18	19.0	12.5	13.2
19	19.0	16.0	16.9
20	19.0	20.0	21.1
20	19.0	18.0	19.0
20	19.0	12.8	13.5
20	19.0	16.0	16.9
21	19.0	13.0	13.7
21	19.0	14.5	15.3
21	19.0	16.2	17.1
22	19.0	17.0	17.9
22	19.0	14.9	15.7
24	19.0	15.5	16.3
24	19.0	16.5	17.4
24	19.0	14.0	14.8

POLYMER = NYLON 6-6

LOAD = 9.8 N

DATE = 05/25/76

PHOTO NO.	PHOTO ANGLE (DEG.)	MEASURED ANGLE (DEG.)	REAL ANGLE (DEG.)
1	19.0	19.5	20.5
1	19.0	9.0	9.5
2	19.0	16.0	16.9
2	19.0	18.0	19.0
2	19.0	15.0	15.8
3	19.0	25.0	26.3
3	19.0	18.0	19.0
4	19.0	13.0	13.7
5	19.0	17.0	17.9
5	19.0	12.8	13.5
6	19.0	25.0	26.3
6	19.0	17.4	18.3
7	19.0	18.0	19.0
7	19.0	19.2	20.2
7	19.0	14.0	14.8
8	19.0	20.0	21.1
8	19.0	24.0	25.2
9	19.0	20.0	21.1
9	19.0	22.0	23.1
10	19.0	12.5	13.2
10	19.0	18.0	19.0
10	19.0	25.0	26.3
11	19.0	32.0	33.5
12	19.0	11.0	11.6
12	19.0	12.0	12.7
12	19.0	21.0	22.1
12	19.0	24.0	25.2
13	19.0	11.0	11.6
13	19.0	14.0	14.8
13	19.0	13.0	13.7
14	19.0	11.0	11.6
14	19.0	19.5	20.5
14	19.0	21.5	22.6
15	19.0	11.0	11.6
15	19.0	17.0	17.9

POLYMER = PCTFE

LOAD = 9.8 N

DATE = 05/24/76

PHOTO NO.	PHOTO ANGLE (DEG.)	MEASURED ANGLE (DEG.)	REAL ANGLE (DEG.)
1	19.0	12.0	12.7
1	19.0	10.5	11.1
1	19.0	11.2	11.8
1	19.0	14.4	15.2
2	19.0	7.5	7.9
3	19.0	14.0	14.8
3	19.0	14.5	15.3
4	19.0	9.4	9.9
4	19.0	12.0	12.7
4	19.0	11.0	11.6
5	19.0	9.0	9.5
5	19.0	11.0	11.6
5	19.0	11.5	12.1
5	19.0	12.0	12.7
6	19.0	11.0	11.6
6	19.0	11.0	11.6
7	19.0	11.0	11.6
8	19.0	14.8	15.6
8	19.0	14.3	15.1
8	19.0	13.0	13.7
9	19.0	15.0	15.8
9	19.0	14.5	15.3
10	19.0	12.5	13.2
11	19.0	11.0	11.6
11	19.0	9.0	9.5
12	19.0	12.0	12.7
12	19.0	12.3	13.0
13	19.0	14.0	14.8
13	19.0	14.0	14.8
14	19.0	10.0	10.6
14	19.0	7.5	7.9
15	19.0	8.7	9.2
16	19.0	14.0	14.8
16	19.0	17.0	17.9
16	19.0	12.5	13.2

PCTFE 9.8 N 05/24/76 (CONTINUED)

PHOTO NO.	PHOTO ANGLE (DEG.)	MEASURED ANGLE (DEG.)	REAL ANGLE (DEG.)
16	19.0	12.5	13.2
17	19.0	12.0	12.7
18	19.0	7.0	7.4
18	19.0	13.0	13.7
18	19.0	11.0	11.6
18	19.0	10.0	10.6
19	19.0	10.0	10.6
19	19.0	14.0	14.8
19	19.0	14.0	14.8
20	19.0	9.5	10.0
20	19.0	11.5	12.1
21	19.0	10.0	10.6
21	19.0	14.0	14.8
21	19.0	12.0	12.7
21	19.0	14.3	15.1
21	19.0	7.5	7.9
22	19.0	13.5	14.2
22	19.0	16.0	16.9
23	19.0	12.0	12.7
23	19.0	11.0	11.6
23	19.0	15.0	15.8
24	19.0	6.5	6.9
24	19.0	8.9	9.4
24	19.0	14.5	15.3
24	19.0	11.0	11.6

NYLON 6-6 9.8 N 05/25/76 (CONTINUED)

PHOTO NO.	PHOTO ANGLE (DEG.)	MEASURED ANGLE (DEG.)	REAL ANGLE (DEG.)
15	19.0	17.0	17.9
15	19.0	20.0	21.1
15	19.0	22.0	23.1
16	19.0	14.5	15.3
16	19.0	10.4	11.0
16	19.0	14.4	15.2
16	19.0	14.5	15.3
16	19.0	14.2	15.0
17	19.0	14.5	15.3
17	19.0	17.0	17.9
17	19.0	18.0	19.0
17	19.0	17.5	18.4
17	19.0	17.5	18.4
18	19.0	21.0	22.1
19	19.0	26.0	27.3
19	19.0	18.5	19.5
19	19.0	20.5	21.6
19	19.0	19.0	20.0
20	19.0	19.0	20.0
20	19.0	22.5	23.7
20	19.0	16.0	16.9
21	19.0	14.5	15.3
22	19.0	32.5	34.0
22	19.0	14.0	14.8
22	19.0	20.9	22.0
22	19.0	20.5	21.6
23	19.0	21.5	22.6
24	19.0	23.0	24.2
24	19.0	16.5	17.4
24	19.0	20.5	21.6

POLYMER = PCTFE

LOAD = 2.45 N

DATE = 05/28/76

PHOTO NO.	PHOTO ANGLE (DEG.)	MEASURED ANGLE (DEG.)	REAL ANGLE (DEG.)
1	19.0	17.7	18.7
1	19.0	17.0	17.9
2	19.0	8.0	8.5
3	19.0	11.0	11.6
3	19.0	12.0	12.7
4	19.0	12.5	13.2
5	19.0	15.5	16.3
6	19.0	9.0	9.5
6	19.0	10.5	11.1
7	19.0	8.0	8.5
7	19.0	10.5	11.1
8	19.0	6.5	6.9
8	19.0	11.0	11.6
9	19.0	10.5	11.1
9	19.0	10.5	11.1
9	19.0	11.5	12.1
10	19.0	11.0	11.6
10	19.0	11.0	11.6
11	19.0	8.6	9.1
11	19.0	15.0	15.8
11	19.0	12.5	13.2
12	19.0	10.0	10.6
12	19.0	14.0	14.8
13	19.0	16.5	17.4
14	19.0	13.6	14.4
15	19.0	10.0	10.6
15	19.0	12.0	12.7
15	19.0	14.5	15.3
16	19.0	11.5	12.1
16	19.0	16.0	16.9
18	19.0	9.8	10.4
18	19.0	10.0	10.6
18	19.0	11.0	11.6
19	19.0	10.0	10.6
19	19.0	13.0	13.7

PCTFE 2.45 N 05/28/76 (CONTINUED)

PHOTO NO.	PHOTO ANGLE (DEG.)	MEASURED ANGLE (DEG.)	REAL ANGLE (DEG.)
19	19.0	13.0	13.7
19	19.0	18.0	19.0
19	19.0	25.0	26.3
20	19.0	12.0	12.7
20	19.0	12.6	13.3
21	19.0	10.0	10.6
21	19.0	12.0	12.7
21	19.0	11.6	12.2
21	19.0	16.0	16.9
22	19.0	19.0	20.0
22	19.0	14.0	14.8
22	19.0	15.5	16.3
23	19.0	12.4	13.1
23	19.0	13.5	14.2
23	19.0	14.8	15.6

POLYMER = NYLON 6-6

LOAD = 2.45 N

DATE = 05/31/76

PHOTO NO.	PHOTO ANGLE (DEG.)	MEASURED ANGLE (DEG.)	REAL ANGLE (DEG.)
1	19.0	21.0	22.1
1	19.0	17.5	18.4
1	19.0	10.0	10.6
2	19.0	13.0	13.7
2	19.0	18.5	19.5
3	19.0	18.0	19.0
3	19.0	13.0	13.7
4	19.0	17.5	18.4
4	19.0	18.0	19.0
4	19.0	16.0	16.9
5	19.0	17.3	18.2
5	19.0	21.0	22.1
6	19.0	17.4	18.3
6	19.0	13.9	14.7
6	19.0	16.0	16.9
7	19.0	27.3	28.6
7	19.0	23.0	24.2
8	19.0	14.0	14.8
8	19.0	16.0	16.9
8	19.0	11.5	12.1
8	19.0	24.0	25.2
9	19.0	19.9	20.9
10	19.0	7.4	7.8
10	19.0	13.5	14.2
11	19.0	20.5	21.6
11	19.0	16.0	16.9
12	19.0	19.0	20.0
12	19.0	24.0	25.2
13	19.0	17.0	17.9
13	19.0	20.0	21.1
14	19.0	20.7	21.8
15	19.0	11.5	12.1
15	19.0	15.0	15.8
16	19.0	25.9	27.2
17	19.0	31.5	32.9

NYLON 6-6 2.45 N 05/31/76 (CONTINUED)

PHOTO NO.	PHOTO ANGLE (DEG.)	MEASURED ANGLE (DEG.)	REAL ANGLE (DEG.)
17	19.0	31.5	32.9
17	19.0	22.0	23.1
17	19.0	24.0	25.2
18	19.0	19.9	20.9
18	19.0	14.5	15.3
18	19.0	24.0	25.2
19	19.0	17.0	17.9
19	19.0	24.5	25.7
19	19.0	18.5	19.5
20	19.0	18.8	19.8
20	19.0	13.0	13.7
20	19.0	12.9	13.6
21	19.0	20.1	21.2
21	19.0	16.0	16.9
22	19.0	14.0	14.8
22	19.0	15.0	15.8
23	19.0	11.2	11.8
23	19.0	11.2	11.8
23	19.0	14.0	14.8
24	19.0	13.0	13.7
24	19.0	15.0	15.8
24	19.0	23.0	24.2

POLYMER = PVC

LOAD = 9.8 N

DATE = 06/03/76

PHOTO NO.	PHOTO ANGLE (DEG.)	MEASURED ANGLE (DEG.)	REAL ANGLE (DEG.)
1	19.0	11.0	11.6
1	19.0	19.5	20.5
1	19.0	13.0	13.7
2	19.0	9.3	9.8
2	19.0	16.0	16.9
2	19.0	8.8	9.3
3	19.0	17.0	17.9
3	19.0	10.0	10.6
3	19.0	16.5	17.4
3	19.0	8.5	9.0
4	19.0	10.5	11.1
4	19.0	15.0	15.8
4	19.0	23.0	24.2
5	19.0	9.0	9.5
5	19.0	9.0	9.5
5	19.0	16.6	17.5
6	19.0	7.0	7.4
6	19.0	13.0	13.7
6	19.0	10.8	11.4
6	19.0	12.3	13.0
7	19.0	13.0	13.7
7	19.0	6.1	6.4
7	19.0	18.3	19.3
7	19.0	15.5	16.3
7	19.0	15.0	15.8
8	19.0	13.0	13.7
8	19.0	6.5	6.9
8	19.0	13.3	14.0
8	19.0	7.0	7.4
9	19.0	7.8	8.2
9	19.0	7.5	7.9
9	19.0	5.2	5.5
9	19.0	12.3	13.0
9	19.0	8.8	9.3
10	19.0	4.0	4.2

PVC 9.8 N 06/03/76 (CONTINUED)

PHOTO NO.	PHOTO ANGLE (DEG.)	MEASURED ANGLE (DEG.)	REAL ANGLE (DEG.)
10	19.0	4.0	4.2
10	19.0	5.5	5.8
11	19.0	17.0	17.9
11	19.0	7.5	7.9
11	19.0	9.5	10.0
11	19.0	14.0	14.8
13	19.0	10.3	10.9
13	19.0	9.6	10.1
13	19.0	15.5	16.3
14	19.0	17.0	17.9
14	19.0	10.0	10.6
14	19.0	8.0	8.5
14	19.0	12.4	13.1
14	19.0	10.8	11.4
15	19.0	12.5	13.2
15	19.0	14.5	15.3
15	19.0	13.5	14.2
15	19.0	11.0	11.6
16	19.0	7.0	7.4
16	19.0	6.2	6.6
16	19.0	3.4	3.6
16	19.0	5.0	5.3
17	19.0	8.0	8.5
17	19.0	13.0	13.7
17	19.0	15.0	15.8
18	19.0	5.9	6.2
18	19.0	13.0	13.7
18	19.0	7.5	7.9
19	19.0	8.5	9.0
19	19.0	13.0	13.7
19	19.0	12.0	12.7
19	19.0	11.5	12.1
20	19.0	9.0	9.5
20	19.0	7.5	7.9
20	19.0	11.0	11.6
20	19.0	10.5	11.1
21	19.0	5.5	5.8
21	19.0	9.0	9.5
21	19.0	9.2	9.7
22	19.0	11.0	11.6
22	19.0	8.3	8.8
22	19.0	6.5	6.9

PVC 9.8 N 06/03/76 (CONTINUED)

PHOTO NO.	PHOTO ANGLE (DEG.)	MEASURED ANGLE (DEG.)	REAL ANGLE (DEG.)
22	19.0	6.5	6.9
22	19.0	8.3	8.8
23	19.0	4.5	4.8
23	19.0	5.0	5.3
23	19.0	4.0	4.2
23	19.0	6.5	6.9
24	19.0	5.0	5.3
24	19.0	6.4	6.8
24	19.0	6.0	6.3

POLYMER = NYLON 6-6

LOAD = 14.7 N

DATE = 06/04/76

PHOTO NO.	PHOTO ANGLE (DEG.)	MEASURED ANGLE (DEG.)	REAL ANGLE (DEG.)
1	19.0	17.4	18.3
1	19.0	20.4	21.5
1	19.0	20.0	21.1
1	19.0	13.0	13.7
1	19.0	6.8	7.2
2	19.0	13.0	13.7
2	19.0	14.5	15.3
3	19.0	13.5	14.2
3	19.0	18.5	19.5
3	19.0	25.0	26.3
4	19.0	24.4	25.6
4	19.0	18.0	19.0
4	19.0	18.5	19.5
4	19.0	12.5	13.2
5	19.0	18.4	19.4
5	19.0	8.5	9.0
5	19.0	19.5	20.5
5	19.0	14.5	15.3
6	19.0	8.0	8.5
6	19.0	20.9	22.0
6	19.0	28.0	29.4
7	19.0	18.0	19.0
7	19.0	21.5	22.6
7	19.0	18.5	19.5
8	19.0	13.5	14.2
8	19.0	15.5	16.3
8	19.0	24.5	25.7
9	19.0	15.0	15.8
9	19.0	16.0	16.9
9	19.0	23.5	24.7
10	19.0	19.5	20.5
10	19.0	21.2	22.3
11	19.0	19.6	20.6
12	19.0	14.1	14.9
12	19.0	24.3	25.5

NYLON 6-6 14.7 N 06/04/76 (CONTINUED)

PHOTO NO.	PHOTO ANGLE (DEG.)	MEASURED ANGLE (DEG.)	REAL ANGLE (DEG.)
12	19.0	24.3	25.5
12	19.0	14.1	14.9
12	19.0	14.0	14.8
12	19.0	16.5	17.4
13	19.0	15.5	16.3
13	19.0	13.6	14.4
13	19.0	19.1	20.1
13	19.0	28.0	29.4
13	19.0	11.5	12.1
14	19.0	20.5	21.6
14	19.0	23.5	24.7
14	19.0	23.5	24.7
14	19.0	24.8	26.0
15	19.0	45.0	46.6
15	19.0	21.6	22.7
15	19.0	21.0	22.1
15	19.0	19.5	20.5
17	19.0	26.5	27.8
17	19.0	24.0	25.2
17	19.0	25.5	26.8
17	19.0	13.8	14.6
18	19.0	27.0	28.3
18	19.0	18.0	19.0
18	19.0	32.0	33.5
19	19.0	16.9	17.8
19	19.0	17.4	18.3
19	19.0	18.5	19.5
19	19.0	25.0	26.3
21	19.0	19.2	20.2
21	19.0	18.0	19.0
21	19.0	24.0	25.2
20	19.0	17.2	18.1
20	19.0	14.1	14.9
20	19.0	17.5	18.4
20	19.0	16.6	17.5
22	19.0	14.6	15.4
22	19.0	21.0	22.1
22	19.0	25.0	26.3
22	19.0	15.0	15.9
23	19.0	16.0	16.9
23	19.0	23.5	24.7
24	19.0	14.2	15.0

NYLON 6-6 14.7 N 06/04/76 (CONTINUED)

PHOTO NO.	PHOTO ANGLE (DEG.)	MEASURED ANGLE (DEG.)	REAL ANGLE (DEG.)
24	19.0	14.2	15.0
24	19.0	15.5	16.3
24	19.0	15.0	15.8
24	19.0	32.5	34.0
24	19.0	20.5	21.6

POLYMER = PVC

LOAD = 14.7 N

DATE = 06/08/76

PHOTO NO.	PHOTO ANGLE (DEG.)	MEASURED ANGLE (DEG.)	REAL ANGLE (DEG.)
1	19.0	7.0	7.4
1	19.0	4.2	4.4
1	19.0	3.5	3.7
1	19.0	7.8	8.2
1	19.0	3.4	3.6
2	19.0	5.7	6.0
2	19.0	9.0	9.5
2	19.0	9.9	10.5
2	19.0	6.0	6.3
3	19.0	3.0	3.2
3	19.0	5.5	5.8
3	19.0	9.0	9.5
3	19.0	8.1	8.6
3	19.0	7.0	7.4
3	19.0	5.6	5.9
4	19.0	8.6	9.1
4	19.0	6.5	6.9
4	19.0	5.7	6.0
4	19.0	11.0	11.6
4	19.0	11.4	12.0
5	19.0	7.7	8.1
5	19.0	8.2	8.7
5	19.0	6.9	7.3
5	19.0	7.0	7.4
6	19.0	8.6	9.1
6	19.0	11.8	12.5
6	19.0	11.0	11.6
7	19.0	10.4	11.0
7	19.0	3.2	3.4
7	19.0	14.6	15.4
8	19.0	5.6	5.9
8	19.0	12.5	13.2
9	19.0	7.0	7.4
9	19.0	9.5	10.0
9	19.0	10.6	11.2

PVC 14.7 N 06/08/76 (CONTINUED)

PHOTO NO.	PHOTO ANGLE (DEG.)	MEASURED ANGLE (DEG.)	REAL ANGLE (DEG.)
9	19.0	10.6	11.2
9	19.0	3.7	3.9
10	19.0	12.0	12.7
10	19.0	9.3	9.8
10	19.0	13.0	13.7
10	19.0	14.5	15.3
10	19.0	10.0	10.6
10	19.0	10.7	11.3
11	19.0	8.0	8.5
11	19.0	2.5	2.6
11	19.0	6.0	6.3
11	19.0	7.0	7.4
11	19.0	11.9	12.6
12	19.0	8.4	8.9
12	19.0	13.4	14.1
12	19.0	12.9	13.6
12	19.0	11.7	12.4
12	19.0	6.5	6.9
13	19.0	13.4	14.1
13	19.0	13.4	14.1
13	19.0	9.1	9.6
13	19.0	6.5	6.9
14	19.0	8.0	8.5
14	19.0	10.9	11.5
14	19.0	6.5	6.9
14	19.0	7.0	7.4
15	19.0	9.9	10.5
15	19.0	33.2	34.7
15	19.0	18.5	19.5
15	19.0	11.5	12.1
16	19.0	16.3	17.2
16	19.0	10.0	10.6
16	19.0	11.8	12.5
16	19.0	14.6	15.4
16	19.0	11.5	12.1
16	19.0	12.0	12.7
17	19.0	18.0	19.0
17	19.0	13.9	14.7
17	19.0	13.9	14.7
17	19.0	8.0	8.5
17	19.0	9.5	10.0
17	19.0	5.5	5.8

PVC 14.7 N 06/08/76 (CONTINUED)

PHOTO NO.	PHOTO ANGLE (DEG.)	MEASURED ANGLE (DEG.)	REAL ANGLE (DEG.)
17	19.0	5.5	5.8
18	19.0	7.0	7.4
18	19.0	5.3	5.6
18	19.0	5.0	5.3
18	19.0	5.0	5.3
19	19.0	3.0	3.2
19	19.0	12.3	13.0
19	19.0	13.3	14.0
19	19.0	10.0	10.6
19	19.0	12.0	12.7
20	19.0	11.9	12.6
20	19.0	12.5	13.2
20	19.0	17.0	17.9
20	19.0	3.5	3.7
21	19.0	11.5	12.1
21	19.0	13.6	14.4
21	19.0	8.0	8.5
22	19.0	7.5	7.9
22	19.0	6.9	7.3
22	19.0	9.5	10.0
22	19.0	8.0	8.5
22	19.0	7.5	7.9
23	19.0	5.1	5.4
23	19.0	6.6	7.0
23	19.0	6.5	6.9
23	19.0	6.8	7.2
24	19.0	9.6	10.1
24	19.0	9.5	10.0
24	19.0	9.7	10.2
24	19.0	5.5	5.8
24	19.0	8.6	9.1

POLYMER = PVC

LOAD = 2.45 N

DATE = 06/08/76

PHOTO NO.	PHOTO ANGLE (DEG.)	MEASURED ANGLE (DEG.)	REAL ANGLE (DEG.)
1	19.0	8.8	9.3
1	19.0	14.0	14.8
1	19.0	12.5	13.2
2	19.0	5.5	5.8
2	19.0	10.0	10.6
2	19.0	12.0	12.7
3	19.0	8.0	8.5
3	19.0	7.0	7.4
4	19.0	8.8	9.3
4	19.0	15.0	15.8
4	19.0	14.4	15.2
5	19.0	15.3	16.1
5	19.0	16.0	16.9
5	19.0	14.5	15.3
5	19.0	14.4	15.2
5	19.0	11.8	12.5
5	19.0	11.5	12.1
6	19.0	18.0	19.0
6	19.0	7.5	7.9
6	19.0	6.0	6.3
6	19.0	7.5	7.9
7	19.0	9.8	10.4
7	19.0	6.0	6.3
7	19.0	9.5	10.0
8	19.0	11.0	11.6
8	19.0	10.4	11.0
8	19.0	13.5	14.2
8	19.0	16.0	16.9
8	19.0	16.5	17.4
8	19.0	18.5	19.5
9	19.0	10.5	11.1
9	19.0	9.0	9.5
9	19.0	15.5	16.3
10	19.0	15.2	16.0
10	19.0	6.0	6.3

PVC 2.45 N 06/08/76 (CONTINUED)

PHOTO NO.	PHOTO ANGLE (DEG.)	MEASURED ANGLE (DEG.)	REAL ANGLE (DEG.)
10	19.0	6.0	6.3
11	19.0	13.0	13.7
11	19.0	7.5	7.9
11	19.0	16.4	17.3
11	19.0	4.2	4.4
11	19.0	6.0	6.3
11	19.0	10.5	11.1
12	19.0	16.5	17.4
12	19.0	7.0	7.4
12	19.0	15.5	16.3
12	19.0	12.0	12.7
12	19.0	12.4	13.1
13	19.0	8.5	9.0
13	19.0	10.0	10.6
13	19.0	14.5	15.3
14	19.0	13.0	13.7
14	19.0	15.5	16.3
14	19.0	17.0	17.9
14	19.0	2.0	2.1
14	19.0	10.0	10.6
15	19.0	14.7	15.5
16	19.0	13.8	14.6
16	19.0	14.5	15.3
16	19.0	10.9	11.5
17	19.0	9.5	10.0
17	19.0	7.5	7.9
17	19.0	9.5	10.0
17	19.0	18.0	19.0
18	19.0	10.0	10.6
18	19.0	9.6	10.1
18	19.0	7.0	7.4
18	19.0	7.5	7.9
19	19.0	15.2	16.0
19	19.0	14.6	15.4
19	19.0	13.0	13.7
19	19.0	15.0	15.8
19	19.0	10.0	10.6
19	19.0	4.5	4.8
20	19.0	13.4	14.1
20	19.0	7.5	7.9
20	19.0	11.1	11.7
20	19.0	11.0	11.6

PVC 2.45 N 06/08/76 (CONTINUED)

PHOTO NO.	PHOTO ANGLE (DEG.)	MEASURED ANGLE (DEG.)	REAL ANGLE (DEG.)
20	19.0	11.0	11.6
20	19.0	8.4	8.9
21	19.0	12.9	13.6
21	19.0	12.4	13.1
21	19.0	11.9	12.6
21	19.0	13.7	14.5
21	19.0	10.5	11.1
21	19.0	7.6	8.0
21	19.0	10.7	11.3
22	19.0	8.0	8.5
22	19.0	9.0	9.5
22	19.0	5.6	5.9
22	19.0	7.9	8.3
23	19.0	13.7	14.5
23	19.0	10.0	10.6
23	19.0	7.5	7.9
23	19.0	11.0	11.6
23	19.0	11.1	11.7
23	19.0	11.4	12.0
24	19.0	11.0	11.6
24	19.0	17.5	18.4
24	19.0	10.0	10.6
24	19.0	11.8	12.5
24	19.0	18.9	19.9

**The vita has been removed from
the scanned document**

THE PREDICTION OF POLYMER WEAR USING
POLYMER MECHANICAL PROPERTIES AND SURFACE
CHARACTERIZATION PARAMETERS

by

Jeffery Howard Warren

(ABSTRACT)

Polymers were slid on rough hard steel surfaces with normal loads which caused full penetration (real and apparent areas equal) and partial penetration (real less than apparent area). Wear data for polyvinylchloride (PVC) and polychlorotrifluoroethylene (PCTFE) was obtained on a pin-on-disk machine using neutron activation analysis (NAA). Observations of the wear process were made in the scanning electron microscope (SEM) both before, during, and after the wear experiment. It was observed that these polymers along with Nylon 6-6 tend to wear in discrete sites rather than continuous films. At these discrete sites the polymer shears at an angle which is dependent on the mechanical properties of the polymer and on the asperity angle. There appears to be a minimum shear angle beyond which no wear occurs. This angle correlates with the energy to rupture (ER) of the polymer.

Orthogonal cutting theory can be modified to predict a shear angle which is dependent on both the asperity angle and the polymer properties if it is assumed that the shear strength of the polymer is a linear function of the normal load. The modified theory requires, however, that

material removing asperities have slopes much larger than those actually measured on the steel surfaces investigated. Thus, assumptions made in the model regarding the shear strength and flow pressure of the polymers should be investigated in future research.

The steel surface roughness was found to be very important in determining the wear of the polymers. For the full penetration case, the peak-to-valley heights, arithmetic average, correlation length times arithmetic average, and average profile slopes all tend to correlate with the wear. The factor S'_S/p_m , where S'_S is the shear strength of the polymer and p_m is the flow pressure of the polymer and the inverse of the energy to rupture of the different polymers also correlate with the wear.

It was shown that surface parameters calculated from traces of the same surface, one trace having a 762 μm waviness filter and one having no filter, made quite a difference in the surface data reported. The data calculated from the trace with no filter were larger than those calculated from the trace with the filter. Thus, when a filter is used it should be made small enough to include wavelengths comparable to the dimensions of the apparent area of the polymer pin in the direction of sliding.

In the partial penetration case, the amount of wear appears to be discriminated by the depth of penetration of the polymer into the steel surface. The depth of penetration appears to be a good parameter

for indicating the amount of wear since it includes both mechanical properties of the polymer and surface properties of the steel disk. Factors such as flow pressure (p_m) used to determine the real area of contact and hence the penetration depth of the polymer need to be investigated along with more experiments of different polymers to determine if indeed the depth of penetration is indicative of the wear.